Hochschule Offenburg
University of Applied Sciences
ECM

DLR Deutsches Zentrum für Luft- und Raumfahrt e.V.
in der Helmholtz-Gemeinschaft

MASTER'S THESIS

AN APPROACH FOR A SIMULTANEOUS SIMULATION OF COOLING AND AIR CONDITIONING SYSTEMS IN ELECTRIC VEHICLES

Course of Study:

M.Sc. Energy Conversion and Management (ECM)

University's Supervisor:

Prof. Dr.- Ing. Peter Treffinger

Institute's name, Department and Thesis Duration:

The German Aerospace Center (DLR)

Institute of Vehicle Concepts

From July 4th, 2013 till January 31, 2014

Institute's Supervisor:

Dipl.- Ing. Mounir Nasri

Name: Ahmed Hussein Saad Hussein (ECM-05)

Study Course: Energy Conversion and Management (ECM) **Date of Submission:** 01 April 2014

Address: Pfaffenwaldring 42 C, 70569 Stuttgart

Foreword

This master's thesis was written during the time-period from Summer 2013 until Spring 2014. For the completion of the master's degree in Energy Conversion and Management, this work has been done under the supervision of Prof. Dr.- Ing. Peter Treffinger, University of Applied Sciences Offenburg and Dipl.- Ing. Mounir Nasri, Institute of Vehicle Concepts, DLR Institute, Stuttgart.

The intent of this thesis is to present a design of an integrated simulation model for the cooling and air conditioning circuits in a fuel cell electric vehicle.

Using the simulation environment Dymola, the coupling of submodels to form the thermal management system has been investigated.

On the account of flexible exchange of submodels and the unsteady operational status of the general model, an approach for a co-simulation using the Building Controls Virtual Test Bed (BCVTB) software to couple between submodels is also analyzed, introduced and tested.

A comparison is to be finally done between coupling in Dymola and co-simulating in BCVTB based on the simulation speed, flexibility of submodels' exchange, ease of coupling and interface.

This thesis contains a good example for modelling and simulating a physical software model for the thermal management system in an electric vehicle from the scratch. It also addresses other attempt to introduce a promising co-simulation tool (BCVTB) developed at Lawrence Berkeley National Laboratory, Berkeley, CA, USA.

I want to thank my supervisors, for being a great help during the development of this thesis, DLR Institute for being so supportive with the necessary softwares.

Author Stuttgart, 1. April 2014

Copyright Clause

I declare in lieu of an oath that the master's thesis submitted has been produced by me without illegal help from other persons. I state that all passages which have been taken out of publications of all means or unpublished material either whole or in part, in words or ideas, have been marked as quotations in the relevant passage or in the bibliography. I also confirm that the quotes included show the extent of the original quotes and are marked as such. I know that a false declaration will have legal consequences.

Author Stuttgart, 1. April 2014

Abstract

Through this dissertation, an approach for a cooling strategy will be exhibited in developing a descriptive software simulation model for the thermal management system inside a fuel cell electric vehicle using the simulation environment Dymola.

Starting from the thermal analogy for the electric devices and then building up the cooling circuits, coupling of all cooling circuits in the thermal management system in Dymola will be finally introduced.

Considering the simulation speed, stability and ease of submodels' exchange, the Building Controls Virtual Test Bed (BCVTB) software; as a co-simulation tool, will be also introduced to couple all submodels founding the thermal management system.

A comparison between the simulation results out of both softwares according to the accuracy and speed of simulation will be executed and used as a validation for both coupling approaches.

Both softwares will be also compared according to stability, flexibility of model exchange, speed of simulation and ease of interface.

By the end of this report, a conclusion is to state the advantages and disadvantages of using both softwares which enables developers at DLR to understand the difference and to choose between them. (© Copyright 2014 All Rights Reserved for DLR & Ahmed Hussein)

Table of Contents

Foreword.... ii
Copyright Clause..... iii
Abstract..... iv
Table of Contents v
List of Figures and Illustrations vi
List of Tables ix
Nomenclature x
List of Abbreviations xi

1 INTRODUCTION 1

2 PROJECT TASKS AND DELIVERABLES 2

2.1 CHOOSING THE APPROPRIATE SOFTWARES 3
2.1.1 For Modelling: 3
2.1.2 For Co-simulation: 3
2.2 THERMAL ANALOGY AND MODELLING OF ELECTRIC DEVICES 5
2.2.1 Thermal Analogy of the Electric Motor 5
2.2.2 Thermal Analogy of Power Electronics Module 12
2.3 THERMAL MANAGEMENT SYSTEM IN THE ELECTRICAL VEHICLE 16
2.3.1 Low Temperature Cooling Circuit (LT Cooling Circuit) 18
2.3.2 Battery Cooling Circuit 32
2.3.3 High Temperature Cooling Circuit (HT Cooling Circuit) 37
2.3.4 Air Conditioning Cycle (A/C Cycle) 44
2.3.5 The Control Module 48
2.3.6 Coupling in Dymola 52
2.4 COUPLING IN BCVTB 58
2.4.1 What is BCVTB? 58
2.4.2 How BCVTB Works? 58
2.4.3 Configuration of Submodels in BCVTB 60
2.4.4 General Model Layout in BCVTB 66
2.4.5 Data Transport between Actors in BCVTB 69
2.4.6 Co-simulation Results and Validation 70
2.5 COMPARISON AND CONCLUSION 73

3 ACKNOWLEDGMENT 74

4 BIBLIOGRAPHY 75

APPENDICES 76

APPENDIX A **76**
APPENDIX B **78**

List of Figures and Illustrations

FIGURE 1: PROJECT PLAN 2
FIGURE 2: UQM MOTOR POWERPHASE SELECT 50 5
FIGURE 3: SANKEY DIAGRAM FOR ENERGY FLOW INSIDE THE EM 6
FIGURE 4: VELOCITY PROFILE OF ONE NEW EUROPEAN DRIVING CYCLE (NEDC) 6
FIGURE 5: RECORDED ELECTRIC AND MECHANICAL POWERS OF THE EM THROUGH DYNO ROLLER TESTBENCH (TEST DATE: 03.09.2013) 7
FIGURE 6: EM EXCLUDED THERMAL SUBMODEL 8
FIGURE 7: EM FINAL THERMAL SUBMODEL 9
FIGURE 8: ABSOLUTE POWER DIFFERENCE FED TO THE EM THERMAL SUBMODEL 9
FIGURE 9: TEMPERATURE RISE INSIDE THE EM 11
FIGURE 10: HEAT GENERATED OUT OF THE EM THERMAL SUBMODEL 11
FIGURE 11: SIDE VIEW FOR THE PEM IN UQM POWERPHASE SELECT 50 12
FIGURE 12: POWER LOSS VALUES FED TO THE PEM THERMAL SUBMODEL (RECORDED THROUGH DYNO ROLLER TESTBENCH (TEST DATE: 03.09.2013)) 13
FIGURE 13: PEM EXCLUDED THERMAL SUBMODEL 13
FIGURE 14: PEM FINAL THERMAL SUBMODEL 14
FIGURE 15: TEMPERATURE RISE INSIDE THE PEM 15
FIGURE 16: HEAT GENERATED OUT OF THE PEM SUBMODEL 15
FIGURE 17: COOLING AND AIR CONDITIONING CIRCUITS' PROPOSED LAYOUT 16
FIGURE 18: LOW TEMPERATURE COOLING CIRCUIT P&ID 18
FIGURE 19: LT COOLING CIRCUIT MODEL 20
FIGURE 20: GENERAL PARAMETERS OF THE SYSTEM 22
FIGURE 21: SYSTEM ASSUMPTIONS 23
FIGURE 22: SYSTEM INITIALIZATION PARAMETERS 24
FIGURE 23: TANK GENERAL PARAMETERS 25
FIGURE 24: PRESCRIBED FLOW PROPERTIES 26
FIGURE 25: DYNAMIC PIPE MODEL WITH MODEL STRUCTURE (AV_VB) & NNODES = 3 27
FIGURE 26: HEX MODEL IN THE A/C LIBRARY 29
FIGURE 27: FREE MODELICA HEX MODEL 29
FIGURE 28: LT HEAT EXCHANGER PARAMETERS 30
FIGURE 29: BATTERY COOLING CIRCUIT P&ID 32
FIGURE 30: THE BATTERY COOLING CIRCUIT MODEL 33
FIGURE 31: AIR MASS FLOW SOURCE IN THE BATTERY COOLING CIRCUIT 34
FIGURE 32: RECORDED BATTERY'S HEAT LOAD THROUGH DYNO ROLLER TESTBENCH (TEST DATE: 03.09.2013) 35
FIGURE 33: BATTERY HEAT EXCHANGER PARAMETERS 36
FIGURE 34: HT COOLING CIRCUIT P&ID 37
FIGURE 35: HT COOLING CIRCUIT MODEL 38
FIGURE 36: RECORDED FC HEAT LOAD THROUGH DYNO ROLLER TESTBENCH (TEST DATE: 03.09.2013) 41
FIGURE 37: MAIN HEAT EXCHANGER PARAMETERS 42
FIGURE 38: EVAPORATOR HEX 43

FIGURE 39: CABIN HEAT EXCHANGER PARAMETERS 43
FIGURE 40: A/C CYCLE P&ID 44
FIGURE 41: A/C CIRCUIT MODEL 45
FIGURE 42: INITIALIZATION PARAMETERS 47
FIGURE 43: SYSTEM'S CONTROL MODULE LAYOUT 48
FIGURE 44: EM TEMPERATURE CONTROL SCHEME 49
FIGURE 45: AIR MASS FLOW CONTROL SCHEME 50
FIGURE 46: FC TEMPERATURE CONTROL SCHEME 50
FIGURE 47: GENERAL MODEL COUPLED LAYOUT IN DYMOLA 52
FIGURE 48: INITIALIZATION BLOCK 53
FIGURE 49: EM COOLING EFFECT 54
FIGURE 50: PEM COOLING EFFECT 55
FIGURE 51: BATTERY COOLING EFFECT 55
FIGURE 52: FC COOLING EFFECT 56
FIGURE 53: A/C CYCLE'S COP 57
FIGURE 54: EVAPORATOR'S OUTLET AIR TEMPERATURE 57
FIGURE 55: ARCHITECTURE OF THE BCVTB WITH THE MIDDLEWARE SHOWN IN THE DOTTED BOX THAT CONNECTS TWO CLIENTS 58
FIGURE 56: AN EXAMPLE OF CONNECTING DYMOLA WITH SIMULINK FOR TESTING BCVTB INTERFACE 59
FIGURE 57: CONTROL MODULE BASE LAYOUT IN BCVTB 60
FIGURE 58: BCVTB BLOCK 61
FIGURE 59: CONTROL MODULE CONFIGURED LAYOUT 61
FIGURE 60: DATA EXCHANGE BETWEEN DYMOLA AND BCVTB 62
FIGURE 61: LT AND BATTERY CONFIGURED MODELS' LAYOUT IN BCVTB 63
FIGURE 62: A/C CONFIGURED MODEL LAYOUT IN BCVTB 64
FIGURE 63: HT CONFIGURED MODEL LAYOUT IN BCVTB 65
FIGURE 64: CONCEPTUAL ARCHITECTURE OF THE GENERAL MODEL IN PTOLEMY II . 66
FIGURE 65: GENERAL MODEL COUPLED IN PTOLEMY II 67
FIGURE 66: SDF DIRECTOR 68
FIGURE 67: DATA TRANSPORT BETWEEN ACTORS IN BCVTB 69
FIGURE 68: COMPARISON BETWEEN EM COOLING EFFECT IN BCVTB AND DYMOLA .. 70
FIGURE 69: COMPARISON BETWEEN PEM COOLING EFFECT IN BCVTB AND DYMOLA 70
FIGURE 70: COMPARISON BETWEEN BATTERY COOLING EFFECT IN BCVTB AND DYMOLA 71
FIGURE 71: COMPARISON BETWEEN FC COOLING EFFECT IN BCVTB AND DYMOLA ... 71
FIGURE 72: COMPARISON BETWEEN COP IN BCVTB AND DYMOLA 71
FIGURE 73: COMPARISON BETWEEN CABIN'S AIR TEMPERATURE IN BCVTB AND DYMOLA 72
FIGURE 74: EM THERMAL SUBMODEL 76
FIGURE 75: UQM BOTH EM AND PEM 77
FIGURE 76: LT AND BATTERY MODELS WITH A/C HEXS 78
FIGURE 77: HT MODEL WITH A/C HEXS 78

List of Tables

TABLE 1: DIFFERENT CONVENTIONS FOR THE EM OPERATIONAL CONDITIONS 7
TABLE 2: COOLANT PROPERTIES IN THE LT CIRCUIT 21
TABLE 3: PIPES' PARAMETERIZATION IN LT MODEL 28
TABLE 4: PIPES' PARAMETERIZATION IN BATTERY COOLING CIRCUIT'S MODEL 35
TABLE 5: COOLANT PROPERTIES IN THE HT CIRCUIT 39
TABLE 6: PIPES' PARAMETERIZATION IN HT COOLING CIRCUIT'S MODEL 40
TABLE 7: REFRIGERANT PROPERTIES IN THE A/C CYCLE 46
TABLE 8: INPUTS AND OUTPUTS TO THE BCVTB BLOCK IN THE CONTROL MODULE ... 62
TABLE 9: INPUTS AND OUTPUTS TO THE BCVTB BLOCK IN THE LT AND BATTERY MODELS 63
TABLE 10: INPUTS AND OUTPUTS TO THE BCVTB BLOCK IN THE A/C MODEL 64
TABLE 11: INPUTS AND OUTPUTS TO THE BCVTB BLOCK IN THE HT MODEL 65
TABLE 12: COMPARISON BETWEEN DYMOLA AND BCVTB COUPLING TOOLS 73

List of Equations

EQUATION 1: HEAT CAPACITY OF ELEMENT 8
EQUATION 2: THERMAL CONVECTION POWER IN WATTS 10
EQUATION 3: EM HEAT TRANSFER AREA 10
EQUATION 4: THERMAL RADIATION POWER IN WATTS 10
EQUATION 5: SURFACE AREA OF THE PEM 14
EQUATION 6: ENERGY BALANCE EQUATION 23
EQUATION 7: COOLANT MASS FLOW RATE EQUATION 25
EQUATION 8: ACCURACY OF DATA EXCHANGE 72
EQUATION 9: ENERGY LOSSES EQUATIONS 76

Nomenclature (Latin Symbols)

Symbol	Unit	Description
B	Wb	Magnetic Flux
C_P	$\frac{\mathrm{kJ}}{\mathrm{kg.K}}$	Specific Heat
f	Hz	Frequency
g	$\frac{\mathrm{m}}{\mathrm{s}^2}$	Gravitational Acceleration
I	A	Electric Current
l	m	Length
m	kg	Mass
$\dot{m}$	$\frac{\mathrm{kg}}{\mathrm{s}}$	Mass Flow
n	$\frac{1}{\mathrm{min}}$	Rotational Speed
P	kW	Power
p	bar	Pressure
$\dot{Q}$	kW	Heat
R	ohm	Electric Resistance
T_{set}	°C	Temperature

Nomenclature (Greek Symbols)

Symbol	Unit	Description
ρ	$\frac{\mathrm{kg}}{\mathrm{m}^3}$	Density
μ	mPa.s	Dynamic Viscosity
K	$\frac{\mathrm{W}}{\mathrm{m.K}}$	Thermal Conductivity
μ	$\frac{\mathrm{H}}{\mathrm{m}}$	Permeability of Material

List of Abbreviations

Abbreviation	Description
BCVTB	Building Controls Virtual Test Bed
COP	Coefficient of Performance
DAE	Differential Algebraic Equation
EM	Electric Motor
EV	Electric Vehicle
FC	Fuel Cell
FCEV	Fuel Cell Electric Vehicle
HEX	Heat Exchanger
MoC	Model of Computation
NEDC	New European Driving Cycle
OS	Operating System
PDE	Partial Differential Equation
PEM	Power Electronics Module
RH	Relative Humidity
XML	Extensible Markup Language

1 Introduction

In the 19th century, the electric vehicles were introduced among the earliest automobiles. In fact, in 1900, 28 % of the cars on the road in USA were electric[i]. Afterwards, the discovery of large petroleum reserves has contributed to decline of electric cars.

Recently, due to ecological and economical reasons, paying more efforts for deploying more electric cars in international markets has become a must. Germany has built up an aim to increase the electric vehicles' production to 1 million units by 2020[ii].

In electric vehicles and besides the power demanded for the road traction, the thermal management system requires a great share of the power stored in the vehicle. The challenge is always in how to keep this share minimized.

As an accurate depiction of reality, modelling and simulation of the thermal management system represent the cornerstone for optimizing the share of the cooling and air conditioning circuits from total electric power consumed by the vehicle.

Considering all heat generative devices (fuel cell stack, electric motor and battery) as well as other influences like ambient temperature and vehicle speed, several stochastic approaches should be introduced not only in modelling the air conditioning and cooling circuits, but also in the simulation for the sake of choosing the most representative strategy.

Using Dymola, thermal analogized submodels for the electric devices inside the FCEV as well as modelling the cooling circuits have been -separately- done and introduced in many scientific papers. In this dissertation, the attempt is to couple all thermal submodels and cooling circuits in one consistent and comprehensive model that represents thermal management and thermal protection inside the electric vehicle the best.

Since the speed of data exchange through coupling has a significant effect on the simulation results; accordingly, the need for a different powerful co-simulation software tool that couples all submodels which form the thermal management system is urgent.

2 Project Tasks and Deliverables

Task 1: Choosing the appropriate softwares for modelling and co-simulation.

Deliverables: Dymola for modelling: A powerful modelica tool with powerful libraries for the cooling, air conditioning and automotive applications.

BCVTB for co-simulation: A promising newly developed co-simulative tool capable of coupling various simulation programs for data exchange.

Task 2: Modelling and thermal analogy for the electric devices inside circuits.

Deliverables: Thermal analogized Dymola submodel for the electric motor (EM).

Thermal analogized Dymola submodel for the power electronics module (PEM).

Task 3: Modelling of low and high temperature cooling circuits. Configuration of the air conditioning circuit from Dymola A/C library then coupling of all submodels in Dymola environment.

Deliverables: Simulation results out of a general model consists of LT, HT and A/C submodels, coupled all together through the air path.

Task 4: Configuration of each circuit and co-simulating in BCVTB.

Deliverables: Validation of co-simulation results out of a new interface for the general model in Ptolemy II software.

Task 5: Coupling's validation based on results from Dymola and BCVTB.

Deliverable: Comparison between two approaches according to the simulation speed, flexibility of model exchange and ease of interface.

In Figure 1, the project schedule is clearly described.

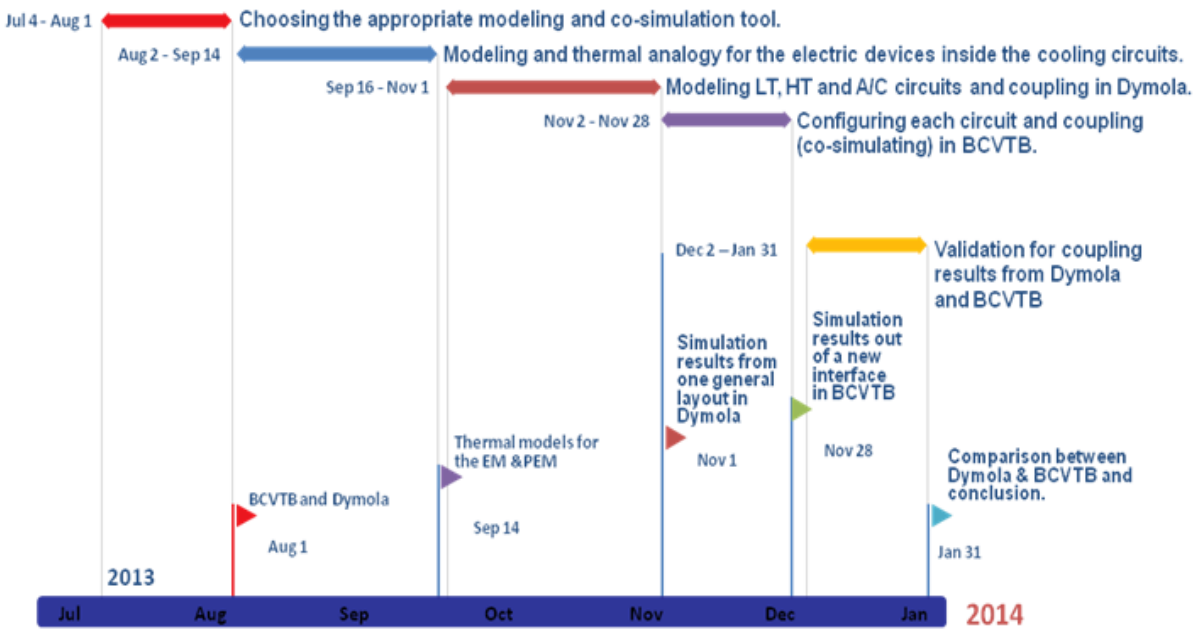

Figure 1: Project Plan

2.1 Choosing the Appropriate Softwares

2.1.1 For Modelling:

As an **object-oriented** software which encapsulates data and operations in objects that interact with each other via the object's interface, Dymola software has been chosen as the main modelling software. As this project is a part of a bigger extended project which; mainly, utilizes the modelica libraries developed by DLR (e.g. Alternative Vehicles library) and Modelon (e.g. Air Conditioning library), Dymola was not only chosen because of the relevance, but also for its academic familiarity.

2.1.2 For Co-simulation:

After a differentiation between Building Controls Virtual Test Bed (BCVTB) and the Functional Mock-up Interface (FMI) developed by MODELISAR, BCVTB has been chosen for the following reasons:

1) Because Dymola is the only modelling environment used, there was no need to involve FMI to provide a unified model interface for model exchange in different modelling environments. However, it would be advisable to use the FMI when several modelling and simulation environments are involved.

2) In Modelica, components are concurrent and communicate via ports. This means, that exporting models to Functional Mock-up Units (FMUs are the FMI compliant exported models) in Dymola environment; represented as FMU blocks, will be subjected to the same synchronization speed of data exchange while simulating as they were before exporting.

3) For any Dymola component, the ports are considered neither inputs nor outputs and the connections between ports impose equation constraints on variables that all lead to actor-like semantics of Modelica. Modelica is actually most suited to modelling physical systems, that can be intuitively described by equations.

4) Ptolemy II (the simulation environment of BCVTB), mainly addresses the heterogeneous modelling, simulation and design of concurrent embedded systems. The major motivation of this project is generating models that can be implemented in a broad variety of computational models such as discrete-event, continuous-time, finite-state machine, synchronous data-flow and etc.

5) The use of the Modelica models in the causal environment of Ptolemy II allows the simulation of the non-causal models of Modelica in combination with variant Models of computation that are realized in Ptolemy II, such as synchronous data-flow to support the design of heterogeneous systems.

6) Some of the fundamental Ptolemy II features are as follows:

- *Java*, Ptolemy II is implemented in Java, which allows Ptolemy II to be:
  - *Platform independent*, currently Ptolemy II runs under Solaris and Windows.
  - *Threaded*, Ptolemy II builds on the threading primitives in Java.
- *Modularity*, Ptolemy II is composed of software packages that can be utilized independently.
- *Mutable System*, Ptolemy II allows the design to be modified as it is running.
- *Software Architecture*, Ptolemy II has designed with object modelling and design patterns in mind.[iii]

7) BCVTB has proven its wide capability of coupling various softwares and still being developed for wider compatibilities. The interface of this model could be expanded to involve other softwares (e.g. Simulink, CATIA or TRNSYS) in other scenarios, therefore BCVTB has been recommended.

2.2 Thermal Analogy and Modelling of Electric Devices

2.2.1 Thermal Analogy of the Electric Motor

As the Electric Motor (EM) in the cooling circuit is considered as a heat dissipative body rather than an electric device, a thermal analogized submodel based on the rate of heat production inside the EM and the heat transfer to the ambience (by convection and radiation) will be introduced supported by the conceptual simple construction of an EM.

2.2.1.1 Motor Specifications

The motor used in the electric vehicle is UQM PowerPhase Select 50.

iv

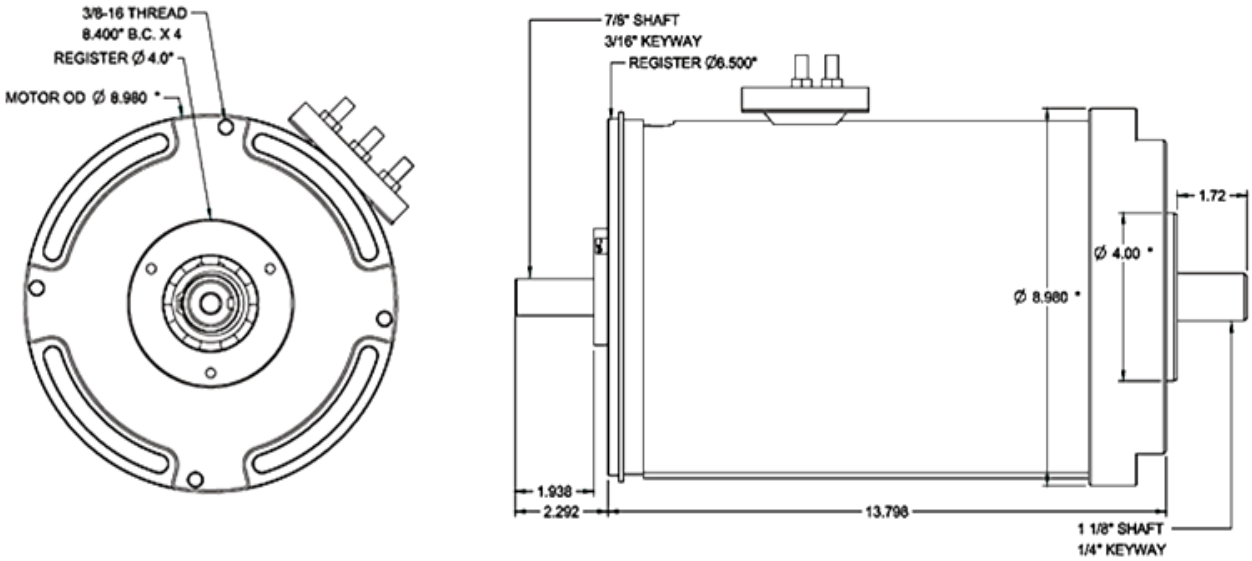

Figure 2: UQM Motor PowerPhase Select 50

Considering Figure 2 and UQM PowerPhase Select 50 spec. sheet, the EM has the following specifications and dimensions in mm:

- Power: 50 kW peak, 30 kW continuous motor/generator power
- Total mass: 50 kg
- Diameter: 305 mm, Length: 381 mm
- Rotational speed: $13 \times 10^3 \frac{1}{\text{min}}$
- Material: 0.5 % silicon low carbon steel
- Average specific heat capacity: 837 $\frac{\text{J}}{(\text{kg.K})}$

2.2.1.2 Power Loss Approach (Absolute Power Difference)

Usually, when a machine transforms energy from a form to another, there are going to be losses. Assuming a steady-state transformation in our case, heat is the energy loss inside the EM. (see Figure 3)

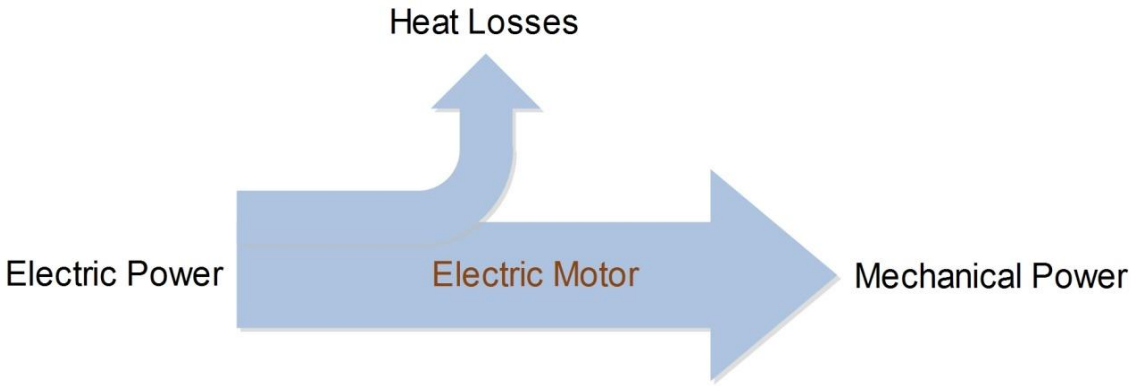

Figure 3: Sankey Diagram for Energy Flow inside the EM

In real life, the heat generated, input and output powers of the EM will so much depend on the driving style. The thermal analogy of the electric components as well as modelling and simulation of the thermal management system are set-up to run on the New European Driving Cycle (NEDC) as a standardized driving cycle.

In an 11 km cycle, the velocity profile indicates the power consumption and hence the thermal performance of the thermal management system in two different driving behaviours inside the FCEV. The first one includes four repeated UDCs and represents an urban drive style, characterized by low speeds and low loads. The second part, called EUDC and represents an extra-urban drive style, corresponds to a more aggressive driving style. (see Figure 4)

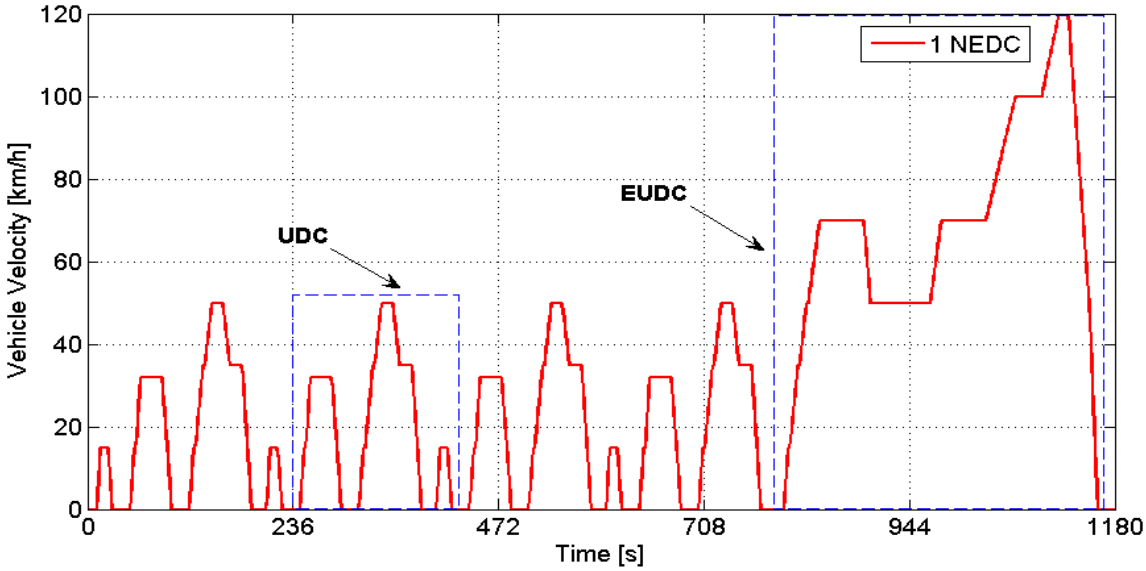

Figure 4: Velocity Profile of One New European Driving Cycle (NEDC)

In the approach above, both the electric and mechanical powers (input and output powers) for the EM in DLR test vehicle HT-BZ-REX were logged for 3 New European Driving Cycles (NEDC). In DC motors, the absolute value of the difference between the electric and mechanical powers ($\mathrm{abs}(P_{elec.} - P_{mech.})$) represents the power lost for the heat generation which will then be fed to the LT cooling circuit. (see Figure 5)

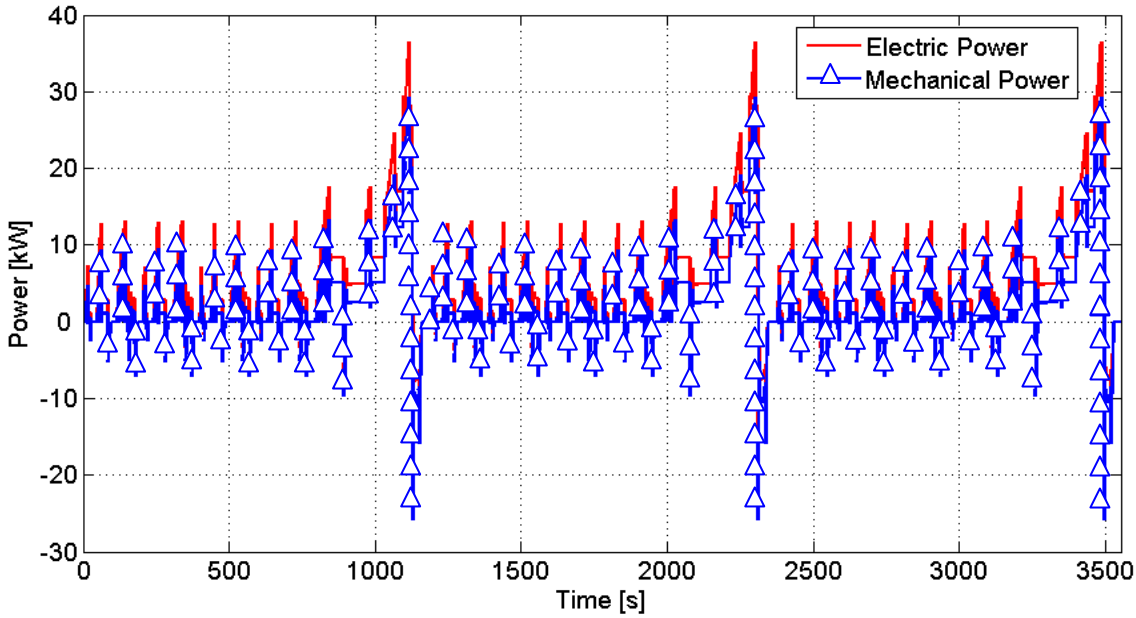

Figure 5: Recorded Electric and Mechanical Powers of the EM through Dyno Roller Testbench (Test Date: 03.09.2013)

For faster simulation, this approach has been chosen between another one that calculates copper, hysteresis energy losses and the eddy current losses as main heat generation sources inside the EM. Using the logged data for coil resistance, magnetic flux density, frequency and current, the three different types of losses are calculated each second. This approach is going to be described in appendix A (page 76). In Figure 5, the operation of the EM is subjected to 3 different conventions. This justifies the existence of negative values for both the electric and mechanical powers while operation depending on the driving conditions and style. (see Table 1)

Table 1: Different Conventions for the EM Operational Conditions

Electrical power	Mechanical power	Condition
Positive	Positive	Motoring
Negative	Negative	Generating
Positive	Negative	Braking

As shown in Figure 5, the time domain has been set to 3 NEDCs (3x1180 s) to have enough observation for the EM performance. Further on, the simulation stop time for each submodel and for the thermal management system will always be 3540 s.

The EM main thermal modelling idea was to cool it down by forced heat convective transfer to the coolant in a cooling jacket surrounding the core. (see Figure 6)

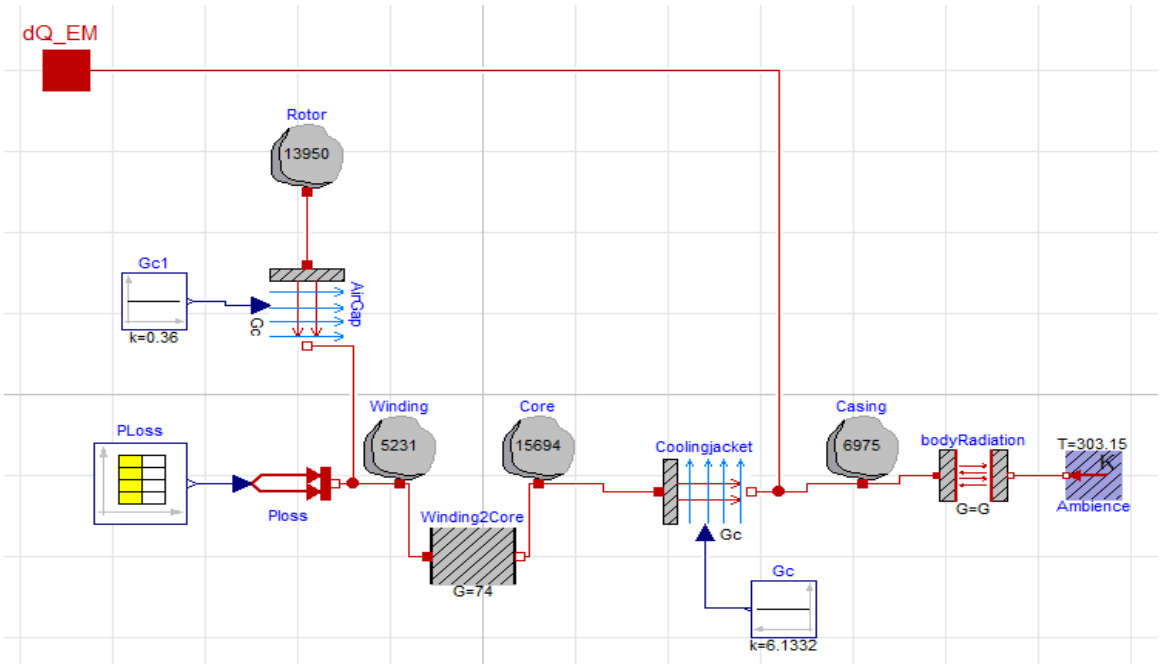

Figure 6: EM Excluded Thermal Submodel

The heat transfers from winding to rotor through air gap by heat convection and to the core by heat conduction. The heat transfer to the ambience would be through radiation from the casing. Because the absolute inlet velocity of coolant to the jacket, jacket's dimensions, flow Reynolds (Re) and Prandtl (Pr) numbers inside the jacket were unknown, this cooling approach has been excluded. Also, because of difficulty in determining the exact weight ratio between the EM construction parts as well as the air gap area, the EM has been then denoted by a single heat capacitor (as shown in Figure 7), where the thermal capacity is calculated using the EM specifications and the equation:

$$C = c_p \cdot m$$

$$C \text{ is the thermal capacity } \left[\frac{\mathrm{J}}{\mathrm{K}}\right], c_p \text{ is the specific heat capacity } \left[\frac{\mathrm{J}}{\mathrm{kg.K}}\right] \quad (1)$$

$$m \text{ is the mass } [\mathrm{kg}]$$

Since the total thermal capacity of the EM will always be the same ;disregarding whether it is modelled as a single heat capacitor or distributed among four heat capacitors, the following thermal submodel should be valid for the analogy. And since there are no means of internal heat transfer between EM's construction parts, there is no subjection to various heat transfer efficiencies that leads; eventually, to a reduction in the heat generated from the EM. In other words, the following thermal submodel expresses a tough heat generation for the LT cooling circuit to sustain.

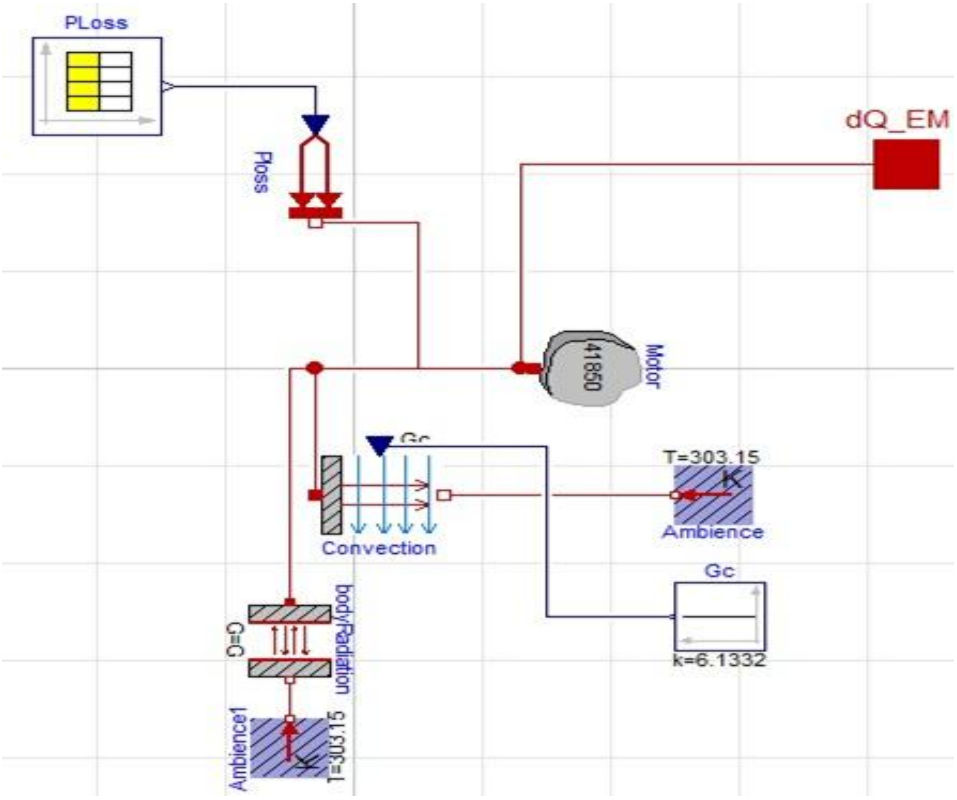

Figure 7: EM Final Thermal Submodel

The difference between the electric and mechanical powers (power loss) is fed to the above model; each <u>second</u> during the simulation, through a prescribed heat flow. (see Figure 8)

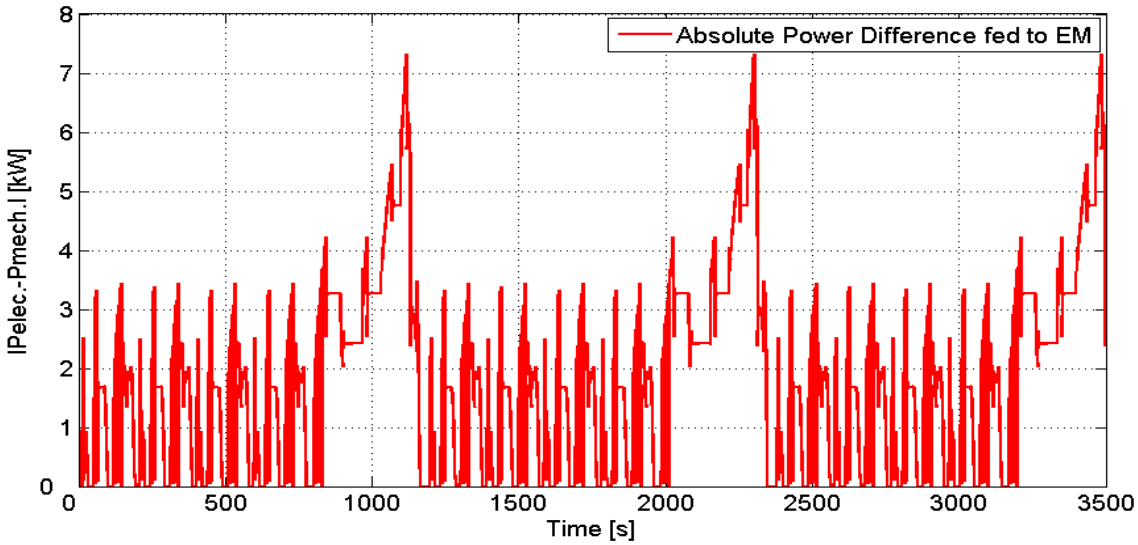

Figure 8: Absolute Power Difference fed to the EM Thermal Submodel

The ambient temperature in this model and all the following models has been set to 30 °C which represents the average air temperature in July 2010 (hottest month in the year) in Germany according to Germany's National Meteorological Service (DWD).[v]

In the above thermal submodel, the thermal heat transfer from the EM will only be to the ambience through free convection by air and radiation.

For a linear free heat convection, the value of the thermal power is calculated as follows:

$$\frac{dQ}{dt} = G_c . \Delta T(t)$$
$$where\ G_c = A \cdot h \tag{2}$$

Q is the thermal energy [J]

$\Delta T(t)$ is the time − dependent thermal gradient between EM and the ambience [K]

A is the motor surface area (heat transfer area) [m^2]

h is the convective heat transfer coefficient $\left[\frac{\mathrm{W}}{\mathrm{m}^2 . \mathrm{K}}\right]$

For air-cooled machines, the amount of h has been empirically approximated to the value of 12 $\left[\frac{W}{m^2 . K}\right]$.[vi]

To calculate the surface area of the EM, the dimensions in page 5 have been used. Since the EM has a cylindrical shape, the heat transfer area consists of the area of both ends plus the side area as follows:

$$A = \left[2 \cdot \left(\frac{\pi}{4} d^2\right)\right] + \pi d l = 0.51111\ m^2 \tag{3}$$

Now to calculate the thermal power by heat radiation, the following equation has been used:

$$Q = G_r \cdot \sigma \cdot (T_1^4 - T_2^4)$$
$$where\ G_r = \epsilon \cdot A \tag{4}$$

Q is the thermal power [W]

σ is Stephan Boltzman constant $= 5.67\mathrm{e}^{-8}\ \left[\frac{\mathrm{W}}{\mathrm{m}^2 . \mathrm{K}^4}\right]$

T_1 and T_2 are Body and ambient temperatures [K]

A is the motor surface area (heat transfer area) [m^2]

ϵ is the thermal emissivity

The thermal emissivity of the EM has been chosen according to the EM's construction material, where ϵ equals to 0.04.

As the thermal submodel simulates, the EM's temperature continues to rise. The curve shown in Figure 9 demonstrates the temperature rise inside the EM's body and Figure 10 shows the net value of heat generation after heat dissipation to atmosphere by means of free convection and radiation.

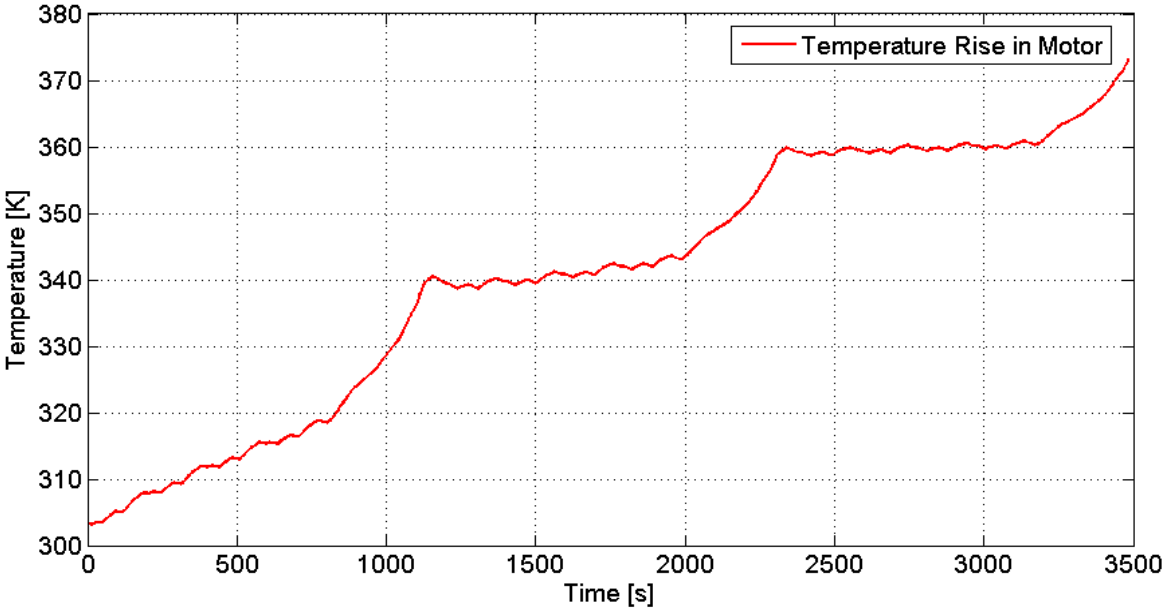

Figure 9: Temperature Rise inside the EM

The illustrated curves in both figures taking into account only the cooling effect of the ambient air and <u>not</u> yet the effect of cooling this thermal submodel by the LT cooling circuit which will be later discussed in details.

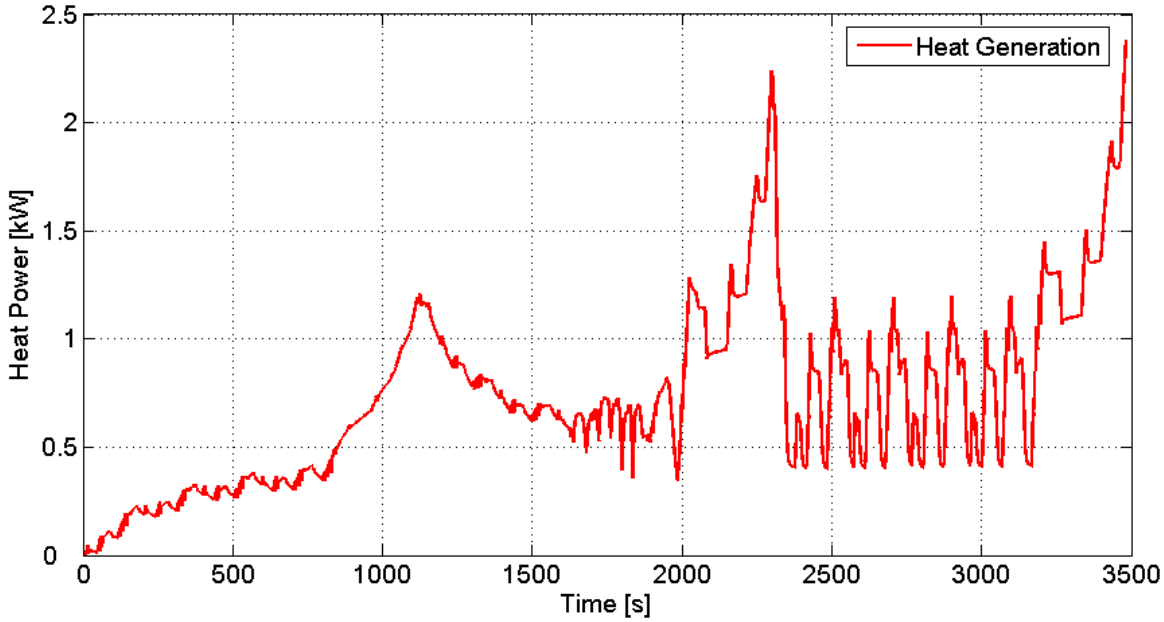

Figure 10: Heat Generated out of the EM Thermal Submodel

The figure above illustrates the final heat generated out of the EM thermal submodel which is measured at the heat port (dQ_EM) and transferred to the LT cooling circuit as will be discussed later on.

2.2.2 Thermal Analogy of Power Electronics Module

The Power Electronics Module (PEM) is a set of solid-state electronics which are accountable for rectifying, inverting and converting the electric power to and from the EM.

At an output power of 100 kW, e.g., 3 kW of losses arise even with 97 % conversion efficiency. These losses concentrate on chip areas getting smaller and smaller that leads to extremely high heat flux densities. Therefore, highly effective cooling is indispensable[vii].

2.2.2.1 Power Electronics Module Specifications

The module used in the electric vehicle is for UQM PowerPhase Select 50 motor.

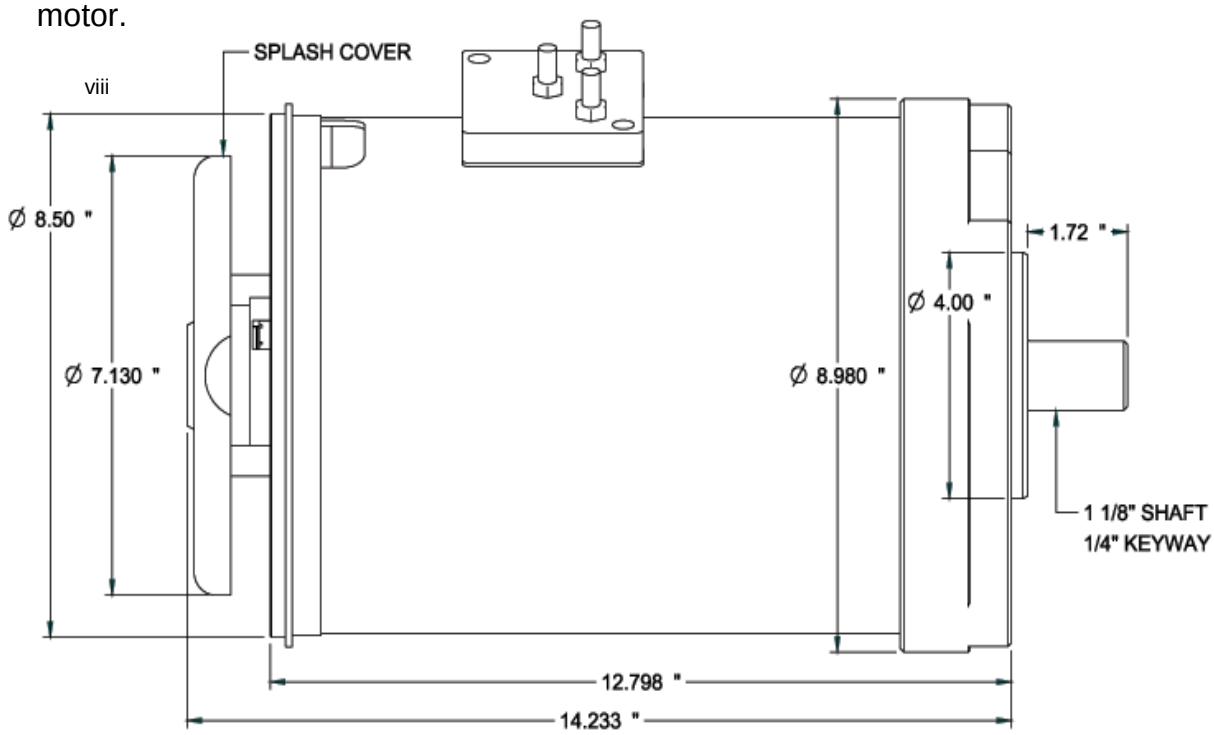

Figure 11: Side View for the PEM in UQM PowerPhase Select 50

Considering Figure 11 and UQM PowerPhase Select 50 spec. sheet, the power electronics module has the following specifications and dimensions in mm:

- Total weight: 10 kg
- Length: 186 mm, Width: 313 mm and Height: 760 mm
- Casing material: Copper
- Average specific heat capacity: 837 $\frac{J}{(kg.K)}$

2.2.2.2 Power Loss (Heat Generation) Approach

Similar to the EM, the data logged for the power loss inside the Power Electronics Module (PEM) in DLR test vehicle HT-BZ-REX was logged for 3 NEDCs. This data will be fed to the PEM thermal submodel as input data of the heat flow in kilowatts. (see Figure 12)

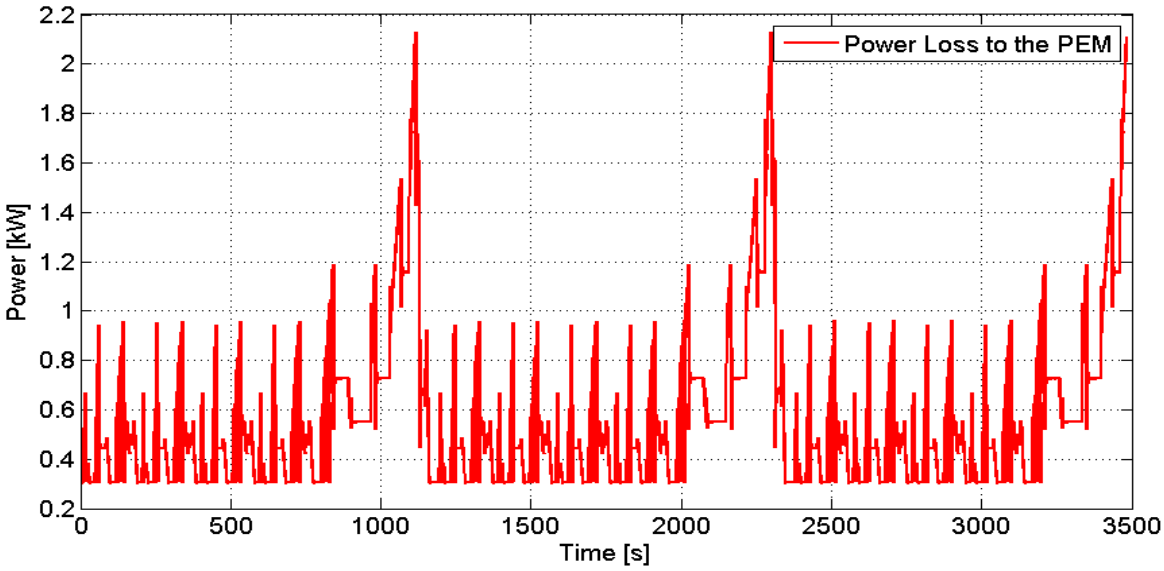

Figure 12: Power Loss Values fed to the PEM Thermal Submodel (Recorded through Dyno Roller Testbench (Test Date: 03.09.2013))

The first modelling approach of the PEM was similar to the EM. The cooling would be done by forced heat convective transfer to the coolant in a cooling bed surrounding the casing and that the heat transfer to the ambience will be through heat radiation. (see Figure 13)

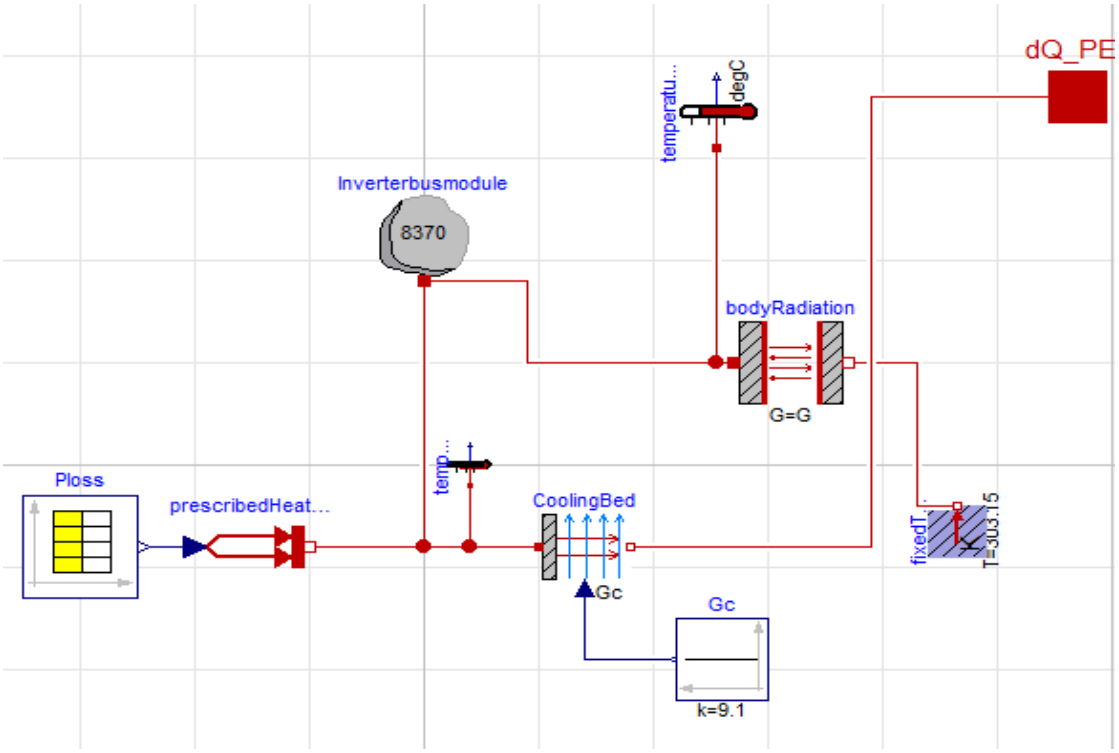

Figure 13: PEM Excluded Thermal Submodel

Also because the absolute inlet velocity of the coolant to the cooling bed, bed's volume, flow Reynolds (R_e) and Prandtl (P_r) numbers were unknown, this cooling approach has been excluded.

The modelling idea in the thermal submodel below depends on cooling the PEM through free heat convection and radiation heat transfer to the ambience.

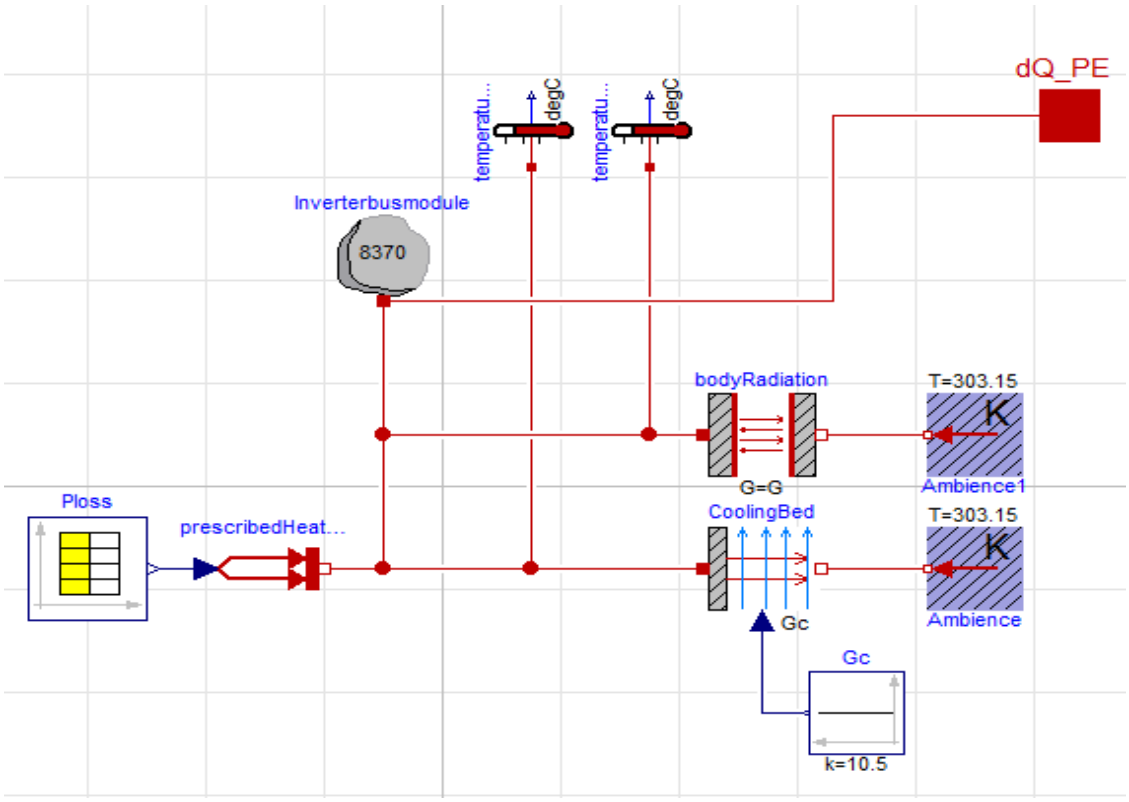

Figure 14: PEM Final Thermal Submodel

In Figure 14, the heat capacity has been calculated using the PEM specifications and equation (1). The heat transferred by free convection and radiation has been calculated using equation (2) and equation (4) respectively.

Since the PEM casing is actually a cuboid with 3 repeated different faces, the total surface area has been calculated as follows:

$$\begin{aligned} A &= (2 \cdot Area\ of\ Face1) + (2 \cdot Area\ of\ Face2) + (2 \cdot Area\ of\ Face3) \\ &= (2 \cdot 0.1860.313) + (2 \cdot 0.186 \cdot 0.760) + (2 \cdot 0.760 \cdot 0.313) \\ &= 0.875\ m^2 \end{aligned} \tag{5}$$

As the thermal submodel simulates, the temperature of the PEM continues to rise. The temperature curve shown in Figure 15 demonstrates the temperature rise inside the PEM's body and Figure 16 shows the net value of heat generation after heat dissipation to atmosphere by means of free convection and radiation.

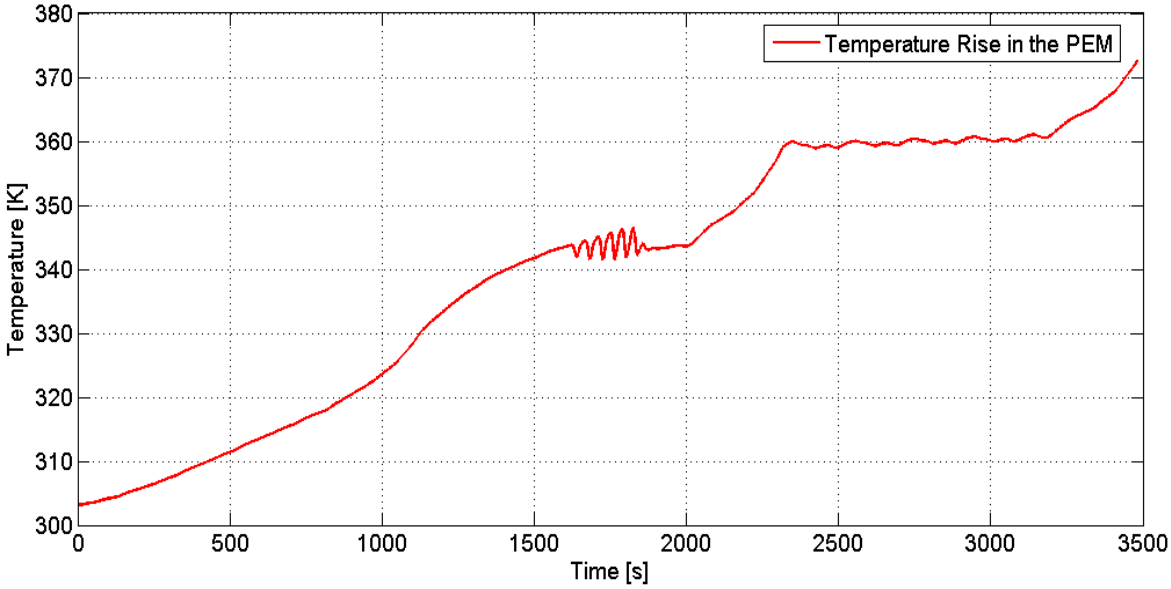

Figure 15: Temperature Rise inside the PEM

The illustrated curves in both figures taking into account only the cooling effect of the ambient air and <u>not</u> yet the effect of cooling this thermal submodel by the LT cooling circuit which will be later discussed in details.

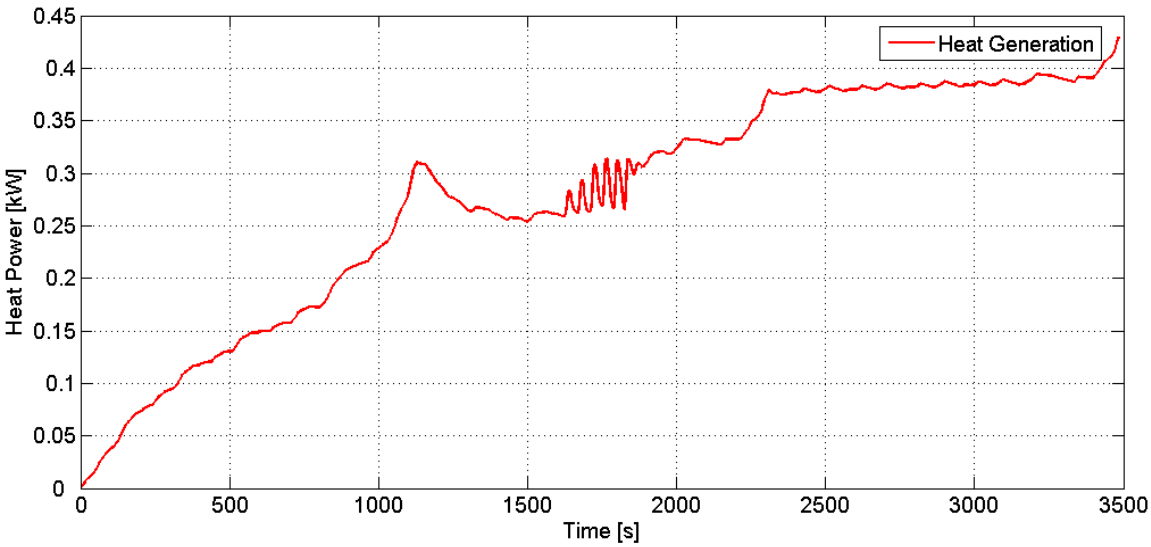

Figure 16: Heat Generated out of the PEM Submodel

The figure above illustrates the final heat generated out of the PEM thermal submodel which is measured at the heat port (dQ_PE) and transferred to the LT cooling circuit as will be discussed later on.

2.3 Thermal Management System in the Electrical Vehicle

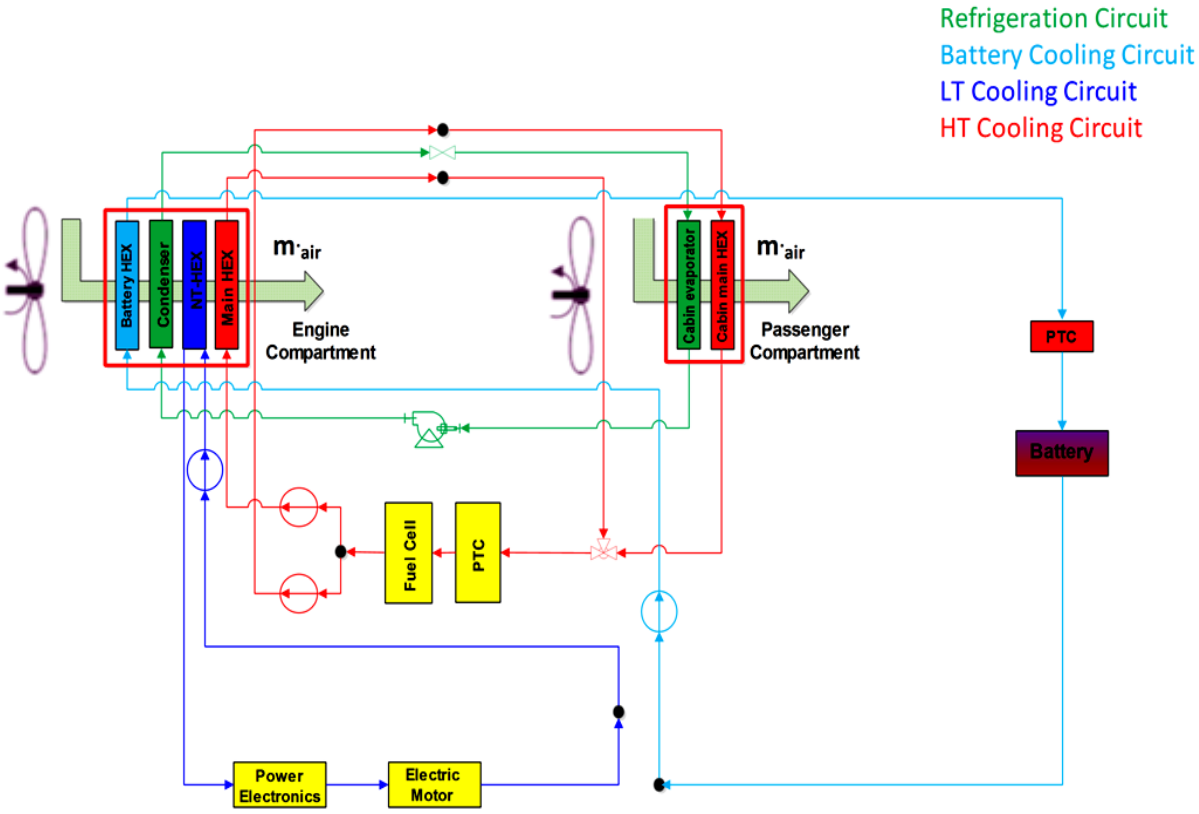

Figure 17: Cooling and Air Conditioning Circuits' Proposed Layout

Figure 17 demonstrates a basic simplified combination of cooling and air conditioning circuits in an EV, using DLR test vehicle HT-BZ-REX as an example for a FCEV.

The thermal management system described above consists of Battery, High, Low temperature cooling circuits and an air conditioning cycle.

The HEXs on the left are contained inside the volume of the engine compartment, while the HEXs on the right are located inside the passengers compartment for air conditioning purposes (summer cooling and winter heating).

The air mass flow rate that flows on (couples) the HEXs' arrangement in the engine compartment is controlled and regulated according to the operating temperatures of the EM and the fuel cell stack as being the top heat generators in the thermal management system.

The HEXs' arrangement proposed in the engine compartment, accounts for the graduation of the operating temperature of each component inside each cooling circuit. As air is the cooling medium inside the engine compartment; where all the HEXs lie, a sufficient temperature difference between the air and the HEX should be maintained at each HEX for sufficient heat transfer.

This means, that the Battery HEX has the lowest radiated heat (according to the logged data of the test vehicle) and the amount of heat radiated from each HEX increases in the direction of the air flow ;gradually, till it reaches the FC stack's HEX. The temperature of the air volumetric flow leaving the Battery HEX per time will then be lower than the temperature of the condenser HEX. Thus, a cooling effect for the air is maintained. This explanation could be also applied on the rest of HEXs in the engine compartment.

Based on the simulation results, other substitutive arrangements will also be suggested in this paper, considering sufficient cooling for the electric devices inside the cooling circuits.

The air volume flow rate flowing on the HEXs' arrangement in the passenger compartment is controlled by the user as in any ordinary air conditioning system inside a passenger car.

In this project, the HEXs' arrangement proposed in the passenger compartment is not of a significant purpose. Since the HEXs will; presumptively, operate alternatively; in summer and winter, to satisfy a thermal comfort inside the cabin, their positions; in different approaches, could be easily altered.

However; in reality, the evaporator of the A/C cycle would operate simultaneously with the heater for air humidification and thermal comfort during cold weather conditions. Therefore, its position should always precedes the heater's location.

Furthermore, each cycle will be separately explained how it is designed, modeled, controlled and simulated in Dymola and BCVTB interfaces in the following sections.

2.3.1 Low Temperature Cooling Circuit (LT Cooling Circuit)

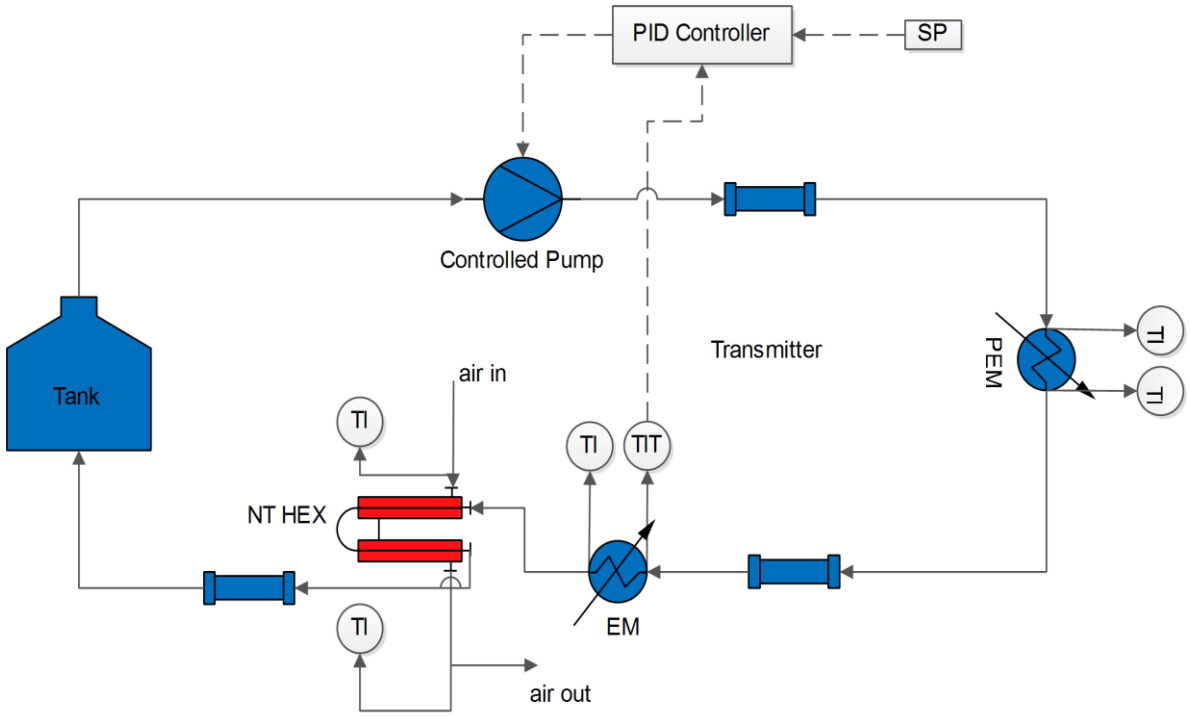

Figure 18: Low Temperature Cooling Circuit P&ID

Now after the thermal analogy for the EM and PEM is done, the second step is to establish the cooling circuit which contains both of them.

In Figure 18, the LT cooling circuit is designed to serve cooling down both the EM and the PEM inside the FCEV. The circuit consists mainly of a tank (coolant source), pump (flow source), hydraulic pipes, hydraulic pipes with heat transfer and a double-pipe HEX. Since EM and the PEM are heat inputs to the circuit, they have been denoted by heat sources in the above P&ID.

The setting temperature for cooling the EM is 70 °C and is used as an input parameter to the proportional-integral-derivative (PID) controller. The temperature of the coolant entering the EM is measured and sent to the PID controller to control the mass flow rate of the cooling pump. The same signal will be also sent to another PID controller to control the air mass flow rate over the HEXs' arrangement in the engine compartment.

The heat generated by the PEM is very low compared with the EM. Therefore; for simplification, the temperatures at the PEM are only measured for observation but not for the feedback control of the cooling pump.

At safe working temperatures, the coolant will be circulated with a small flow rate as a product of a low coolant pump rotation speed.

The NT HEX is to cool down the coolant inside the circuit by air. Therefore, one of its 2 paths is filled with coolant and the other is filled with air from the cooling fan positioned inside the engine compartment in front of the HEXs' arrangement.

The air mass flow rate that flows in the HEX above is the same which flows over all the HEXs' arrangement in the engine compartment as they are coupled from the air side inside the engine compartment. (see Figure 17)

Since the air flow over the HEXs' arrangement in the engine compartment starts at the Battery HEX in the Battery cooling circuit, it will later be illustrated and explained when discussing the layout of the Battery cooling circuit in section 2.3.2.

As mentioned before, the air mass flow rate is controlled in accordance to the temperatures of the EM and the fuel cell stack (FC) being the top heat generators in the thermal management system. The control strategy will be clearly discussed through the layout of the circuit's control module in the following sections.

In translation to Figure 18, the following Dymola model signifies a basic and simplified example that describes the main structure for a LT cooling circuit in an EV.

The cooling circuit will basically consist of a tank (coolant source), prescribed flow (acts as a pump), dynamic pipes, dynamic pipes with heat transfer (heat sources), temperature sensors, system block (defines the ambient conditions), control bus and a HEX. (see Figure 19).

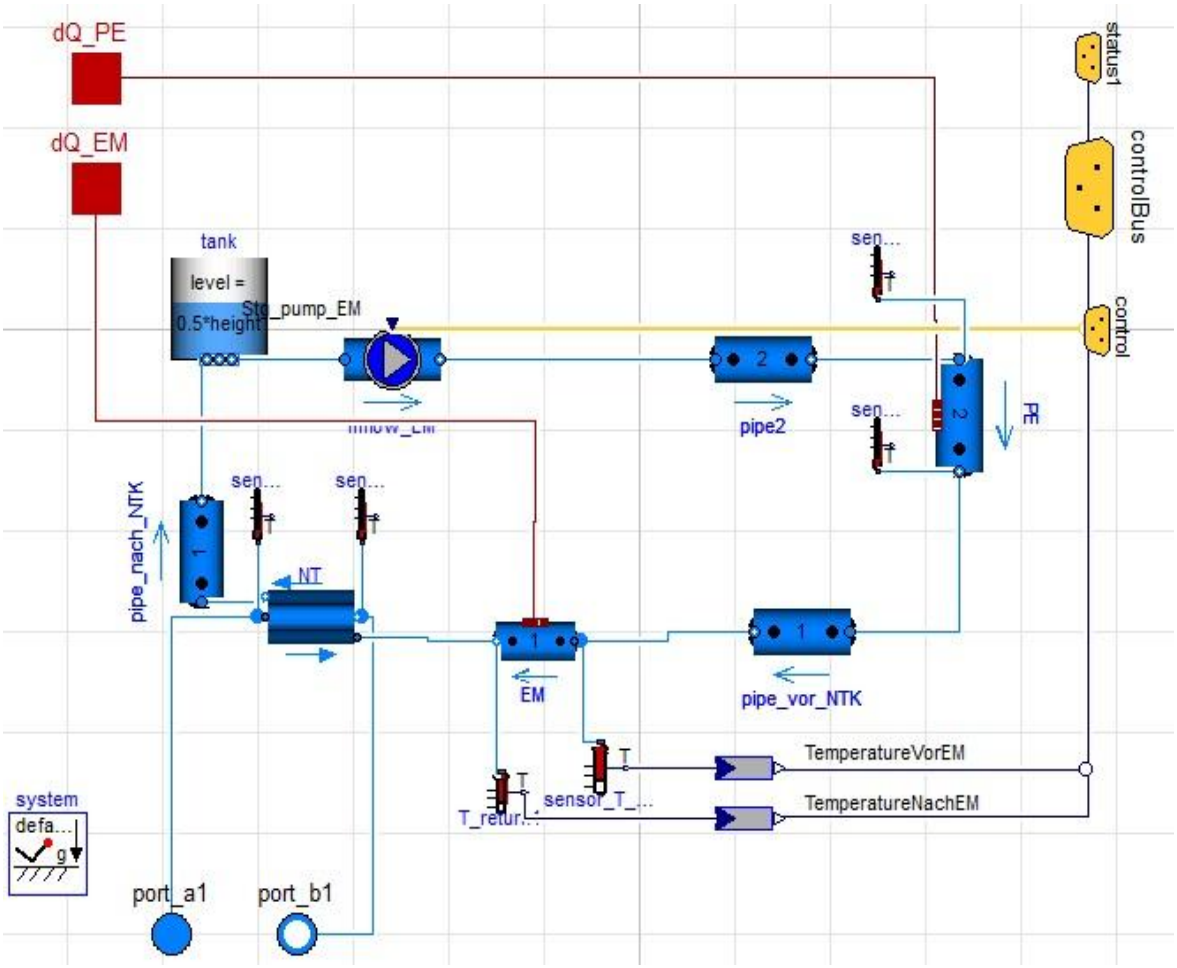

Figure 19: LT Cooling Circuit Model

The aim of developing this model and the following subsequent models is to study the sustainability of heat load and effectiveness of cooling on a substantial level.

It might not signify the exact structure of a real cooling circuit, but it basically contains the main components for the cooling operation. On the modelling basis, this model and the following models represent a good elementary approach for engineers in DLR to develop a sophisticated and plausible models that simulate an actual thermal management system in details.

2.3.1.1 Fluid Properties

In Figure 19, the coolant is pumped to the system by the prescribed flow block which is controlled by the control module that will be described later in details.

The coolant is then directed to straight dynamic hydraulic pipes with distributed mass, energy and momentum balances. Two of these pipes are provided with heat transfer which comprise the heat load of the EM and PEM to the circuit. The coolant is then directed to a double-pipe HEX with a counter flow. One of those pipes contains the liquid coolant (1,2-Propylene glycol, 47 % mixture with water); designated by (Medium_inner) and having the following properties:

Table 2: Coolant Properties in the LT Circuit

Properties	Value
Boiling Point (°C)	105-107 at 1 bar
Freezing Point (°C)	-29 at 1 bar
Corrosion Rate (mm/year)	0.25 mm/year for Steel 0.004 mm/year for Copper
Specific Heat [kJ/(kg.K)]	3.875 at 30 °C
Density (kg/m^3)	1024 at 30 °C
Thermal Conductivity (W/m.K)	0.4529 at 30 °C
Dynamic Viscosity (mPa.s)	2.5886 at 30 °C[ix]

This coolant is commercially wide-spread as an anti-freezing noncorrosive organic solution. It is also; like most glycols, has very low volatility and very low toxicity.

In the other pipe of the HEX flows Moist Air (240 ... 400 K) designated by (Medium_outer). The air side in the HEX will be then connected with the Condenser in the A/C cycle from a side and with the Main HEX in the HT cooling circuit from the other side; inside the engine compartment, to apply the coupling between models. This air package has been chosen to account for moist air-cooling under near atmospheric pressures. It also covers the possibility of moist presence inside the HEX in foggy days. Plus its wide operational temperature range (from 240 to 400 K) and its properties' validity, even with the presence of excess water in the cooling air.

2.3.1.2 Defining Ambient Conditions

Defining the ambient conditions is something that should be done from the beginning.

Due to common interfaces and base classes, most of the models contain similar configuration parameters.

It would be boring to open all individual configuration dialogs in order to change the same setting in all models. This is why Modelica.Fluid defines a System object providing global defaults for all components in the LT model. (see .Figure 20)

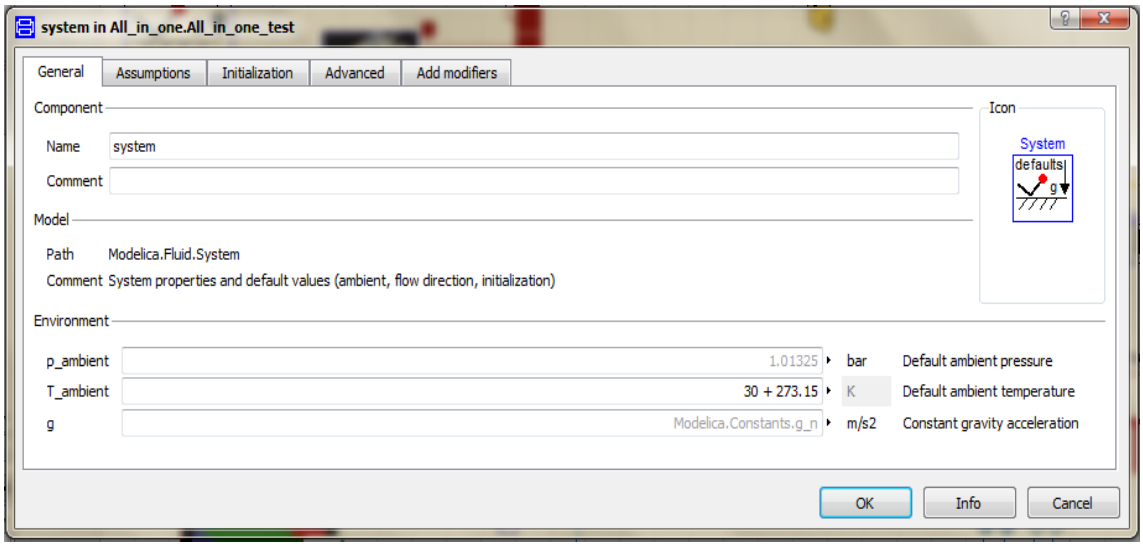

Figure 20: General Parameters of the System

If a parameter is changed inside the system block, the selection will be propagated to all model's components.

In the figure above, the ambient temperature for the whole circuit components has been also set to 30 °C just like for the EM and the PEM thermal submodels. (see page 9)

The default values for the ambient pressure and the gravity are 1.01325 bar and 9.8 m/s^2, respectively.

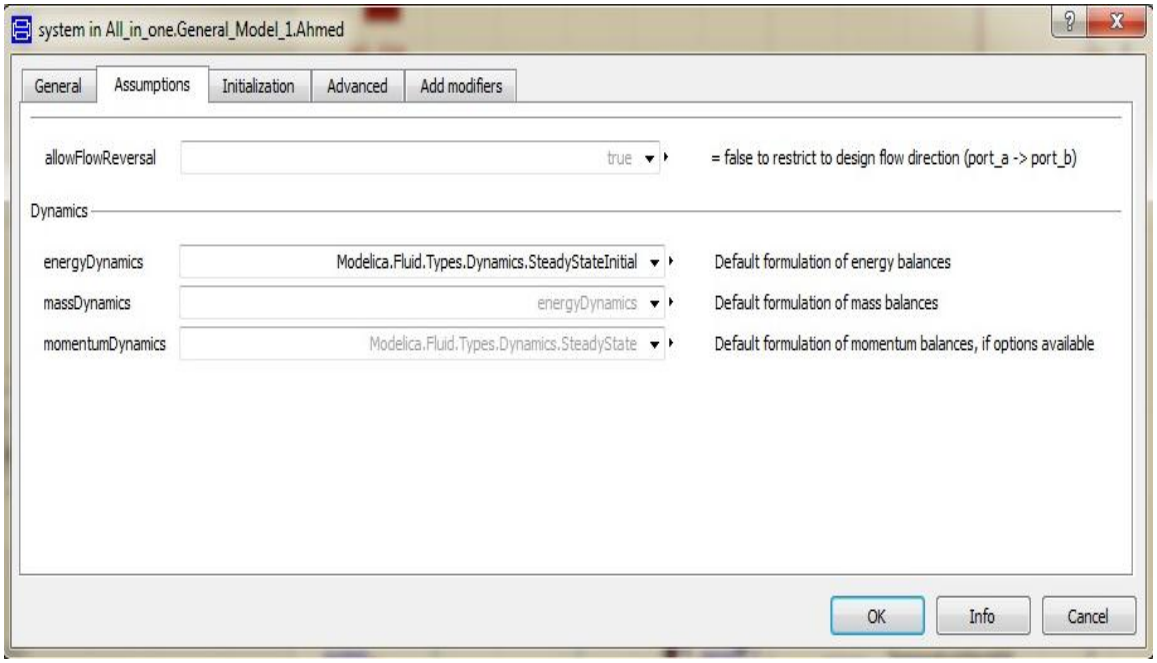

Figure 21: System Assumptions

A typical fluid model would have dynamic energy and mass balances together with steady-state momentum balances.

In Figure 21, the enumeration chosen to define the formulation of energy balances in the LT model was set to "SteadyStateInitial".

Because the thermal phenomena in the whole model is mainly of an interest, a <u>zero</u> change in temperature or enthalpy (der(T), der(h)) of a one-substance fluid will be used as initial condition to solve the Differential Algebraic Equation (DAE) of the energy balance which calculates the heat flow along all model components.

$$\underbrace{\frac{\partial(\rho u A)}{\partial t}}_{\text{Energy change}} = \underbrace{-\frac{\partial\left(\rho\vartheta\left(u+\frac{p}{\rho}\right)A\right)}{\partial x}}_{\text{Enthalpy change}} + \underbrace{\vartheta A\frac{\partial p}{\partial x} + \vartheta F_F}_{\text{Work change}} + \underbrace{\frac{\partial}{\partial x}\left(kA\frac{\partial T}{\partial x}\right) + \dot{Q}_e}_{\text{Heat change}} \qquad (6)$$

This maintains a lossless heat transfer along each pipe's flow model, such that the temperature measured at the input port will be as same as the temperature measured at the output port of the same pipe.

In Figure 22, the initialization guess value for the coolant mass flow rate inside the LT circuit has been set to 0.0001 kg/s. This value has been chosen as the minimal and to be smaller than the minimum value in the operation range of the pump's mass flow rate inside the LT circuit (0.01-0.5 kg/s).

This operational range has been chosen according to empirical values for the mass flow rate used for cooling down water-cooled EMs with 50 kW output power.

This initial guess value is needed for the iterative solution for the mathematical model that the LT circuit represents during the simulation.

At safe operational temperatures for the EM and the PEM, the flow will circulate with the minimum value in the operational range of the cooling pump which is 0.01 kg/s.

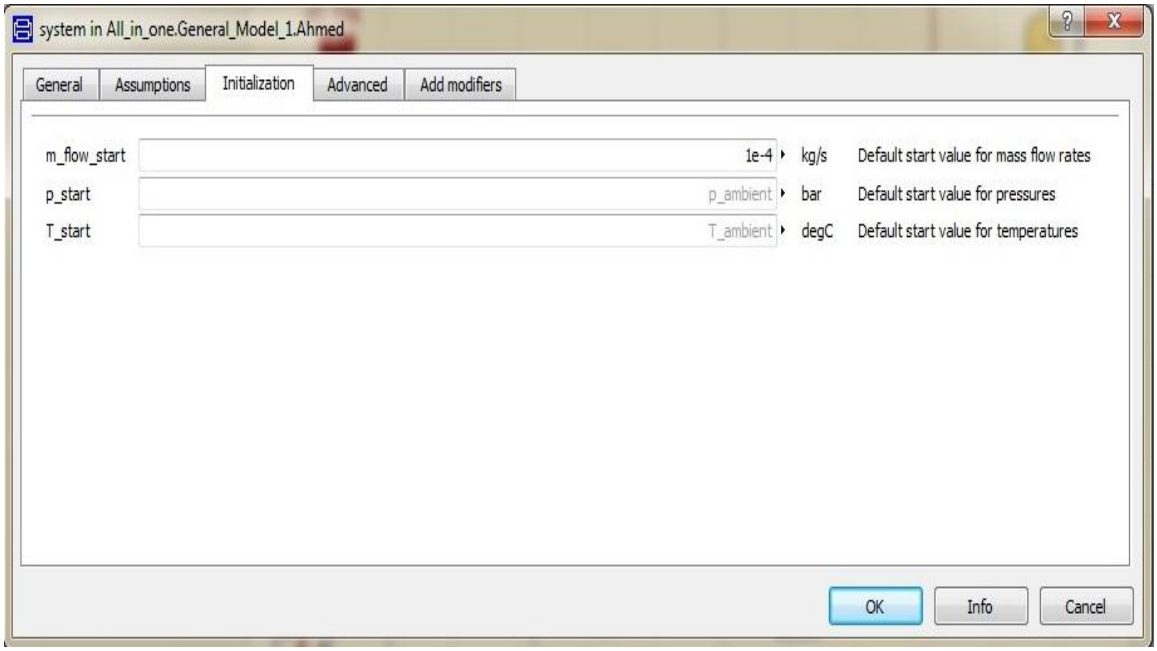

Figure 22: System Initialization Parameters

2.3.1.3 The Tank

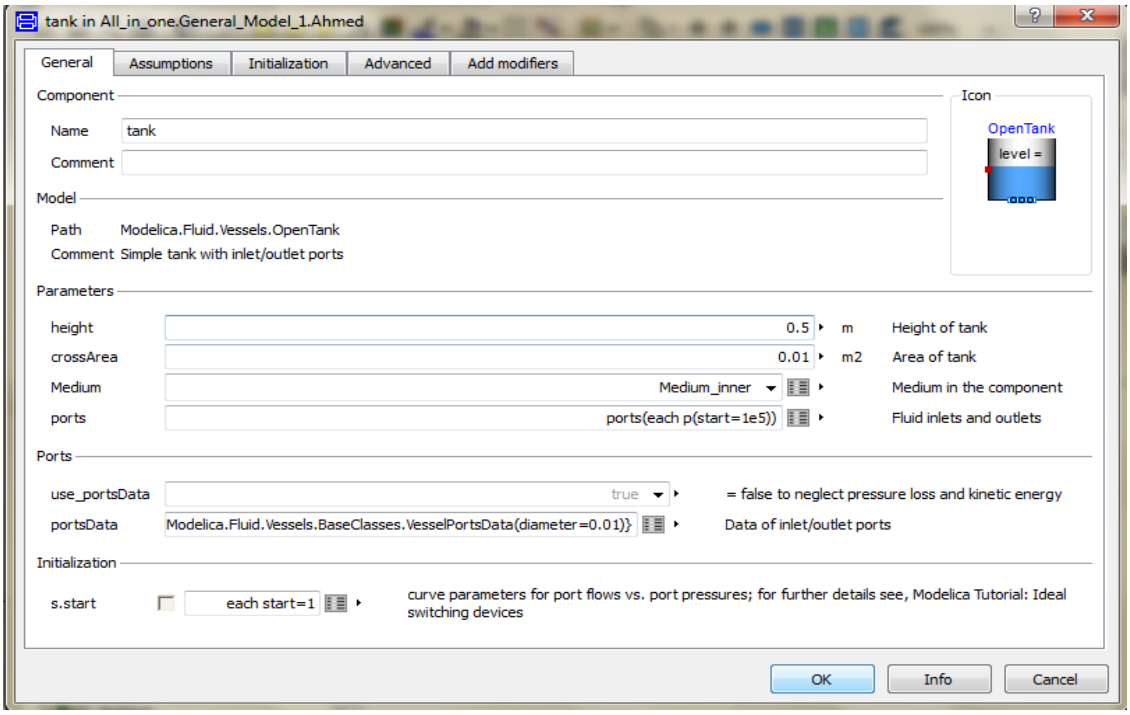

Figure 23: Tank General Parameters

As mentioned before, the open tank is only considered as a coolant source which doesn't characterize the actual tank tokens.

While choosing the tank, the most important factor was to calculate the volume which is a multiplication product of both tank's area and height. Both parameters are so much dependants on the available volume in the engine compartment. Thus, they could be simply changed keeping the volume available for the coolant constant as calculated below. (see Figure 23)

By default and for initialization, the coolant's level equals to 0.5 of the tank's height. This means; at constant area, that the tank's volume should be double the coolant's volume required for the circuit.

As will be discussed later, the total length of coolant pipes in the LT circuit model; including the coolant path length inside the HEX is 7 m with a diameter equals to 0.015 m. According to empirical values from water-cooled EMs with 50 kW output power, the maximum operational mass flow rate to cool down the EM is 0.5 kg/s. Applying the mass flow rate equation:

$$\dot{Q} = \rho \left[\frac{kg}{m^3}\right] \cdot A[m^2] \cdot v \left[\frac{m}{s}\right], \qquad 0.5 = 1024 \cdot \frac{\pi}{4}(0.015)^2 \cdot v, \qquad (7)$$
$$v \approx 2.8 \frac{m}{s} = \frac{x}{t}$$

The flow rate with 0.5 kg/s consumes 2.6 seconds with the velocity 2.8 m/s to circulate one cycle through the LT circuit from the output port of the tank back to the input.

This means, that the pump pumps around 1.3 kg of coolant (0.00127 m^3) to accomplish one cycle through the circuit. To compensate for coolant's vaporization, the coolant's volume inside the tank should be double of this value (≈0.0025 m^3). Hence, the tank's volume will be 0.005 m^3, which is the multiplication product of the tank's height and cross sectional area in Figure 23.

2.3.1.4 Prescribed Flow

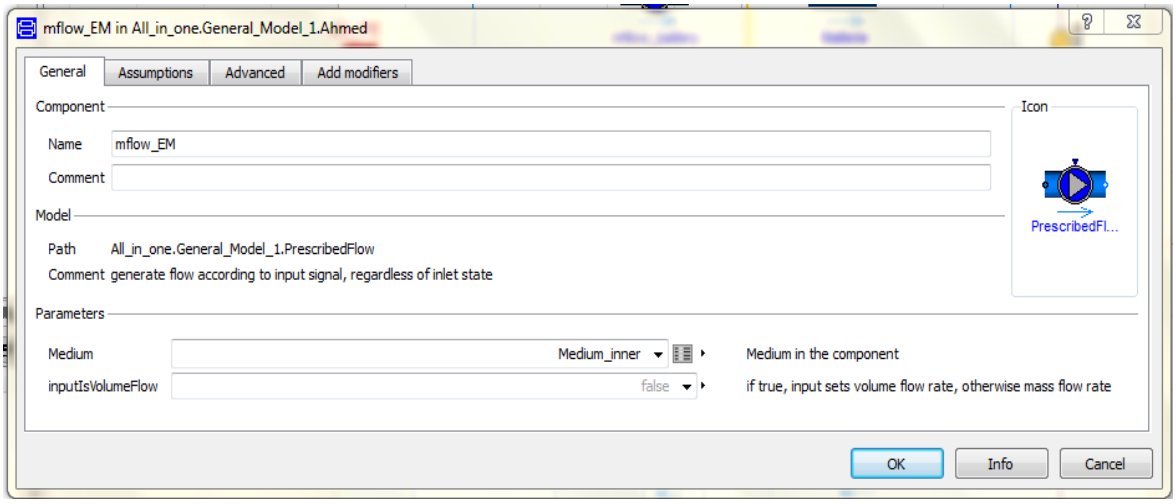

Figure 24: Prescribed Flow Properties

As seen in Figure 24, only the medium inside the prescribed flow has been designated to the coolant inside the circuit and that the flow rate will be controlled by the control module; as will be illustrated later when discussing the control, according to the EM's setting temperature (T_{set}).

As mentioned before, according to the empirical values from DLR test vehicle, the operational range of the pump's mass flow rate inside the LT model is (0.01-0.5 kg/s).

2.3.1.5 The Piping System in the LT Cooling Circuit

The pipes inside the LT model are dynamic pipe models with storage of mass and energy. Each pipe represents a model of a straight pipe with distributed mass, energy and momentum balances. It provides the complete balance equations for one-dimensional fluid flow. (see Figure 25)

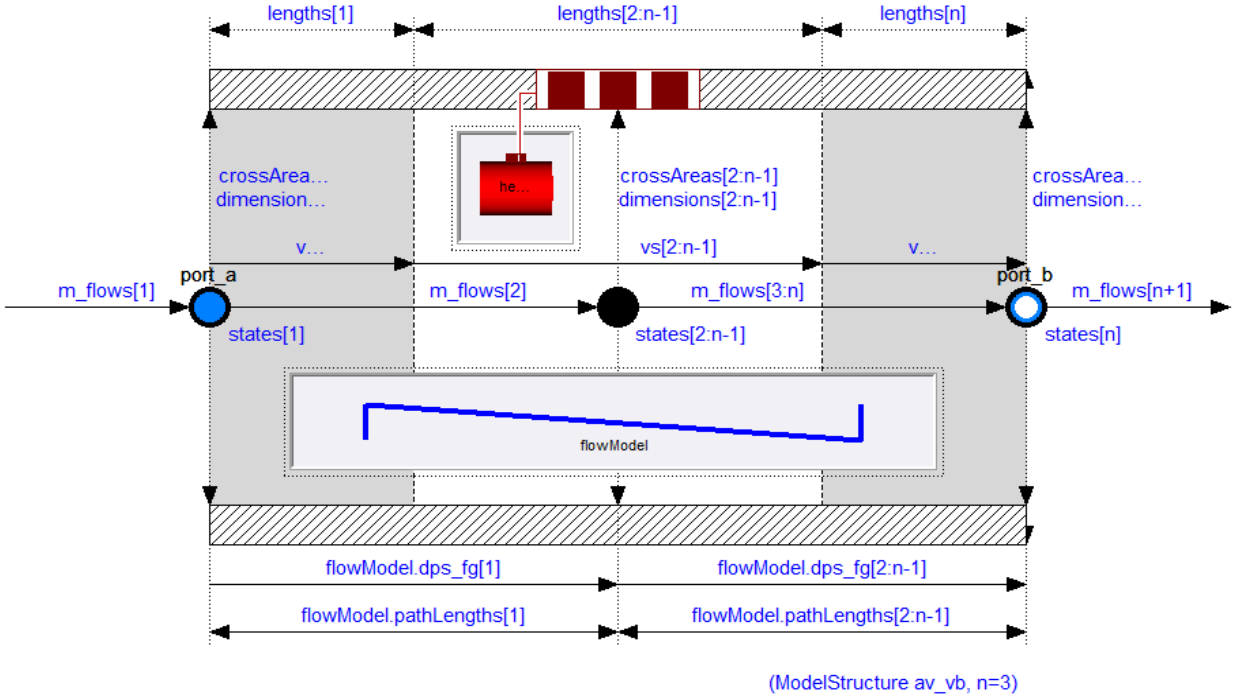

Figure 25: Dynamic Pipe Model with Model Structure (av_vb) & nNodes = 3

In DLR HT-BZ-REX test vehicle, the pipes used in the cooling system have DN 15 standard with an approximated inner diameter of 15 mm.

The total length of the pipes in the LT circuit <u>might not</u> signify the actual length of the water path in the test vehicle. However; for a rear drive vehicle, the path from the radiator at the vehicles front to EM in the rear multiplied by two (for a closed cycle) plus accounting for the cycle's pressure loss, the value of 7 m would seem reasonable.

The number of pipe models used in the model was decided for the model consistency in Dymola.

As seen in Figure 25, each pipe is split into n-Nodes equally spaced segments along the flow path. The partial differential equations are treated with the finite volume method and a staggered grid scheme for momentum balances. The default value is nNodes=2. This results in two lumped mass and energy balances and one lumped momentum balance across the dynamic pipe.

The default model structure is "av_vb". The ports port_a and port_b expose the first and the last thermodynamic state, respectively. Connecting two or more flow devices therefore may result in high-index DAEs for the pressures of connected flow segments.[x]

The simplest possible alternative symmetric configuration, avoiding potential high-index DAEs at the cost of the potential introduction of nonlinear equation systems, is obtained with the setting nNodes=1, model structure=a_v_b.

Depending on the configured model structure, the first and the last pipe segment, or the flow path length of the first and the last momentum balance, are of half size.

Therefore, in Table 3, only two pipes had the model structure av_vb, while the rest had the simplified model structure of a_v_b to avoid the high-index DAEs' error.

The heat transfer component in Figure 25 specifies the source term $\dot{Q}_e$ in equation (6). Since the pipes PE and EM represent the heat load from the PEM and EM thermal submodels to the LT circuit, the heat transfer model in those pipes have been activated to allow for the heat load transfer.

The heat transfer model in the PE and EM pipes has been set to "IdealHeatTransfer" allowing no thermal resistance by the pipes since it has been already considered in the thermal submodels for both PE and EM devices.

The table below describes the pipes' parameters and details:

Table 3: Pipes' Parameterization in LT Model

Pipe in model	**Parameter**			
	Length (m)	Heat transfer	Model structure	nNodes
pipe2	1	not allowed	av_vb	2
PE	1	allowed	av_vb	2
pipe_vor_NTK	2	not allowed	a_v_b	1
EM	1	allowed	a_v_b	1
pipe_nach_NTK	2	not allowed	a_v_b	1

2.3.1.6 Heat Exchanger in LT Cooling Circuit

The first approach was to use the HEX from the A/C library for better ability to control the spatial discretization between the fins and between the coolant baffles on both the air and refrigerant paths; respectively. For better control of the heat transfer area, the width and depth of the HEX could also be changed along with the refrigerant flow scheme inside the HEX. (see Figure 26)

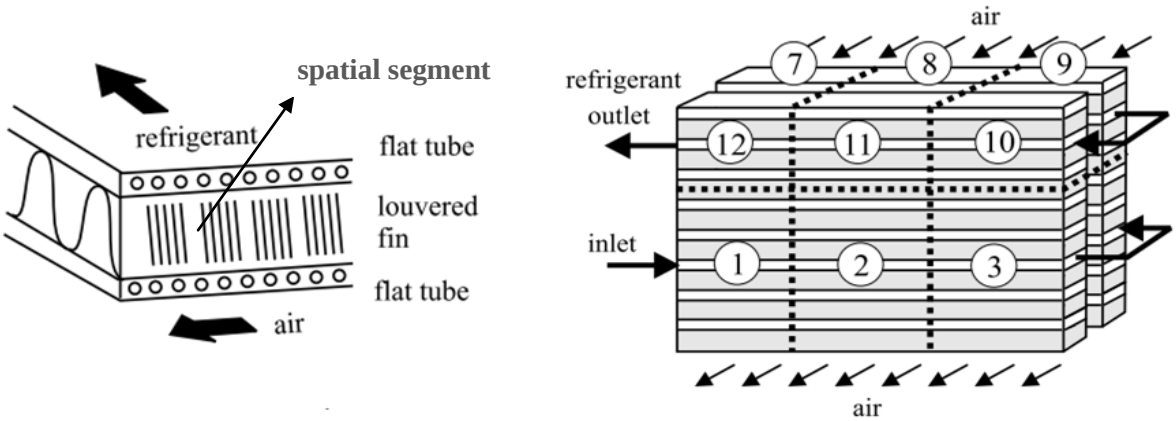

Figure 26: HEX Model in the A/C Library

When both air and refrigerant flow models inside the HEXs from the A/C library have been changed to match with the mediums of the free modelica library (1,2-Propylene glycol, 47 % mixture with water and Moist Air) used in the LT model, compilation errors have been resulted due to the difference in the fluid model properties between both of them. Therefore, this approach has been excluded. The second option is to use the simple HEX model from free modelica fluid library. It basically consists of two heat generating pipes with countered flow connected with each other through a wall. (see Figure 27)

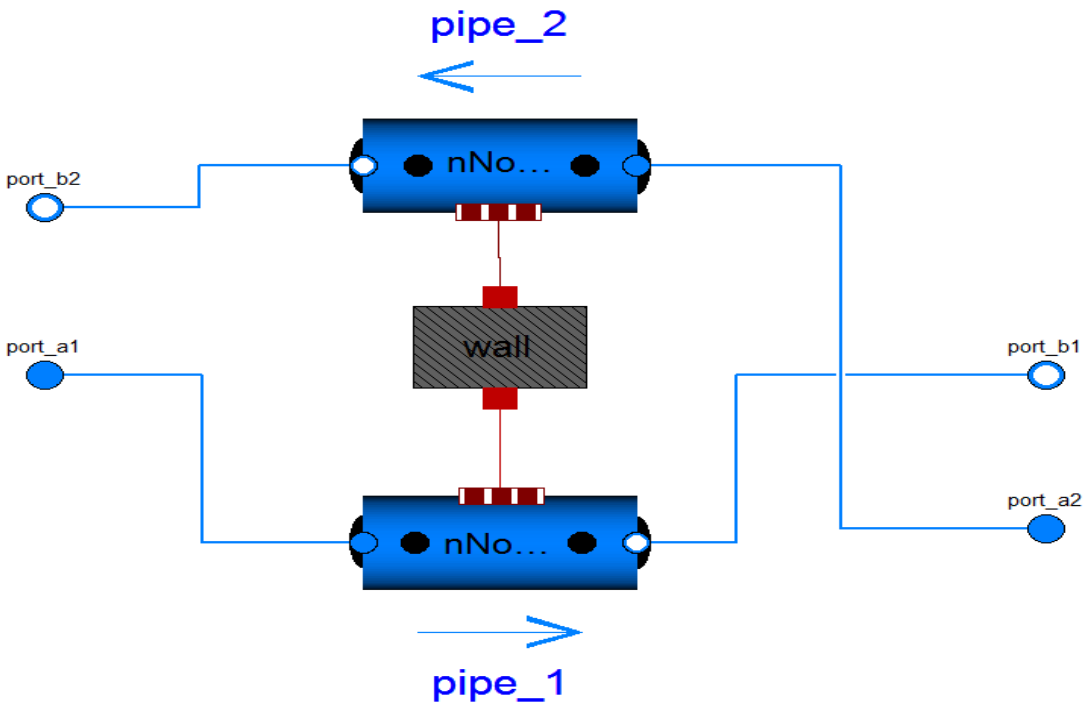

Figure 27: Free Modelica HEX Model

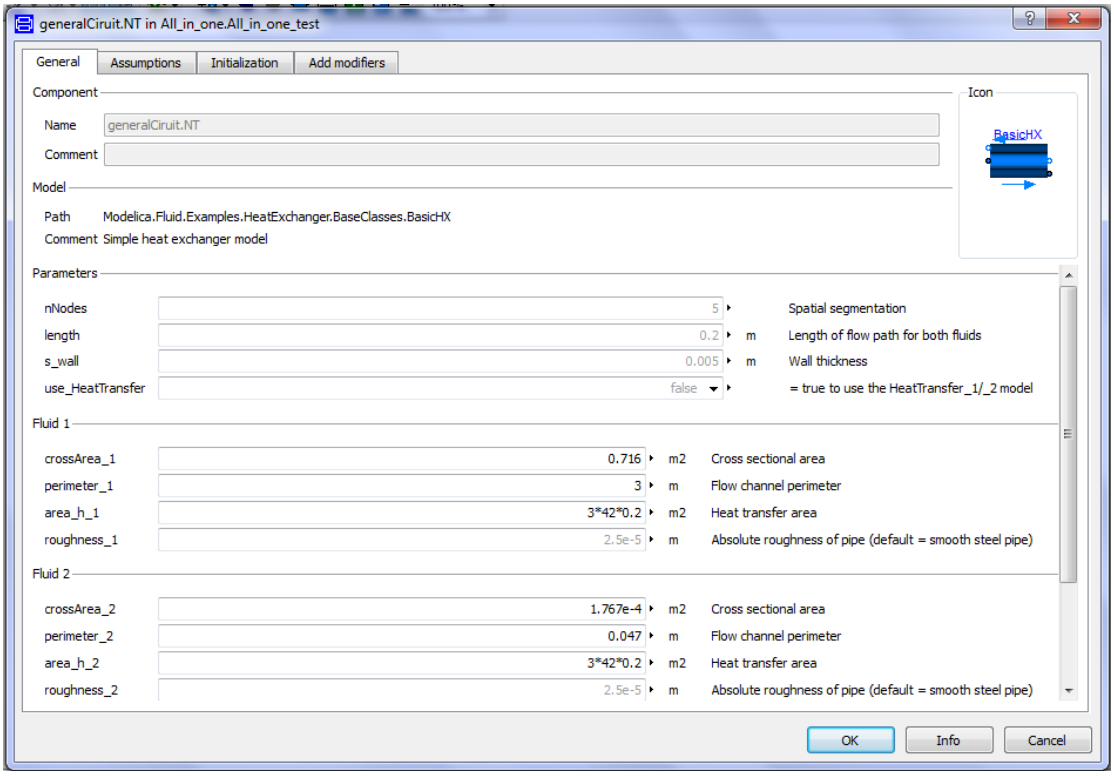

Figure 28: LT Heat Exchanger Parameters

In Figure 27 and unlike the HEX from the A/C library where the coolant would have been cooled down by the ambient air flowing over louvered fins (first excluded approach); in the simple model of modelica HEX, the first pipe (denoted by Fluid_1) will carry the ambient air flowing over the HEX, while the second pipe (denoted by Fluid_2) carries the coolant flow inside the LT circuit for heat transfer.

Since this HEX will be connected with the condenser from the A/C model which is actually a HEX from the A/C library, the sizing of the air and coolant paths in the HEX above; in this case, is necessary. The sizing has been based on calculating the air flow segmentation and discretization inside the condenser with the recourse of the fin geometry and spacing. To account for the perimeters' difference, a calculated value of 42 has been multiplied by the multiplication product of the flow path length and channel perimeter in the LT HEX's heat transfer area.

The keyword for enhancing the cooling effect of a HEX is to increase its surface area. The surface area of the LT HEX is a product of the flow path length, flow channel perimeter and the number of the tubes' discretization inside the flow path.

As a main requirement, the sizing of the HEXs in the whole circuit was a top challenge from the beginning. Since the whole project relies on the idea of designing a sufficient cooling system to be as much convincing as applicable in reality, the compromise has arisen between designing a system that cools down the components and to have as minimal (able to be manufactured) measurements as possible to be introduced as a feasible solution.

The alternative for using one large HEX with the above measurements, is to double or sometimes triple the number of the HEXs used inside the model. This approach has not been only used in the LT model, but also in the other circuits.

In Figure 28, the perimeter of the air flow channel was the changed value to increase the area of the HEX. The value has been increased; gradually, with observing the temperature rise during the simulation run along with the cooling process till it reached the value of 3 m, when increasing the perimeter will no further have an enhancing effect on the cooling process.

The cross sectional area of the air flow channel was then calculated with correspondence.

The nNodes for the spatial segmentation (42) as well as the length of the flow channel (0.2 m) have been always constants.

In correspondence on the coolant side, the heat transfer area would be the same and the flow channel cross sectional area and flow perimeter were calculated based on the diameter of 0.015 m, which is the same diameter used for the coolant pipes in the LT model. The nNodes for the spatial segmentation (42) as well as the length of the flow channel (0.2 m) have been always constants.

2.3.2 Battery Cooling Circuit

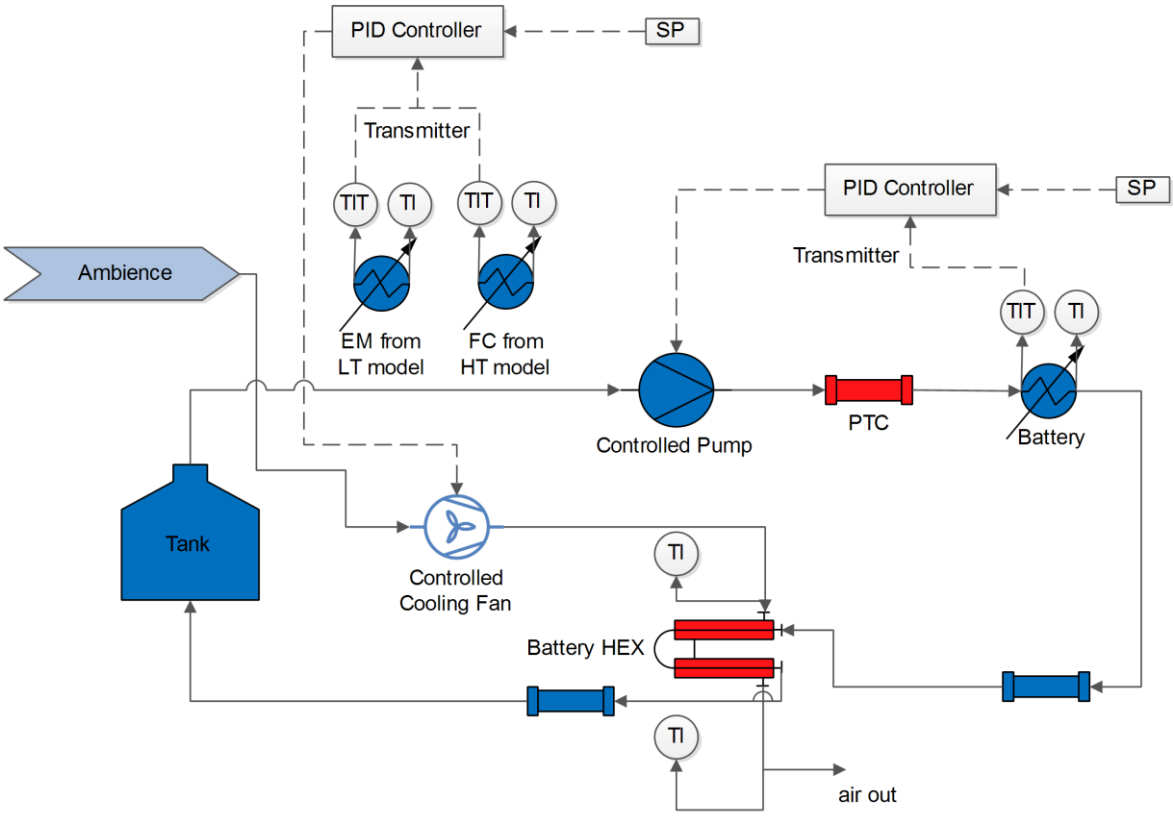

Figure 29: Battery Cooling Circuit P&ID

In Figure 29, the battery cooling circuit is designed to serve cooling down the Battery inside the FCEV, while the PTC (Positive Temperature Coefficient) device serves as a heater to heat up the Battery to the operational temperature.

As the operating temperature for the Battery should not exceed the amount of 40 °C, the mass flow rate for the cooling pump will also be controlled and regulated just like in the LT model. The temperature of the coolant entering the Battery is measured and sent to the PID controller for the feedback control. The mass flow rate of the cooling pump is then controlled and regulated to maintain a safe operating temperature and sufficient cooling.

At safe working temperatures, the coolant will be circulated with a small flow rate as a product of a low coolant pump rotation speed.

As mentioned before, the air flow entering the HEXs' arrangement in the engine compartment and couples the HEXs, starts from the Battery cooling circuit model. The air volume flow rate of the fan is controlled by a PID controller which uses the temperature of the coolant entering the EM in LT model and the fuel cell stack (FC) in the HT model; being the maximum heat sources in the thermal management system, for the feedback control.

In translation to Figure 29, the model illustrated below represents a basic and simplified cooling circuit that cools down the Battery. Its structure and components are similar to the LT cooling circuit. The Battery has been denoted by a dynamic pipe model with heat transfer, while the air mass flow rate to the system will be through an air mass flow source connected to the HEX and controlled by the control module. (see Figure 30)

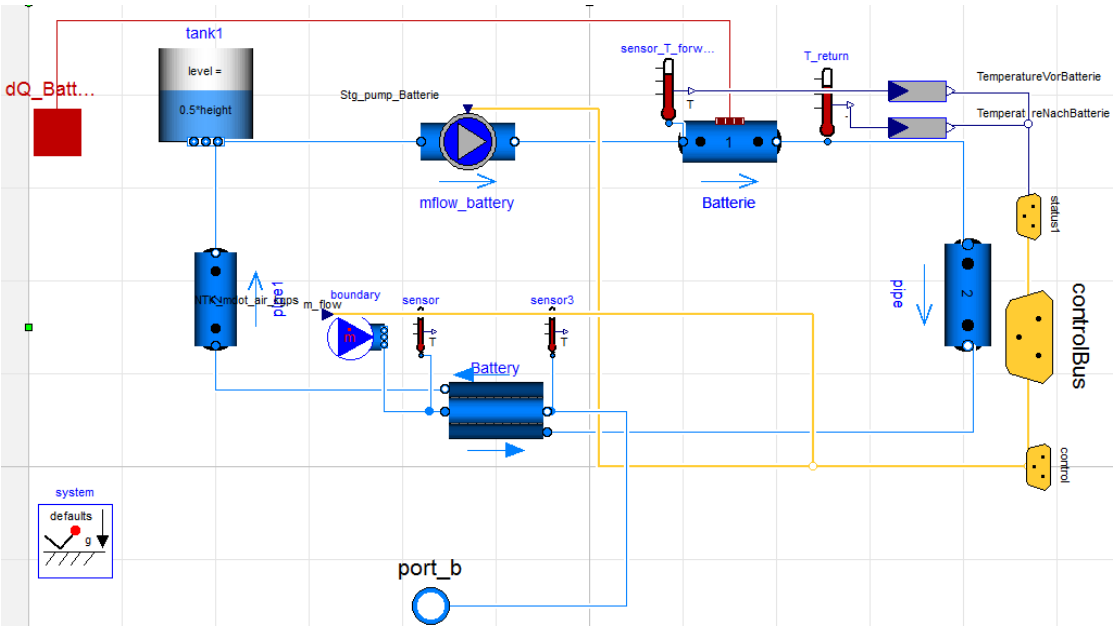

Figure 30: The Battery Cooling Circuit Model

Since the cooling phenomena is what of importance in the model above, the PTC has not been included. Additionally, it only operates when the battery's operational temperature has not been yet reached, which is the condition for the vehicle's operation.

2.3.2.1 Fluid Properties

The same coolant used in the LT model, is also used in the Battery cooling circuit (1,2-Propylene glycol, 47 % mixture with water). Since the HEXs in both circuits are coupled from the air side, they will also share the same air properties of the Moist Air (240 ... 400 K) package. (see 2.3.1.1p. 21)

2.3.2.2 Defining Ambient Conditions

The ambient conditions defined for this model are similar to the ambient conditions defined for the LT cooling circuit model. (see pp 22-24)

The initialization guess value for the coolant mass flow rate inside the Battery cooling circuit's model has been also set to 0.0001 kg/s. According to the empirical values from DLR test vehicle, the operational range of the pump's mass flow rate inside the Battery model is (0.01-0.2 kg/s).

2.3.2.3 The Tank

Since both LT and Battery circuits were separately modelled and tested before coupling, a separate tank was specified for each of them. In reality, only one tank; as a coolant source, will be used for both the LT and Battery cooling circuits since they are sharing similar coolant properties.

As a separate tank, it should be dimensioned up on the maximum coolants' mass flow rate inside the circuit, the pipes' lengths and diameters.

The diameter of the pipes is always 0.015 m and the total length of the pipes in the Battery's circuit is 3 m. Using equation (7), the coolant's volume inside the tank will be 0.002 m^3.

2.3.2.4 Prescribed Flow

Only the medium inside the prescribed flow has been designated to the coolant inside the circuit and that the flow rate will be controlled by the control module; as will be illustrated later when discussing the control, according to the Battery's setting temperature (T_{set}).

Since the air mass flow to the HEXs in the engine compartment starts from the Battery cooling circuit, an air mass flow source with prescribed flow rate and temperature has been connected to the air side of the HEX in the circuit and controlled by the control module which uses the temperatures of the EM and the fuel cell stack for regulation. (see Figure 31)

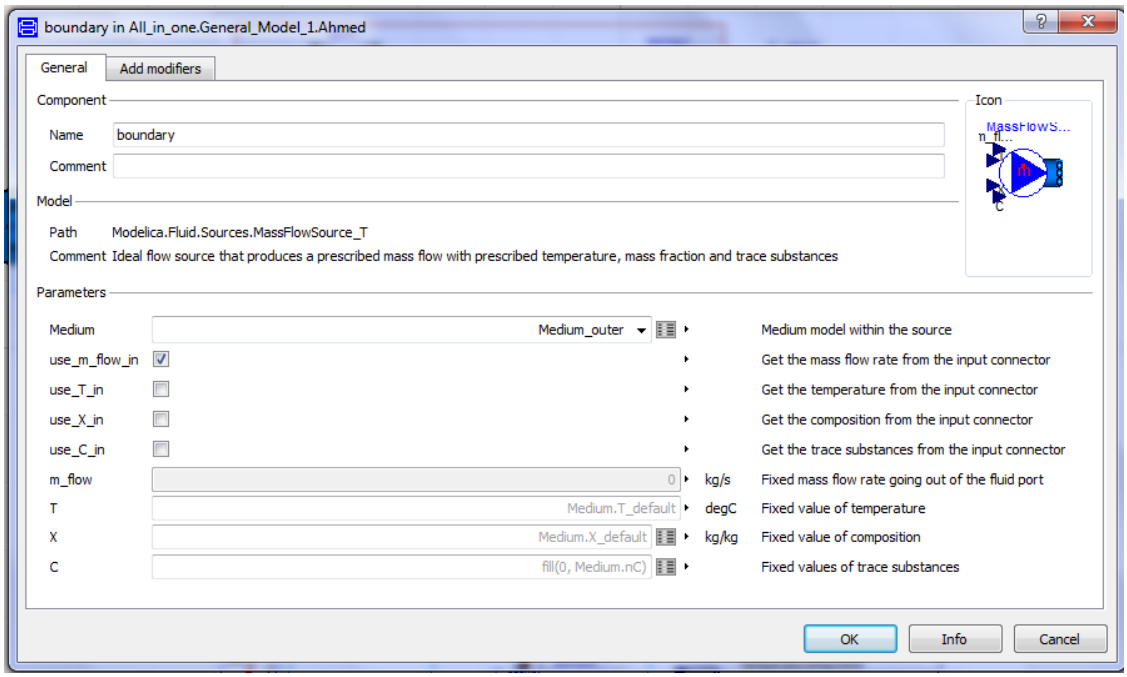

Figure 31: Air Mass Flow Source in the Battery Cooling Circuit

Based on empirical values from DLR test vehicle, the operational range of the cooling fan (air mass flow rate) in the HEXs' arrangement inside the engine compartment is (0.16-0.66 kg/s).

2.3.2.5 The Piping System in the Battery Cooling Circuit

The pipes inside the Battery cooling circuit's model are dynamic pipe models with storage of mass and energy. The diameter of all pipes is 0.015 m and their total length is 3 m according to DLR test vehicle. In the total pipe length, the cycle's pressure loss has been accounted for. The number of pipe models used in the model was decided for the model consistency in Dymola.

In order to avoid high-index DAEs, the model structures of the pipes in the Battery cooling circuit's model have been chosen as follows:

Table 4: Pipes' Parameterization in Battery Cooling Circuit's Model

Pipe in model	Parameter			
	Length (m)	Heat transfer	Model structure	nNodes
Batterie	1	allowed	a_v_b	1
pipe	1	not allowed	av_vb	2
pipe1	1	not allowed	av_vb	2

The thermal load of the Battery was measured during DLR test vehicle's trip for 3 NEDCs in kilowatts and fed to the Battery cooling circuit's model by a prescribed heat flow through the "Batterie" pipe with the heat transfer model. (see Figure 32)

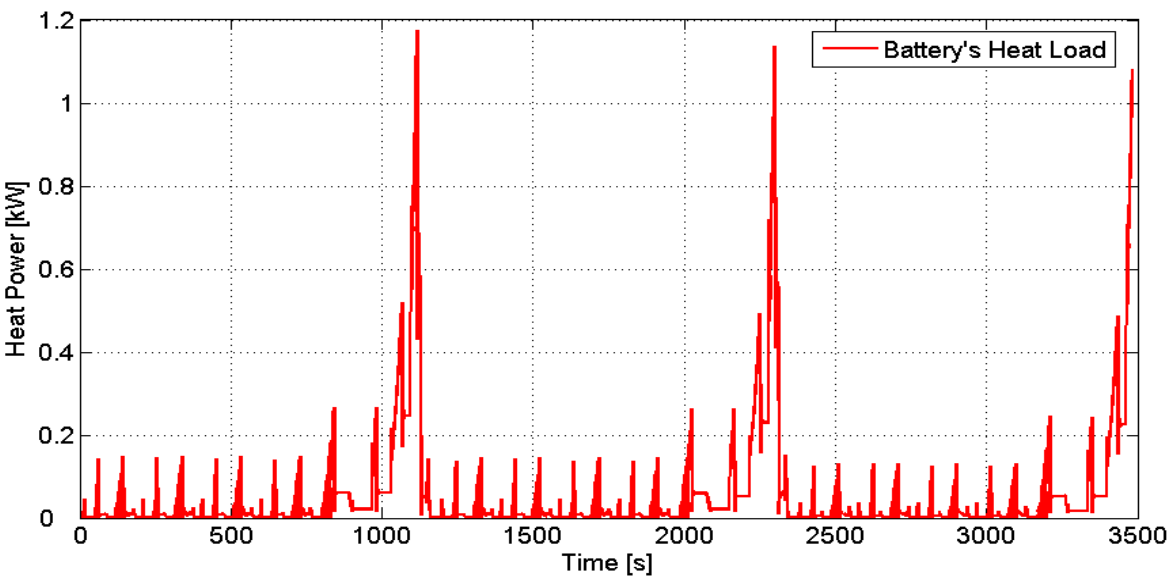

Figure 32: Recorded Battery's Heat Load through Dyno Roller Testbench (Test Date: 03.09.2013)

2.3.2.6 Heat Exchanger in Battery Cooling Circuit

The HEX used in the Battery cooling circuit's model is simple HEX from the modelica fluid library. (see Figure 27)

Similar to the approach used in the LT model, the HEXs from the A/C library were to be used in the Battery cooling circuit model and for the same reason, this approach has been excluded.

The approach used in sizing the HEX in the Battery cooling circuit is the same used in sizing the HEX used in the LT cooling circuit.

In Figure 33, the perimeter of the air flow channel was the changed value to increase the area of the HEX. The value has been increased; gradually, with observing the temperature rise during the simulation run along with the cooling process till it reached the value of 0.25 m, when increasing the perimeter will no further have an enhancing effect on the cooling process.

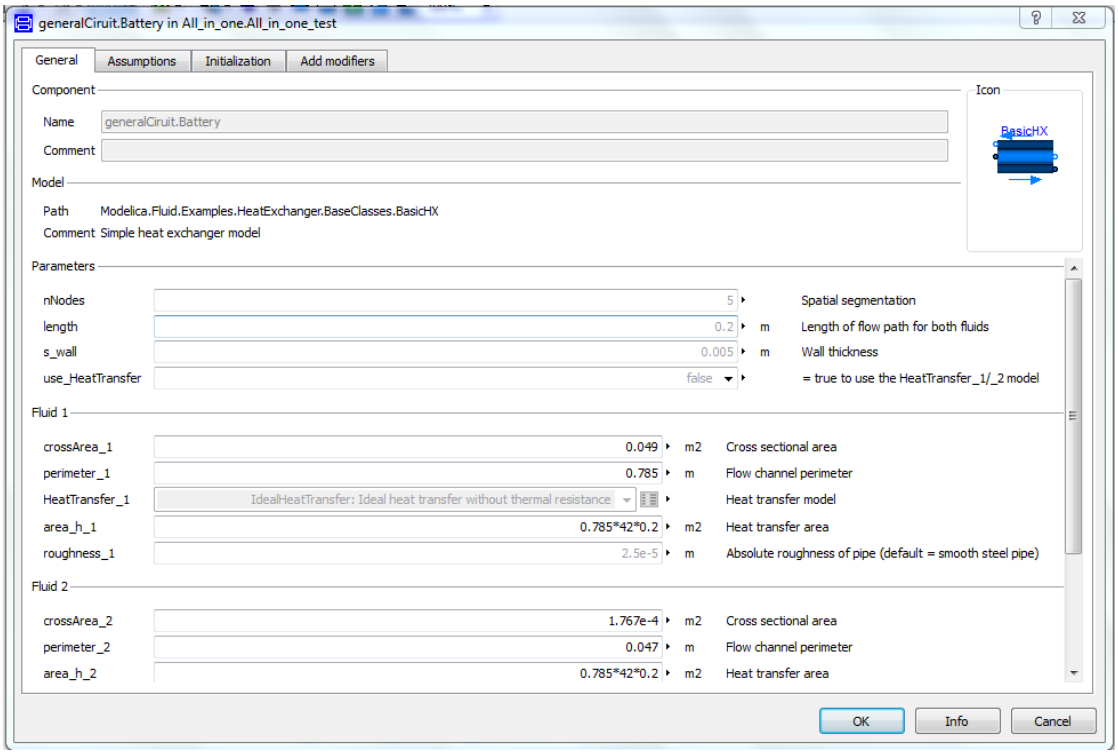

Figure 33: Battery Heat Exchanger Parameters

In correspondence on the coolant side, the heat transfer area would be the same and the flow channel cross sectional area and flow perimeter were calculated based on the diameter of 0.015 m, which is the same diameter used for the coolant pipes in the Battery model. The nNodes for the spatial segmentation (42) as well as the length of the flow channel (0.2 m) have been always constants.

2.3.3 High Temperature Cooling Circuit (HT Cooling Circuit)

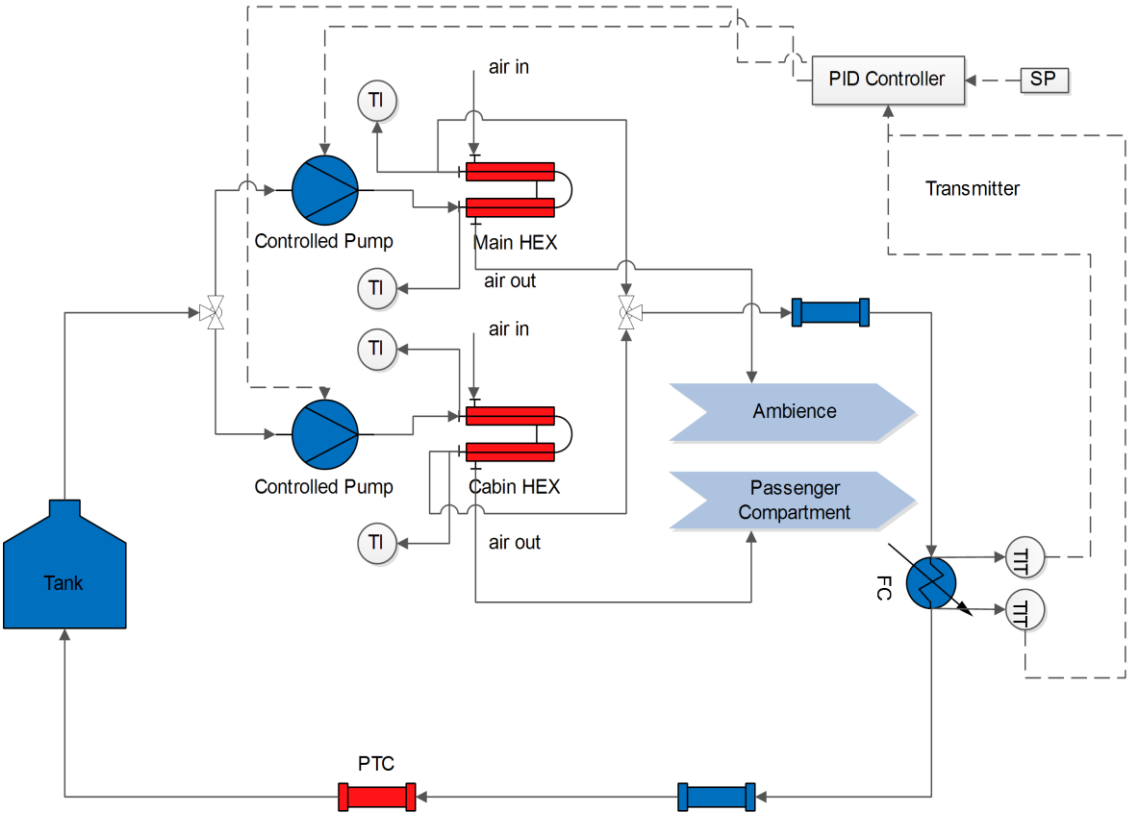

Figure 34: HT Cooling Circuit P&ID

In Figure 34, the HT cooling circuit is designed to serve cooling down the fuel cell stack in the FCEV. As it is clearly illustrated above, there are two HEXs connected to the FC cooling circuit. One of each exchanges the heat with the ambience (Main HEX) and the other exchanges the heat with the passengers' compartment (Cabin HEX). As the air-conditioning load is the largest ancillary load in the vehicle, the idea depends on mitigating the working temperature of the fuel cell stack to remain within the safe range and at the same time make use of the heat generated to heat up the compartment (cabin) of the vehicle as an air conditioning technique; when required, at cold weather conditions.

Since the operating temperature for the fuel cell stack should not exceed the amount of 160 °C, the temperature of the coolant entering the FC will be sent to a PID controller to control the air mass flow rate over all the HEXs' arrangement contained in the engine compartment. (see Figure 29)

Since the coolant temperature difference between the inlet and outlet ports of the FC should not exceed the amount of 10 °C, the temperature difference between the coolant entering and exiting the FC will be sent to another PID to control the coolant mass flow rates to the Main and Cabin HEXs.

In Figure 34, since the heat transfer from the coolant inside the circuit to the working mediums (ambient air and cabin air) will so much depend on the pump's mass flow rate, a separate pump has been specified for each HEX for better and simpler mass flow rate control.

The pumps' combined mass flow rates required to cool down the FC are controlled so that the share of each HEX from the coolant's volume through its pump will be defined by the user according to the air conditioning demand for heating.

The HT cooling circuit will basically consist of a tank (coolant source), prescribed flows (act as a pumps), dynamic pipes, dynamic pipes with heat transfer, temperature sensors, system block (defines the ambient conditions), control bus, tee junction and HEXs. (see Figure 35)

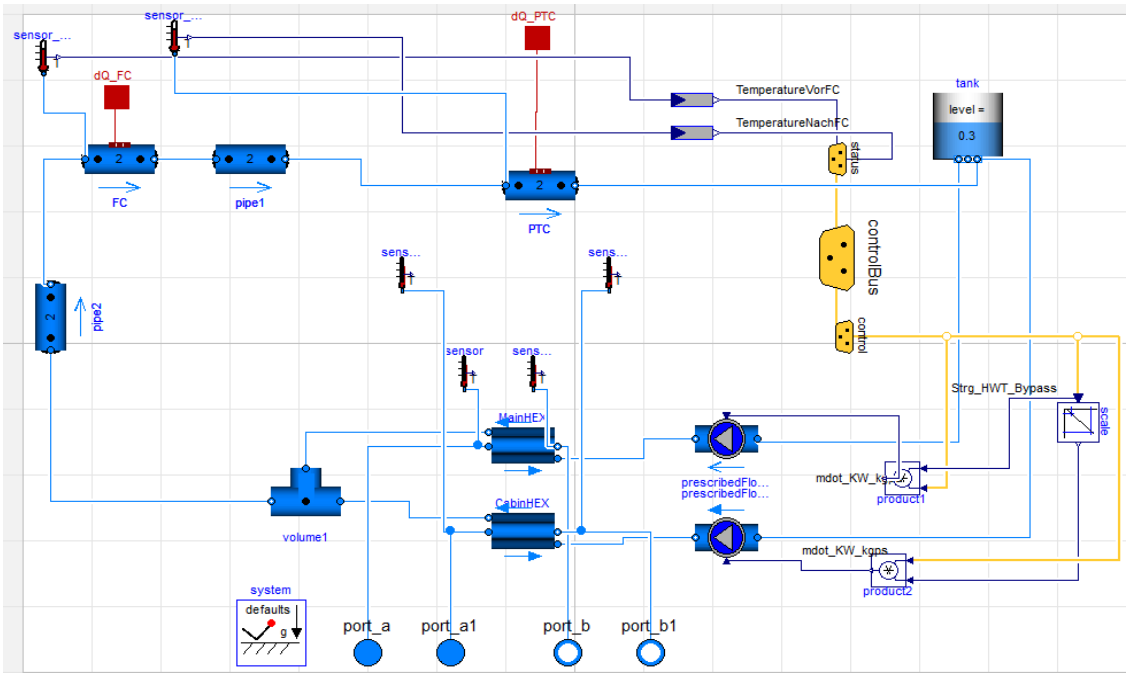

Figure 35: HT Cooling Circuit Model

The HEXs are controlled so that the Main HEX will mainly exchange heat with the ambience to cool down the FC, while the cooling pump for the Cabin HEX will only work according to the passenger's will in cold weather conditions for air conditioning. So, the cooling action of the HEXs will be divided between cooling down the FC and heating up the Cabin.

Just like in the Battery cooling circuit, the PTC has not been included, because the cooling phenomena in the model is what of importance. Additionally, it only operates when the FC's operational temperature has not been yet reached, which is the condition for the vehicle's operation.

2.3.3.1 Fluid Properties

Since the HEXs in the vehicle are coupled from the air side, the air flowing over the HEXs in each arrangement will always have the same properties (assuming 100 % fresh air to the Cabin). Therefore, the air model in the HT circuit has been chosen to be Moist Air (240 ... 400 K).

As the temperature inside the HT circuit increases above 150°C, the vapour pressure of the water content inside the coolant increases rapidly, and the problems of structural strength for processing equipments becomes more and more severe. Thus; with high temperature systems, it becomes increasingly important to consider fluids with vapour pressures lower than water. That is why Essotherm thermal oil is chosen.

Essotherm 650 is a heat transfer fluid recommended where bulk temperature does not exceed 340 °C in closed systems. Essotherm is used for most conventional applications because of its low volatility, good low temperature performance, low corrosivity, relatively low viscosity, and good heat transfer properties.

Table 5: Coolant Properties in the HT Circuit

Properties	Value
Boiling Point (°C)	430 at 1 bar
Flow Point (°C)	-9 at 1 bar
Flash Point (°C)	300 at 1 bar
Vapour Pressure (mbar)	0.1 at 160 °C
Specific Heat [kJ/(kg.K)]	1.88 at 30 °C
Density (kg/m^3)	890 at 30 °C
Thermal Conductivity (W/m.K)	0.128 at 30 °C
Dynamic Viscosity (mPa.s)	1172 at 30 °C[xi]

2.3.3.2 Defining Ambient Conditions

The ambient conditions defined for this model are similar to the ambient conditions defined for the LT and Battery cooling circuit models. (see pp 22-24)

The initialization guess value for the total coolant mass flow rate inside the HT cooling circuit's model has been also set to 0.0001 kg/s. According to the empirical values from DLR test vehicle, the combined operational range of the pumps' mass flow rates inside the HT model is (0.16-0.5 kg/s).

2.3.3.3 The Tank

Since the coolant properties in the HT circuit is different than the coolant in both LT and Battery circuits, a separate tank has been specified.

As a separate tank, it should be dimensioned up on the maximum coolants' mass flow rate inside the circuit, the pipes' lengths and diameters.

Based on empirical values, the diameter of the pipes is always 0.015 m and the total length of the pipes in the HT circuit is 4 m. Using equation (7), the coolant's volume inside the tank will be 0.003 m^3.

2.3.3.4 Prescribed Flow

Only the medium inside the prescribed flows has been designated to the coolant inside the circuit and that the flow rates will be controlled by the control module; as will be illustrated later when discussing the control, according to the temperature difference between the inlet and outlet ports of the FC.

2.3.3.5 The Piping System in the HT Cooling Circuit

The pipes inside the HT cooling circuit's model are dynamic pipe models with storage of mass and energy. The diameter of all pipes is 0.015 m and their total length is 4 m according to DLR test vehicle. In the total pipe length, the cycle's pressure loss has been accounted for. The number of pipe models used in the model was decided for the model consistency in Dymola.

In order to avoid high-index DAEs, the model structures of the pipes in the HT cooling circuit's model have been chosen as follows:

Table 6: Pipes' Parameterization in HT Cooling Circuit's Model

Pipe in model	Parameter			
	Length (m)	Heat transfer	Model structure	nNodes
pipe2	1	not allowed	a_v_b	2
FC	1	allowed	av_vb	2
pipe1	1	not allowed	a_v_b	2
PTC	1	allowed	av_vb	2

The thermal load of the FC was measured in kilowatts and fed to the HT cooling circuit's model by a prescribed heat flow through the "FC" pipe with the heat transfer model. (see Figure 36)

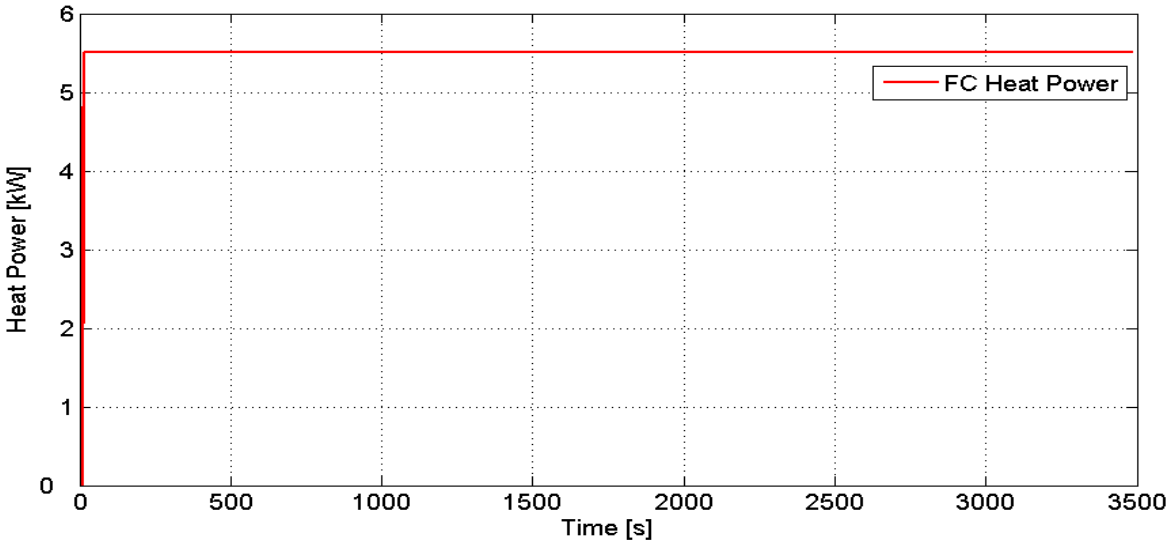

Figure 36: Recorded FC Heat Load through Dyno Roller Testbench (Test Date: 03.09.2013)

The heat load represented above is for a range-extended FC that will only be switched on when the power of the Battery inside the vehicle is depleted. This means, that the curve does not represent a steady state operation for the FC, but it captures the interval when the FC is set into operation to test the cooling performance of the HT cooling circuit.

2.3.3.6 Heat Exchangers in HT Cooling Circuit

The HEXs used in the HT cooling circuit's model are simple HEXs from the modelica fluid library. (see Figure 27)

Similar to the approach used in the LT and Battery models, the HEXs from the A/C library were to be used in the Battery cooling circuit model and for the same reason, this approach has been excluded.

Also, the approach used in sizing the HEX in the LT and Battery cooling circuits is the same used in sizing the HEXs in the HT cooling circuit.

In Figure 37, the perimeter of the air flow channel in Main HEX was the changed value to increase the area of the HEX. The value has been increased; gradually, with observing the temperature rise during the simulation run along with the cooling process till it reached the value of 4 m, when increasing the perimeter will no further have an enhancing effect on the cooling process.

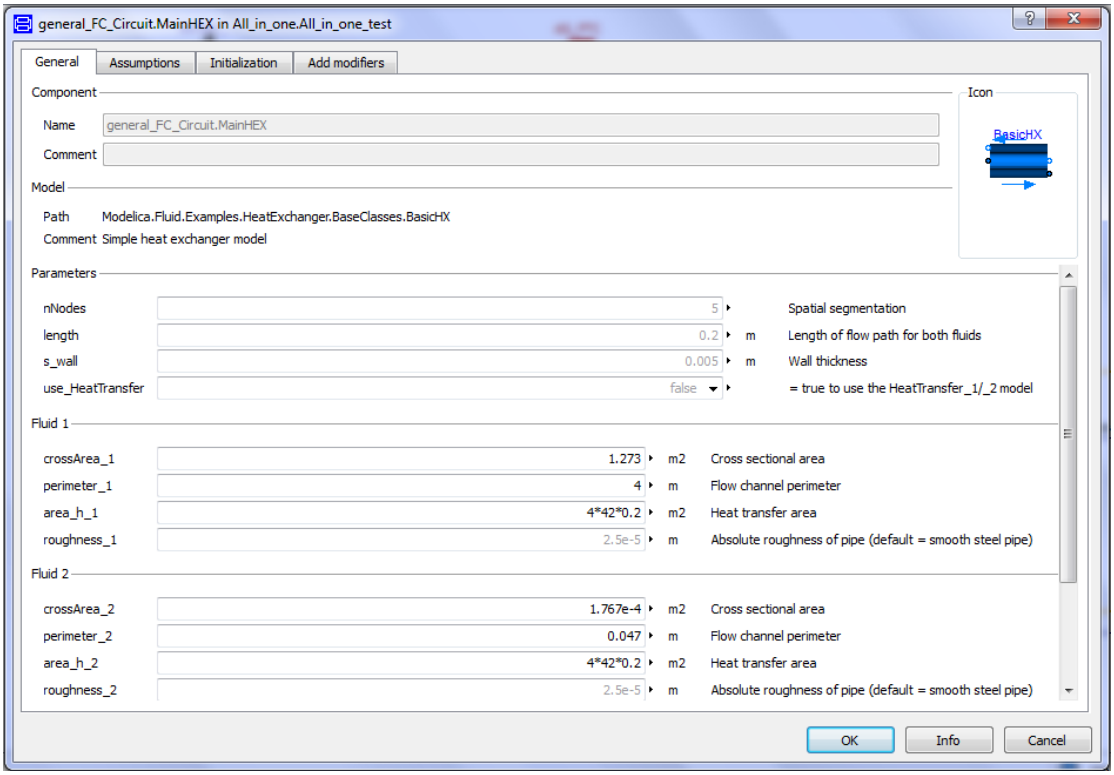

Figure 37: Main Heat Exchanger Parameters

In correspondence on the coolant side, the heat transfer area would be the same and the flow channel cross sectional area and flow perimeter were calculated based on the diameter of 0.015 m, which is the same diameter used for the coolant pipes in the HT model. The nNodes for the spatial segmentation (42) as well as the length of the flow channel (0.2 m) have been always constants.

The sizing of the Cabin HEX was of another perspective. Although the coolant's flow to the Cabin HEX shares a part of the total flow required to be delivered into both HEXs (Main and Cabin) for cooling, the Cabin HEX was not meant to cool down the FC as much as it should; primarily, be used for heating the passenger compartment in winter. Therefore, the sizing of the Cabin HEX was considering the size of the Evaporator inside the A/C cycle as they are both coupled together from the air side and contained inside the passenger compartment for air conditioning.

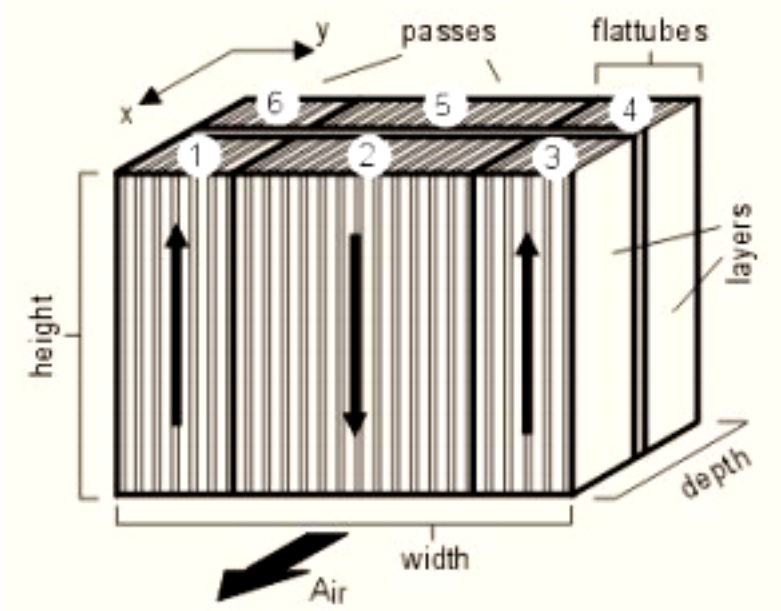

Figure 38: Evaporator HEX

In Figure 38, the evaporator HEX used in the A/C cycle has a total heat transfer area of 0.17 m^2. Thus, the perimeter of the air flow channel in the Cabin HEX should have the value of 0.02 m. (see Figure 39)

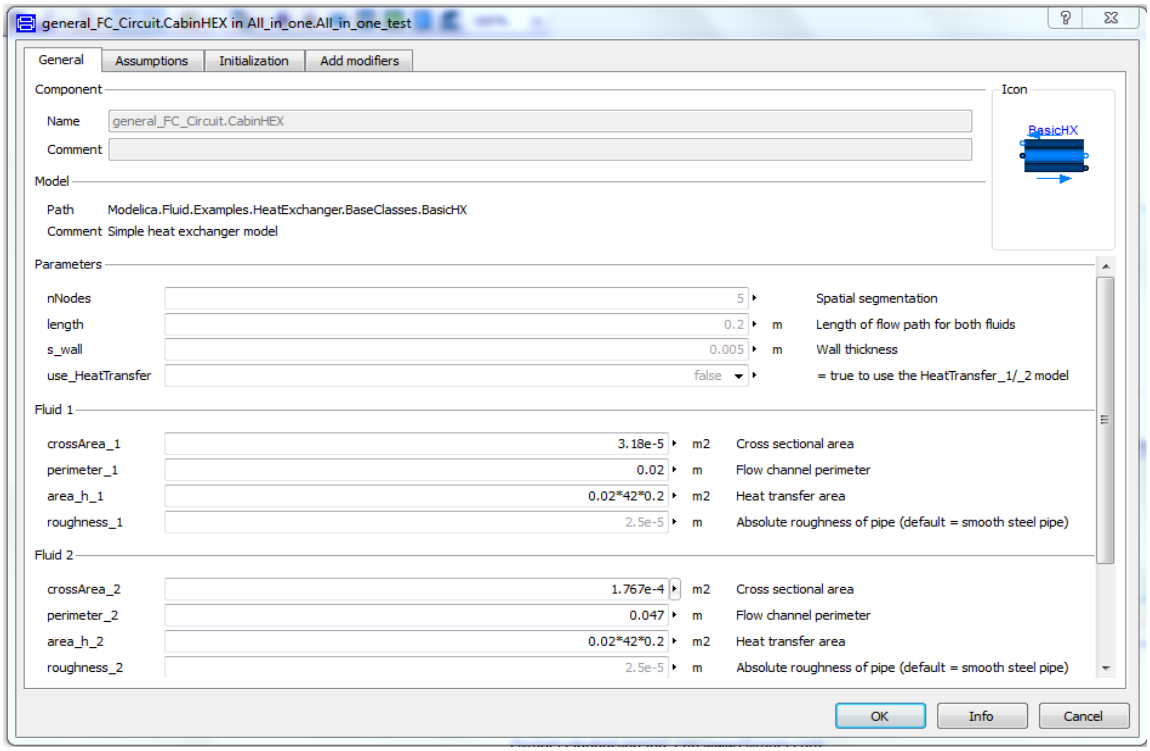

Figure 39: Cabin Heat Exchanger Parameters

In correspondence on the coolant side, the heat transfer area would be the same and the flow channel cross sectional area and flow perimeter were calculated based on the diameter of 0.015 m, which is the same diameter used for the coolant pipes in the HT model. The nNodes for the spatial segmentation (42) as well as the length of the flow channel (0.2 m) have been always constants.

2.3.4 Air Conditioning Cycle (A/C Cycle)

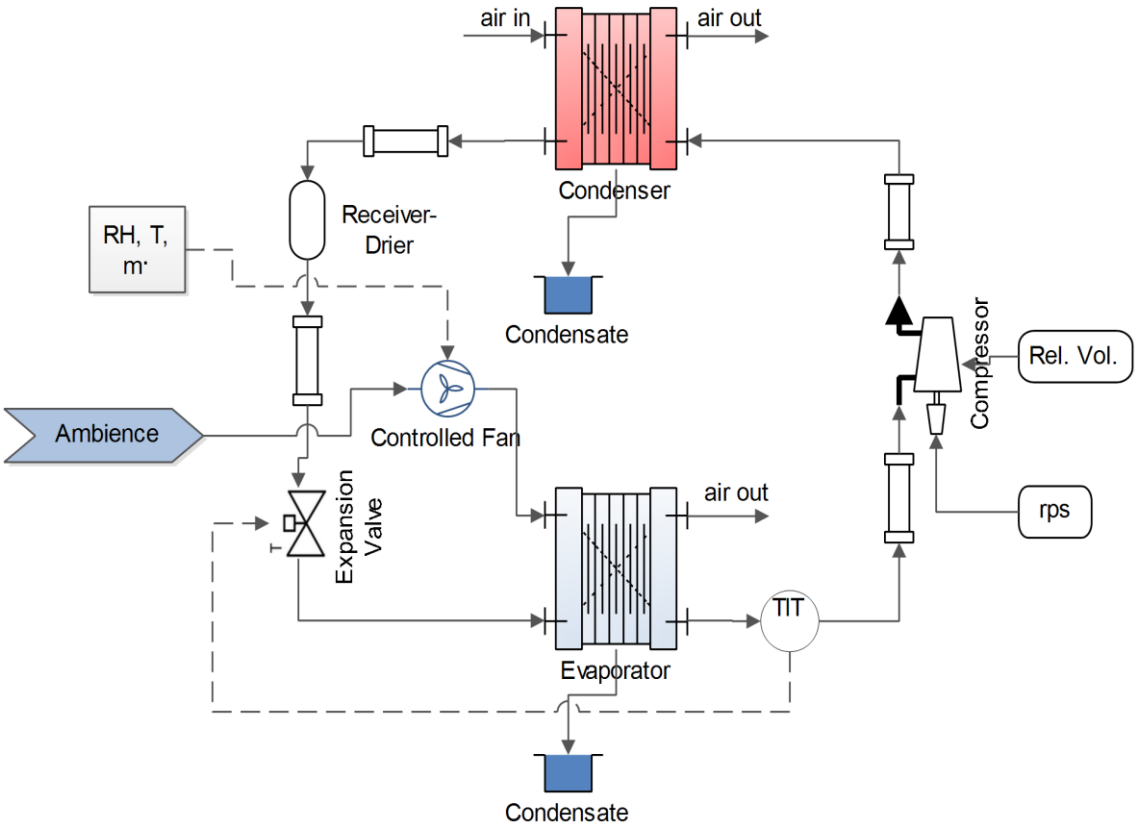

Figure 40: A/C Cycle P&ID

In Figure 40, the A/C Cycle represents an example for an ordinary air conditioning cycle used in vehicles. As it is clearly illustrated above, that the cycle consists mainly of a condenser, evaporator, compressor and expansion valve. Both condenser and evaporator are HEXs from Dymola air conditioning library which exchange heat with ambience and passenger compartment inside the vehicle consequently.

The size of the cycle in the figure above may; slightly, deviate from the actual sizing of the cooling capacity required by the vehicle. However it represents an actual thermal performance with which the thermal management system could be manipulated and studied.

As illustrated in Figure 17, the condenser is a HEX that takes a part and shares the same air flow over the HEXs' arrangement inside the engine compartment, while the evaporator is a HEX that exists inside the passenger compartment where the air flow is controlled by the user.

The A/C model below has been quoted from the examples presented inside the air conditioning library in Dymola. The refrigerant super heating temperature has been measured right after the evaporator to be used as an input for the expansion valve, while the relative volume inside the compressor and its rotational speed have been controlled by constant and ramp functions consequently. (see Figure 41)

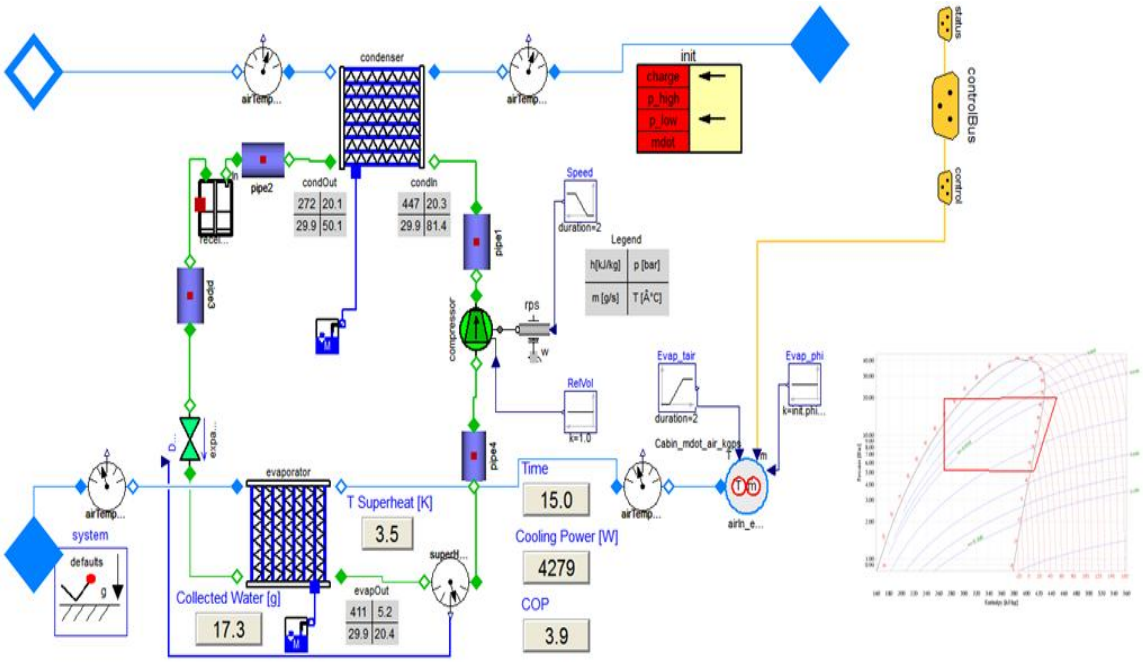

Figure 41: A/C Circuit Model

In the model above, the air flow model inside the condenser and evaporator has been changed to match with the used medium inside the other coupled models. The air mass flow rate entering the evaporator is the same that flows over the HEXs' arrangement inside the passenger compartment. The values of the RH and temperature have been set as constants to 50 % and 30 °C; respectively, while the mass flow rate has been controlled by the control module.

2.3.4.1 Fluid Properties

The air flowing over the HEXs in each arrangement will always have the same properties (assuming 100 % fresh air to the Cabin). Therefore, the air model in the HT circuit has been chosen to be Moist Air (240 ... 400 K).

The refrigerant used in the cycle is R134a with the following properties at 30 °C and 1 bar:

Table 7: Refrigerant Properties in the A/C Cycle

Properties	Value
Specific Enthalpy (kJ/kg)	428.8
Specific Entropy (kJ/kg.K)	1.916
Specific Heat [kJ/(kg.K)]	1.627
Density (kg/m^3)	4.127
Thermal Conductivity (W/m.K)	0.0141
Dynamic Viscosity (mPa.s)	0.012[xii]

2.3.4.2 Defining Ambient Conditions

The ambient conditions defined for this model are similar to the ambient conditions defined for the earlier cooling circuit models. (see pp 22-24)

The initialization guess value for the mass flow rates inside the A/C cycle has been also set to 0.0001 kg/s. However, the values for both air and refrigerant mass flow rates have been set up to constants; according to the empirical values from DLR test vehicle, the maximum value of air mass flow rate is 0.066 kg/s.

2.3.4.3 Flow Sources

The fluid flow inside the A/C cycle is varied between 2 types of flow sources. First, is the compressor which controls the compression ratio of the refrigerant and hence, the cycle's COP. Second, is the air mass flow source to the passenger compartment, which is maintained by a controlled fan. As it seems in Figure 41, that both of them were given constant parameters for operation. However, these parameters have been changed in consideration with the maximum cooling capacity of the air conditioning system under the former specified tough ambient conditions.

2.3.4.4 Model Initialization

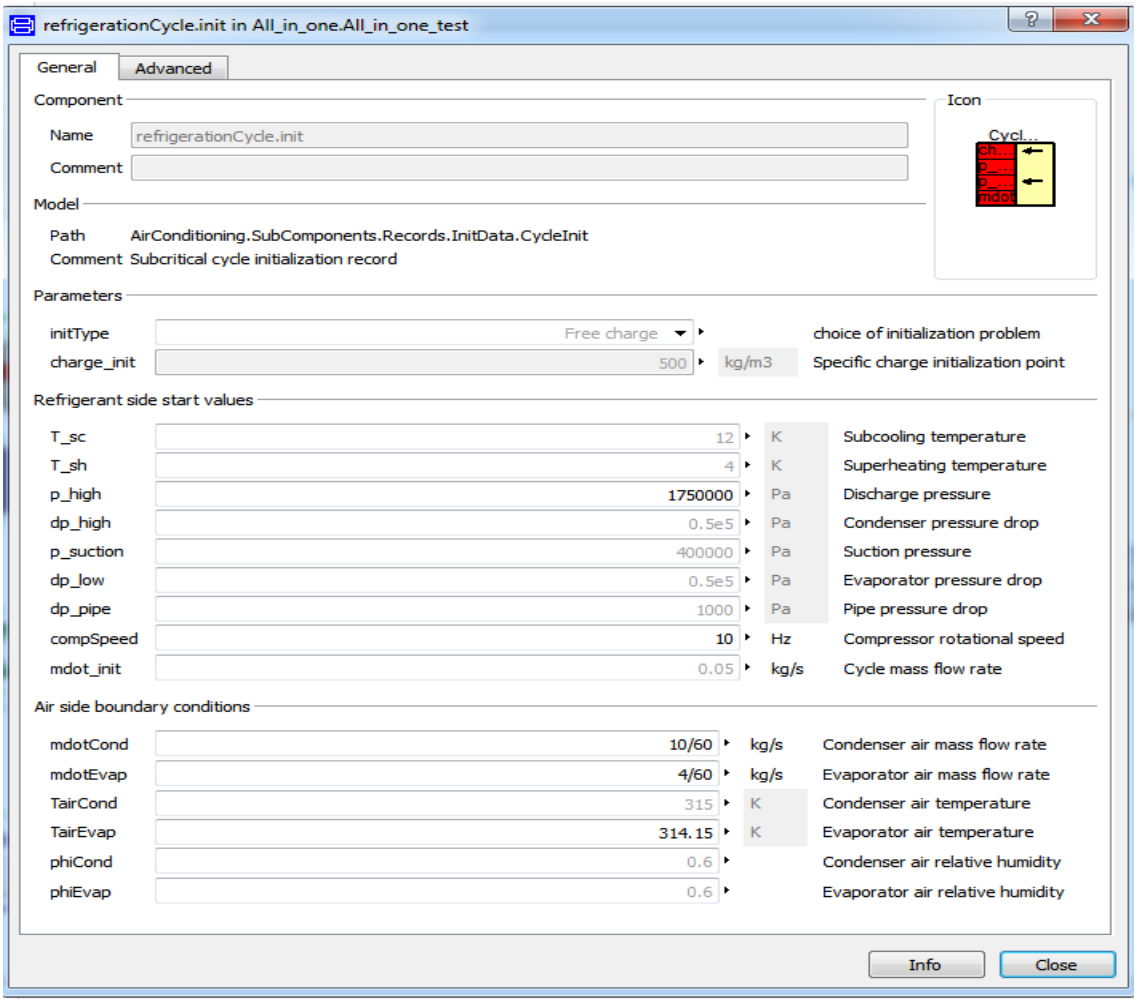

Figure 42: Initialization Parameters

In order to have a quick access to the controlling parameters inside the A/C model, an initialization block has been established to adjust parameters like air mass flow rate, pressures, temperatures and compressor's speed. (see Figure 42)

Since the existence of the A/C cycle inside the system represents an extra thermal load, studying the thermal performance of the cycle was prior to maintaining the right cooling capacity for the vehicle. Thus, the adjustment of the above parameters was based on the observation of the cooling performance for the thermal management system.

2.3.5 The Control Module

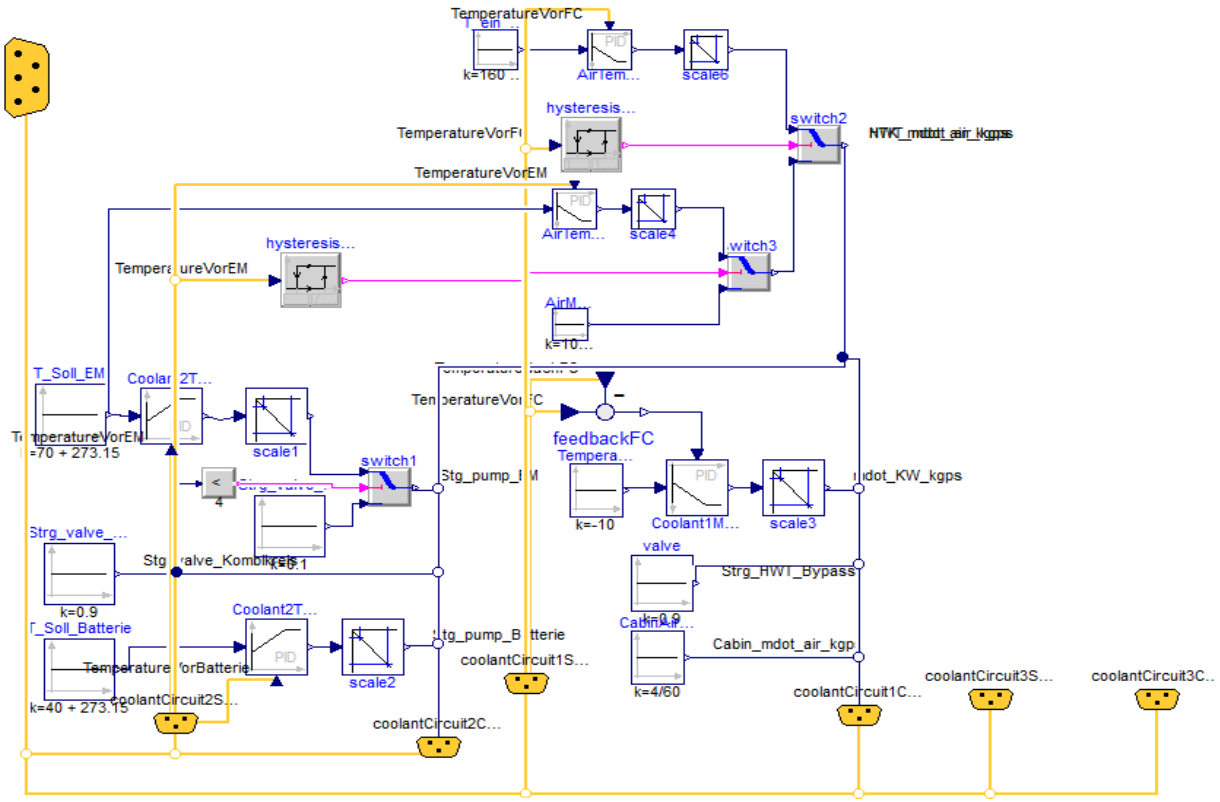

Figure 43: System's Control Module Layout

The control module is the brain for the whole thermal management system. It is what controls the mass flow rates for safe operational temperatures. It combines, compares and triggers the signals with which the cooling process is being operated.

As seen in Figure 43, the module consists of several control loops connected together in duets. One branch of each represents the measured signals which are going to be used in the feedback control loop for an active control process (status) and the other represents the controlling signals which are going to be sent to the prescribed flows and flow sources inside the submodels for the control (control).

2.3.5.1 LT Model Control

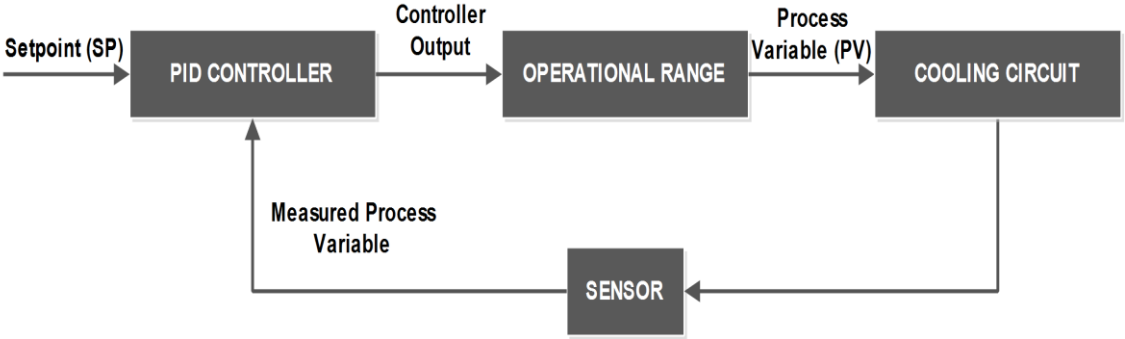

Figure 44: EM Temperature Control Scheme

The idea of controlling the EM's temperature depends on measuring the temperature of the coolant entering the EM pipe (the pipe which denotes the thermal load of the EM in LT cooling model), then sending the signal to a proportional-integral-derivative controller (PID controller).

Along with the T_{set} of the motor (70 °C), the PID will compare between both signals within an active control loop then fires a signal to the coolant pump inside the model to increase the flow rate; within the specified operational range, when the setting temperature is breached. The operational range of the cooling pump is 0.01-0.5 kg/s. (see Figure 44)

2.3.5.2 Battery Model Control

- **Coolant Mass Flow Control**

  Similar to Figure 44, the temperature of the coolant entering the Batterie pipe (the pipe which denotes the thermal load of the Battery in Battery cooling model) is sent to a PID controller along with the T_{set} (40 °C), the PID will compare between both signals within an active control loop then fires a signal to the coolant pump inside the model to increase the flow rate; within the specified operational range, when the setting temperature is breached. The operational range of the cooling pump is 0.01-0.2 kg/s.

- **Air Mass Flow Control**

Controlling the air mass flow rate over the HEXs' arrangement in the engine compartment uses the temperature of both the fuel cell stack and the EM in 2 connected feedback control loops. Whichever breaches its T_{set} first (160 °C for FC or 70 °C for EM), a signal to the cooling fan will be fired to increase its flow rate within the specified operational range (0.166-0.66 kg/s).

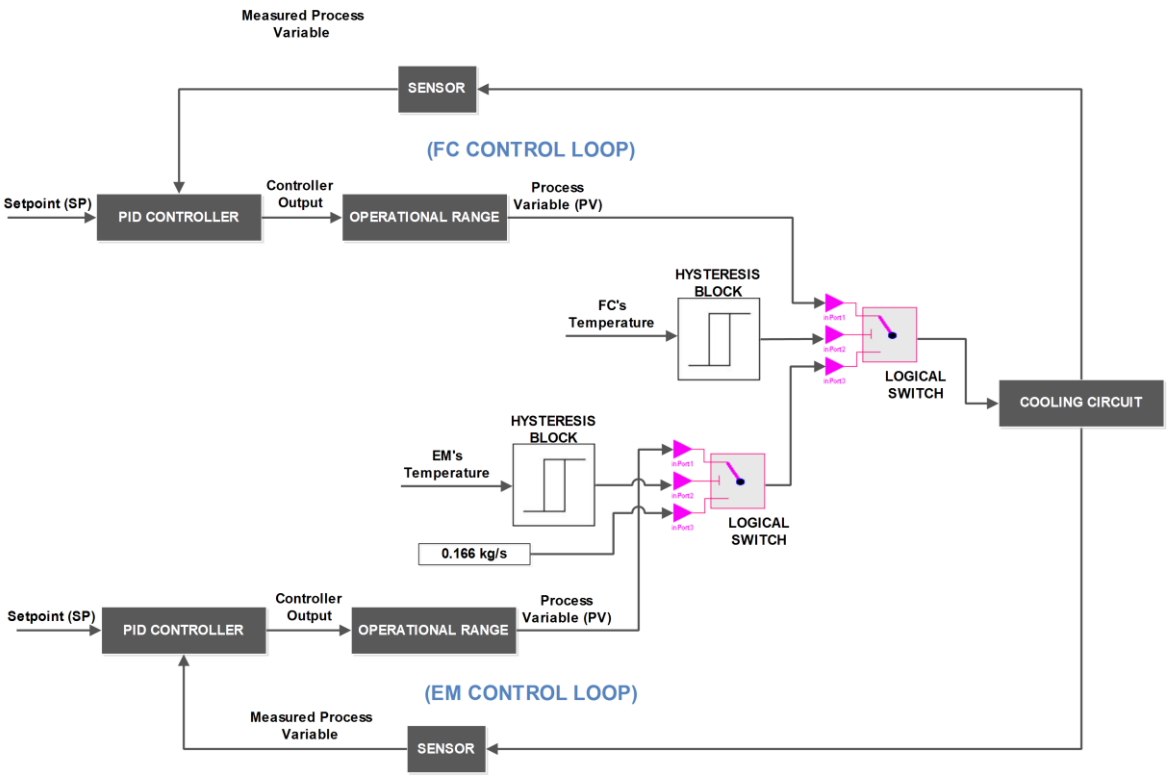

Figure 45: Air mass Flow Control Scheme

In Figure 45, the cascade control scheme involves two control loops that use two measurement signals to control one primary variable. The hysteresis blocks used in the module are responsible for firing signals; only if the upper temperature limit for EM <u>or</u> FC (70 °C or 160 °C) has been reached, to the logical switch. The logical switch will; in return, activate either the EM or FC control loop with the air mass flow rate's operational range of 0.166-0.66 kg/s. Else, the flow rate will have the value of 0.166 kg/s.

2.3.5.3 HT Model Control

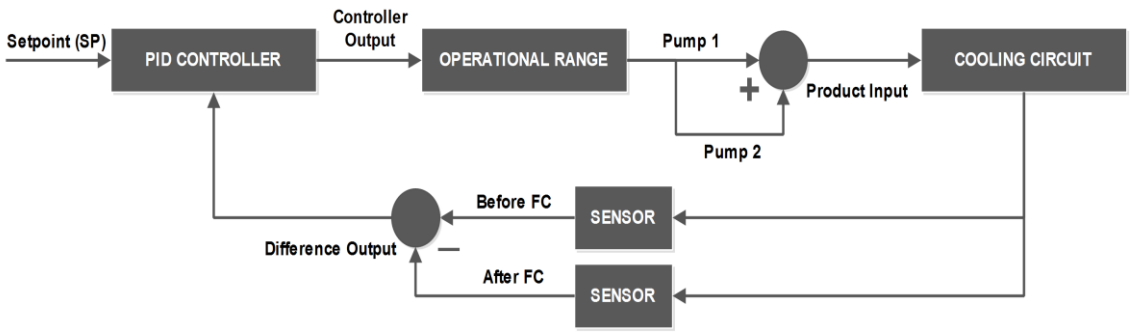

Figure 46: FC Temperature Control Scheme

In Figure 46, the difference between the coolant's entering and exiting temperatures to the FC should always be kept at 10 °C. Therefore, the operational range of the pumps' mass flow rates is 0.16-0.5 kg/s. Referring to Figure 35, the calculated mass flow rate to the circuit is divided between the Main and Cabin HEXs. Since the model is studied in summer, 100 % of the flow will be directed to the Main HEX only.

2.3.5.4 A/C Model Control

Referring to Figure 42, the initialization parameters of the A/C model have been changed with respect to the Battery cooling model. The initial value of the condenser air mass flow rate has been set to 0.166 kg/s, which is similar to the minimum value of air mass flow rate in the flow source inside the Battery model.

The compressor's speed has been lowered down to 10 Hz; after observation, to decrease the amount of heat exhausted by the output air port of the condenser which is used to cool down the NT HEX inside the LT model.

Respectively, the evaporator air outlet temperature has been increased but within an acceptable range for cooling the vehicle compartment in hot summer conditions.

The air mass flow rate inside the evaporator has been set to the maximum value inside DLR test vehicle passenger compartment. All other parameters were kept as default.

2.3.6 Coupling in Dymola

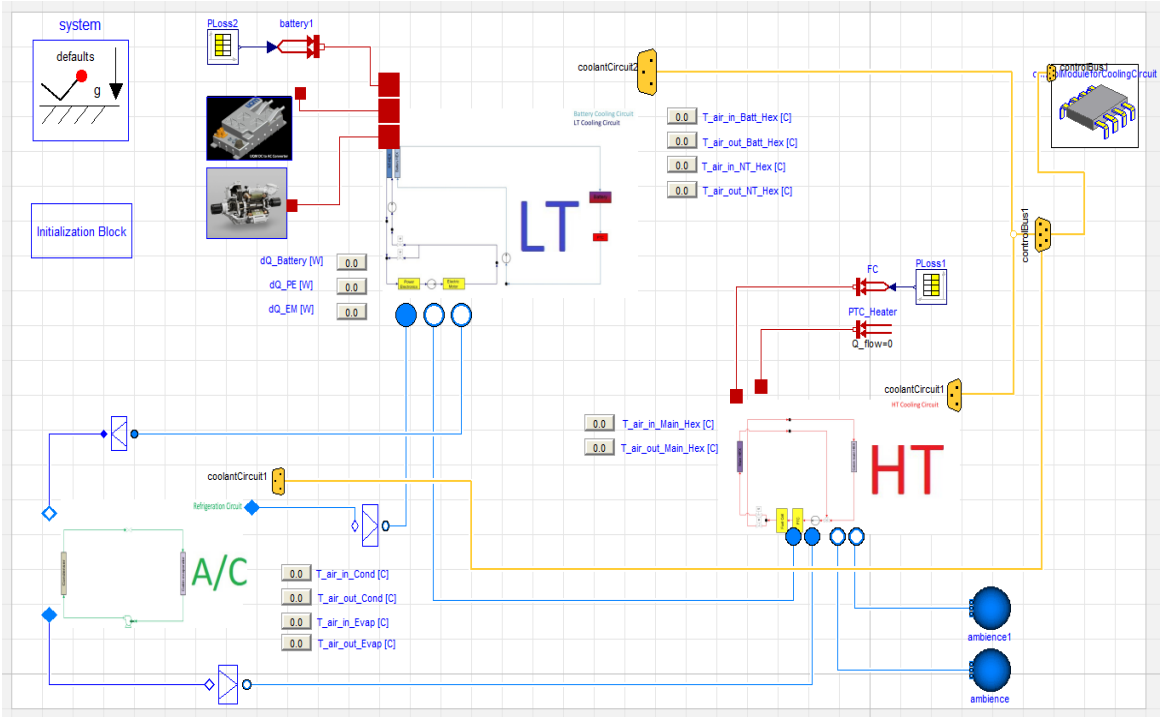

Figure 47: General Model Coupled Layout in Dymola

As seen in Figure 47, the 4 models which were build singularly have been now coupled all together from the air side. This is typically a translated model for the layout seen in Figure 17 in the simulation environment Dymola.

In the figure above, both Battery and LT models have been inserted in one package named "LT".

For the direct monitoring of temperatures, an IntegerExpression block has been used to interface the inlet and outlet air temperatures of the NT, Battery, Condenser, Evaporator and Main HEXs. Also the heat output flow from the Battery, PEM and EM submodels has been monitored.

For rapidly changing the initialization parameters, an initialization block has been used for changing the starting temperatures of EM, Battery, PEM, FC , evaporator air, condenser air and the refrigerant mass flow rate in the A/C model. (see Figure 48)

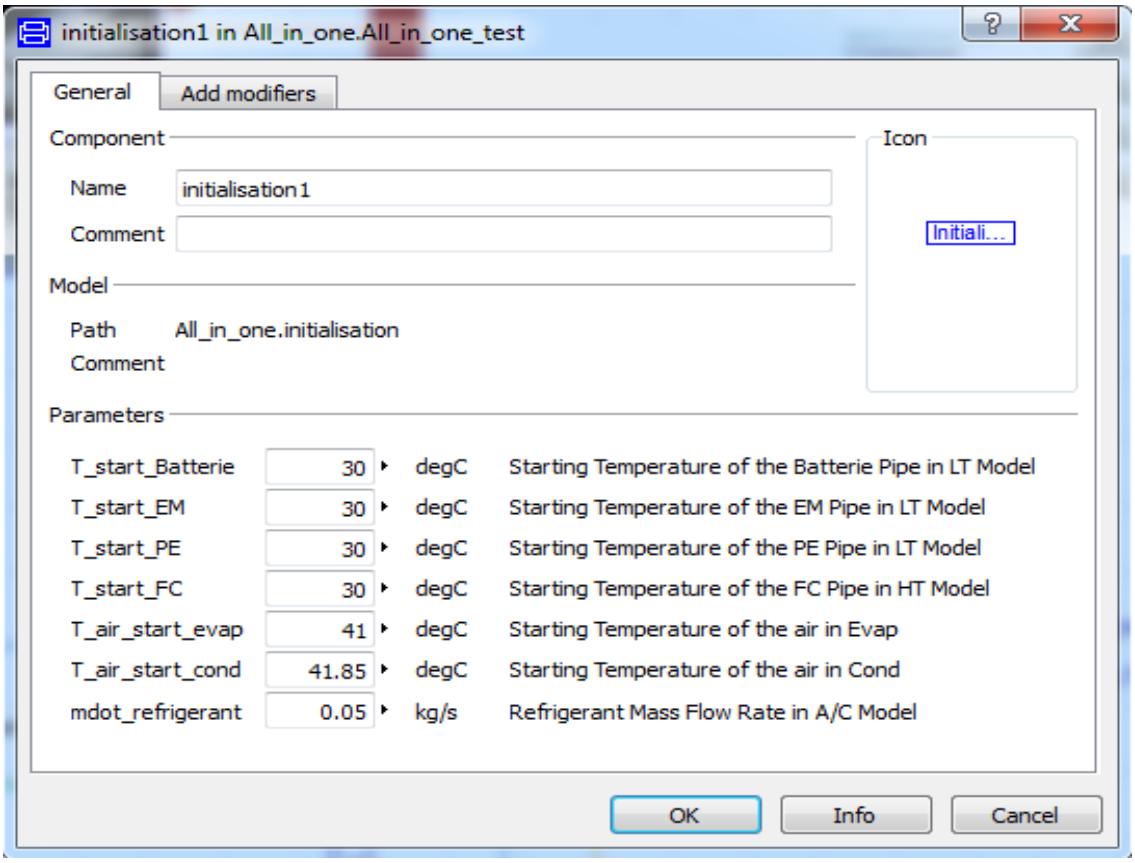

Figure 48: Initialization Block

The general model has been simulated till a stop time of 3500 s which is equivalent to a 3 NEDCs and a number of intervals of 500. The simulation real runtime was 13380 s.

Due to the stiffness of the differential equations inside the model, the solver (Radau IIA – order 5 stiff) has been used instead of Dassl.

2.3.6.1 Simulation Results

➢ **Electric Motor**

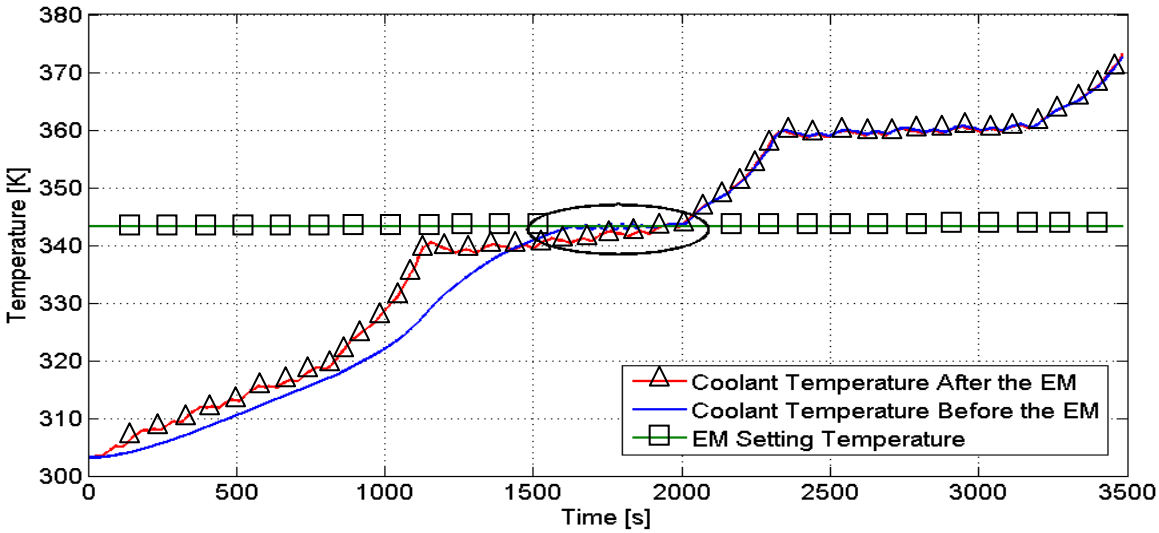

Figure 49: EM Cooling Effect

In Figure 49, the blue curve represents the coolant temperature before the EM pipe (controlled EM's temperature) and the red curve represents the coolant temperature after the EM pipe (after heat is transferred from the EM to the coolant).

Obviously, that the temperature of the coolant before the EM has shown a decreasing attitude being less than the temperature that exits out of the EM. At the circled area (at approx. 2nd NEDC), the control module tries to lower down the temperature of the coolant to T_{set} (70 °C) but the temperature of the EM has arisen to a limit where the NT HEX's size and the pump's flow rate were not able to cool it down.

As increasing the heat transfer area of the HEX is no longer having a cooling effect, we can:

- Change the arrangement of the HEXs or even separate the LT cooling circuit.
- Change the coolant type.
- Use water chiller instead of HEX to cool down the EM.
- Use cooling fan (blower) as a forced convection magnitude inside the motor thermal submodel.

- **Power Electronics Module**

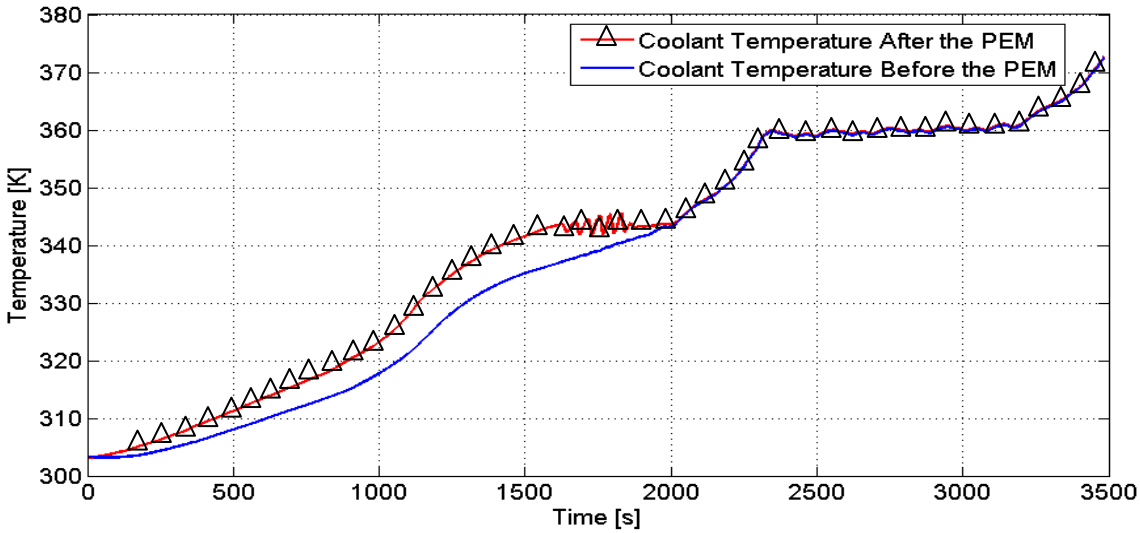

Figure 50: PEM Cooling Effect

As shown in Figure 50 and due to the cooling effect in the LT circuit, the temperature of the PEM has also been decreased as the blue line represents the temperature after cooling and the red line represents the temperature before cooling down the PEM.

- **Battery**

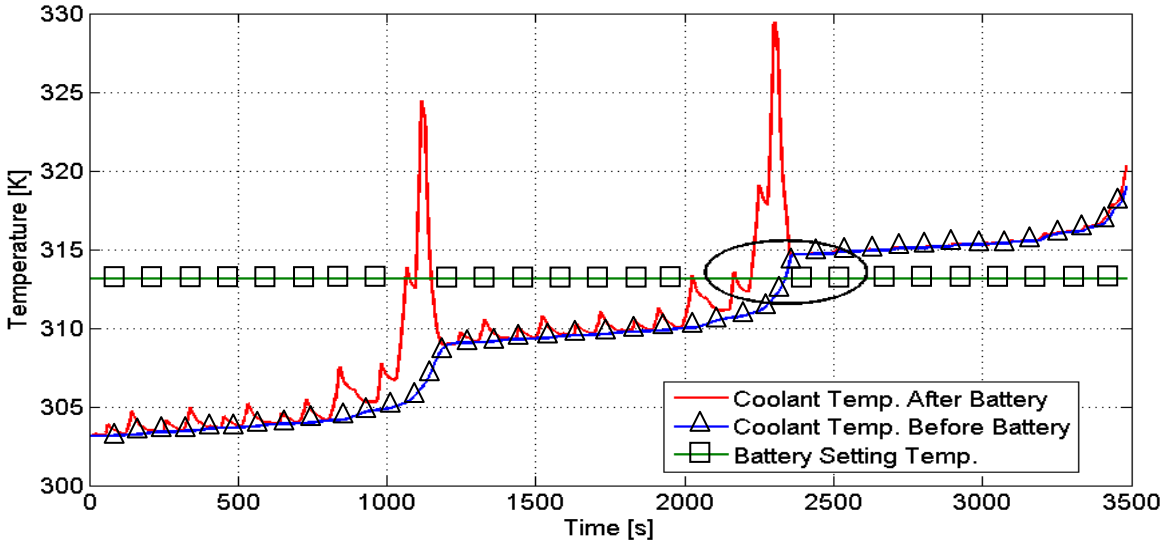

Figure 51: Battery Cooling Effect

As shown in Figure 51, that the temperature before and after the Battery is showing a cooling effect by the control module till the region where the temperature of the Battery has arisen to a limit where the battery HEX and the pump's flow rate were not able to cool it down and at 2 NEDC.

As increasing the heat transfer area of the HEX is no longer having a cooling effect, we can:

- Change the arrangement of the HEXs or even separate the LT cooling circuit.
- Change the coolant type.
- Use water chillers instead of HEX to cool down the EM.

➢ **Fuel Cell**

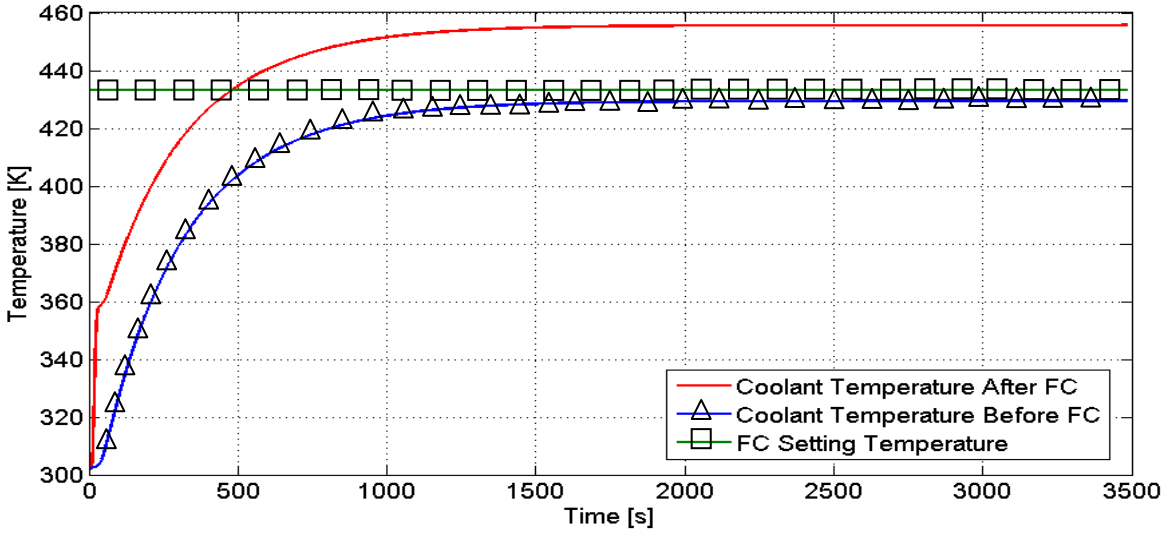

Figure 52: FC Cooling Effect

As illustrated in Figure 52, the cooling process of the FC has shown a reasonable result as the temperature of the coolant entering the stack is lower than the coolant temperature which exits the stack being always less than the FC setting temperature defined in the control module and hence maintaining a safe operating condition.

- **A/C Model**

2.3.6.2 A/C Cycle's Coefficient of Performance

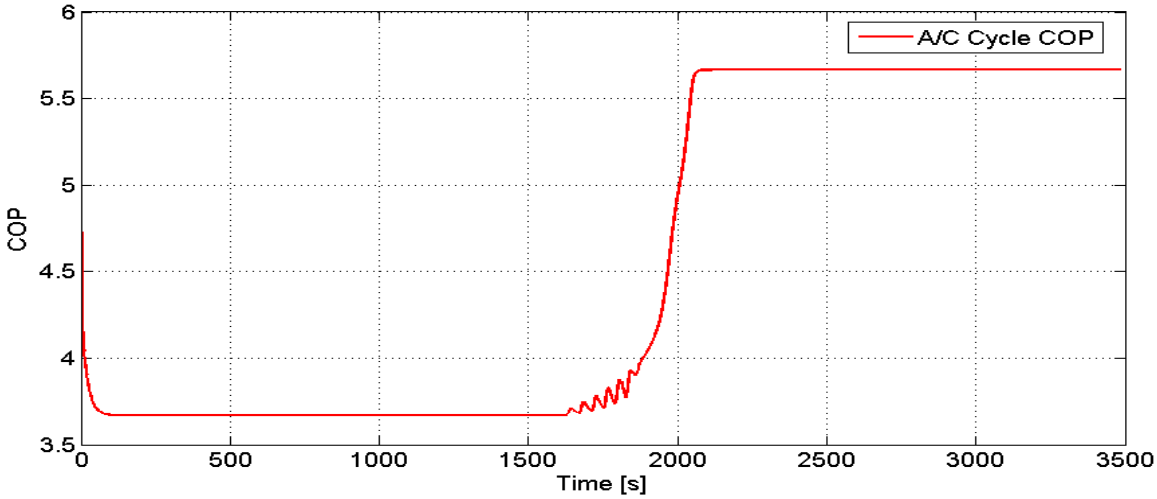

Figure 53: A/C Cycle's COP

In Figure 53, the COP has been oscillating in the range 3.7-5.7 which is quite high. The COP value is an indication for the efficiency of air conditioning cycle's operation under the given conditions of ambient temperature, humidity and mass flow rates.

- **A/C Cycle's Evaporator Outlet Air Temperature**

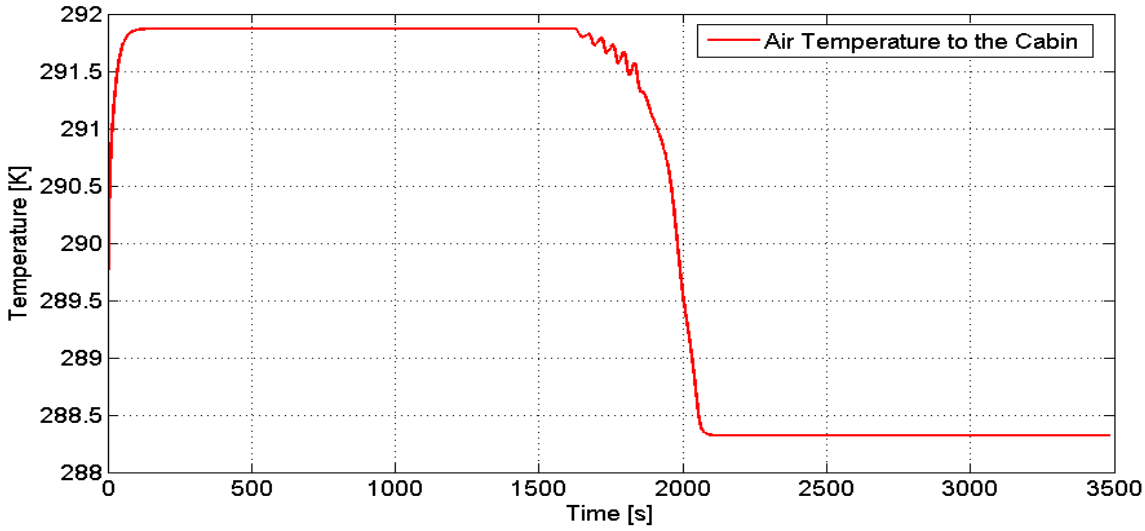

Figure 54: Evaporator's Outlet Air Temperature

In Figure 54 and under the compressor speed of 10 Hz, the outlet air temperature range to the cabin is 15-19 °C. This range seemed to be reasonable at the toughest summer conditions. The temperature could be lowered down at higher compressor speeds but it will higher up the condenser air outlet temperature and hence reduce the cooling effect on the NT HEX inside the LT cooling circuit consequently.

2.4 Coupling in BCVTB

2.4.1 What is BCVTB?

The Building Controls Virtual Test Bed is a software environment that allows expert users to couple different simulation programs for co-simulation, and to couple simulation programs with actual hardware.[xiii]

The BCVTB software has a wide compatibility with softwares like Dymola, MATLAB, TRNSYS and many more. The functioning idea of BCVTB depends on its action as a middleware for the data exchange between the coupled softwares as they simulate.

The BCVTB is based on Ptolemy II software which is an open source software framework supporting experimentation with actor-oriented design. Actors are software components that execute concurrently and communicate through messages sent via interconnected ports. A director in Ptolemy II software implements a model of computation.[xiv]

2.4.2 How BCVTB Works?

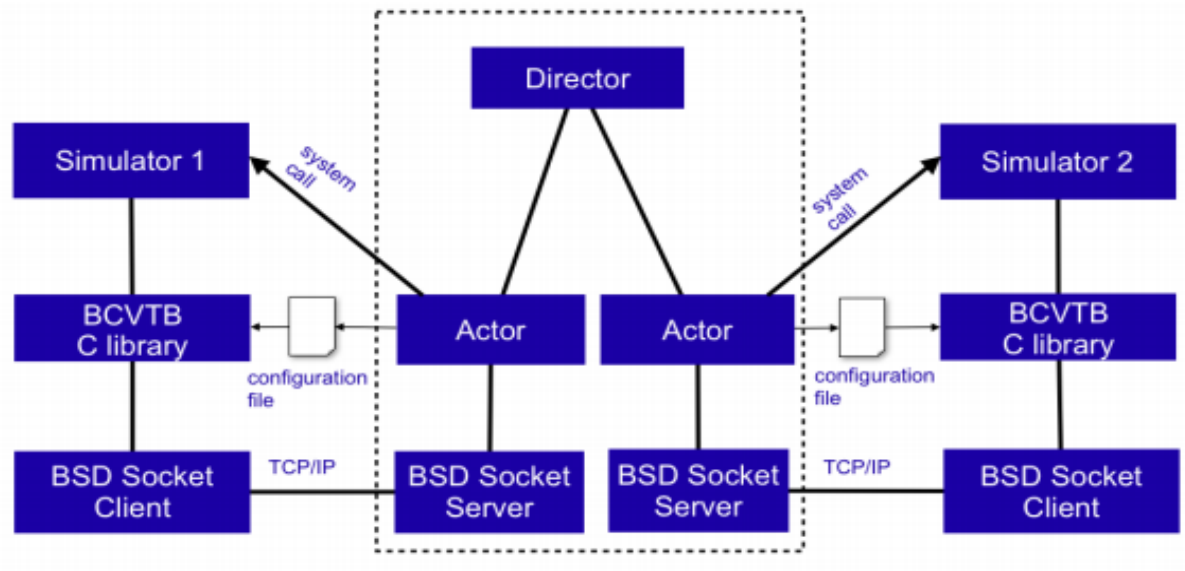

Figure 55: Architecture of the BCVTB with the middleware shown in the dotted box that connects two clients

The interaction between the actors is defined by a Model of Computation (MoC). The MoC specifies the communication semantics among ports. The director controls the communication of the actors which are connected to simulation programs[xv]. (see Figure 55)

In Figure 55, when the co-simulation starts, the director orders the actors to send a system call (firing signals) to the simulators in order to start up the simulation programs. In Ptolemy II software interface, the simulators are actually classes inside the "Actors" library. The class simulator then makes an instance of the class server through the BCVTB C library for the interprocess communication with the simulation program, which is the client. The interprocess communication is implemented using the Berkeley Software Distribution socket interface (BSD sockets). To connect to the server, the client needs to know the number of the port on which it needs to connect.

To pass the port number from the server to the client, the class Simulator writes an XML file using XML Writer, which is then read by the client at the program's start. This implementation allows the actor "Simulator" to use a system call to start any executable (such as a batch file on Windows, a shell script in Mac OS X or Linux) or to start directly any executable program that may have been compiled by the user.

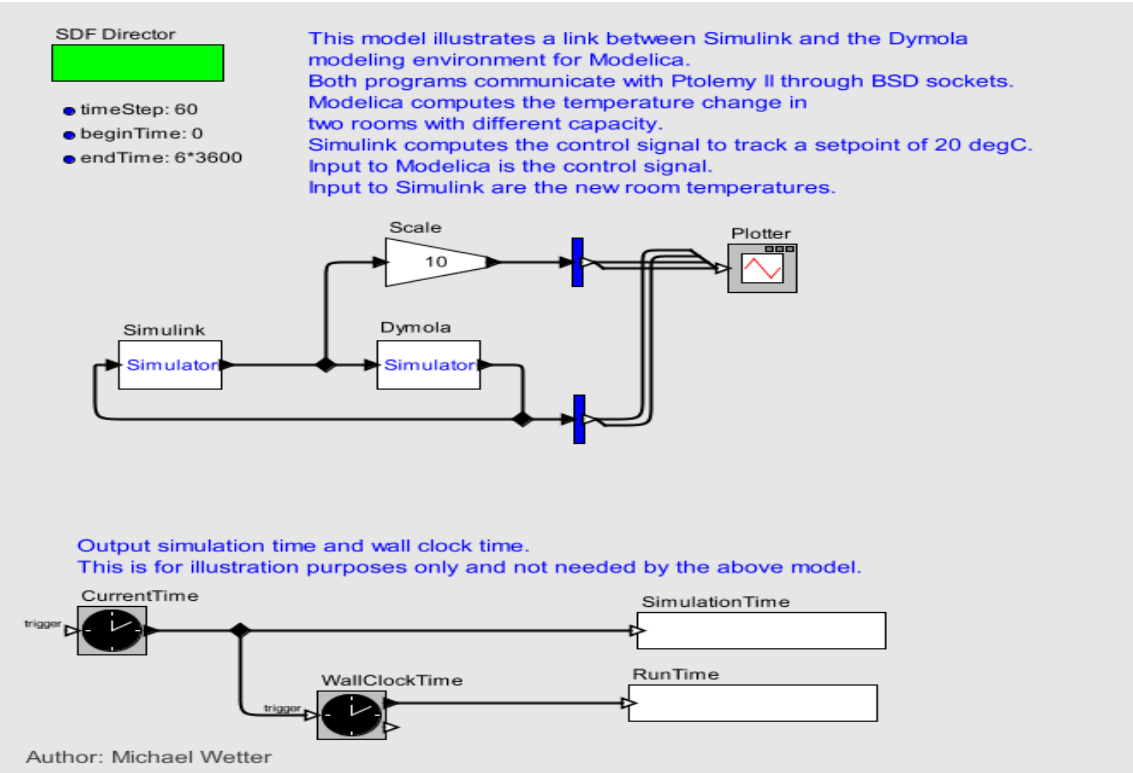

Figure 56: An Example of Connecting Dymola with Simulink for Testing BCVTB Interface

From Figure 56, we can apparently recognize that the model in Ptolemy II software basically consists of a Director (the green rectangle), Actors (Simulators), Relations (Black Diamonds), Connectors (signals), Vectors' assemblers and disassemblers.

2.4.3 Configuration of Submodels in BCVTB

As our general model consists mainly of 4 submodels (LT, HT, A/C and Control Module) coupled all together, the idea is to develop a new interface in BCVTB using "Simulator" actors denoting each submodel and connected all together with relations through input and output ports and directed by a MoC.

Before architecturing the layout of the general model in Ptolemy II, each submodel should be separately reconfigured according to the output and input parameters to it.

2.4.3.1 Configuring Control Module

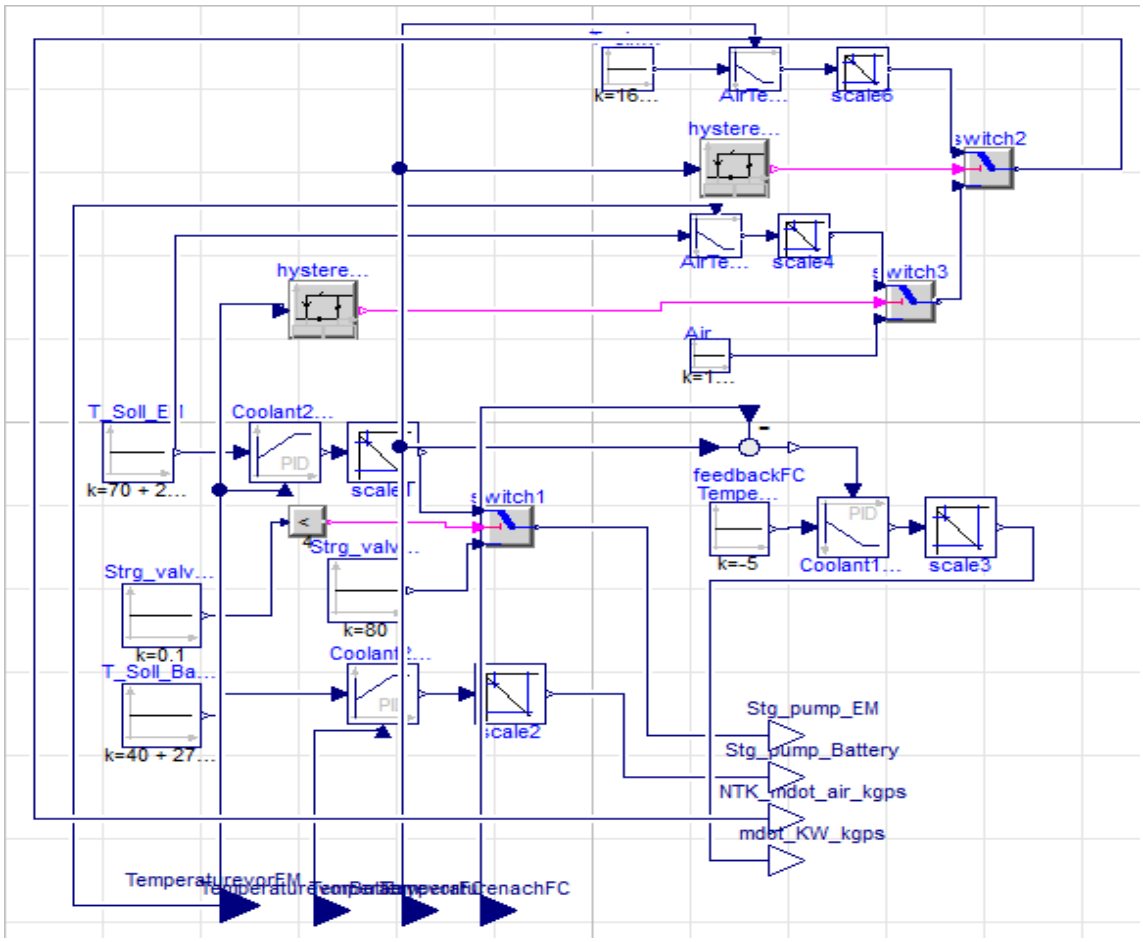

Figure 57: Control Module Base Layout in BCVTB

Compared to the layout of the control module in Dymola model and instead of connecting the input signals and distributing the output signals out of the module through signal buses, the input signals have been connected to input ports and the output signals have been connected to output ports from modelica library, each has been signified and given the name of the signal itself for designation. The setting parameters, temperatures and operating ranges have been always kept the same. (see Figure 57)

To connect the model in Dymola with BCVTB, Berkeley Lab has developed a modelica block inside modelica buildings library to exchange inputs and outputs with Ptolemy II. Inside the block, the user is able to define the synchronization time step when the data will be exchanged between Dymola and BCVTB, number of inputs and outputs (ports) sent from and to the simulator actor that represents the model in Ptolemy II interface and the initial values for each input. (see Figure 58)

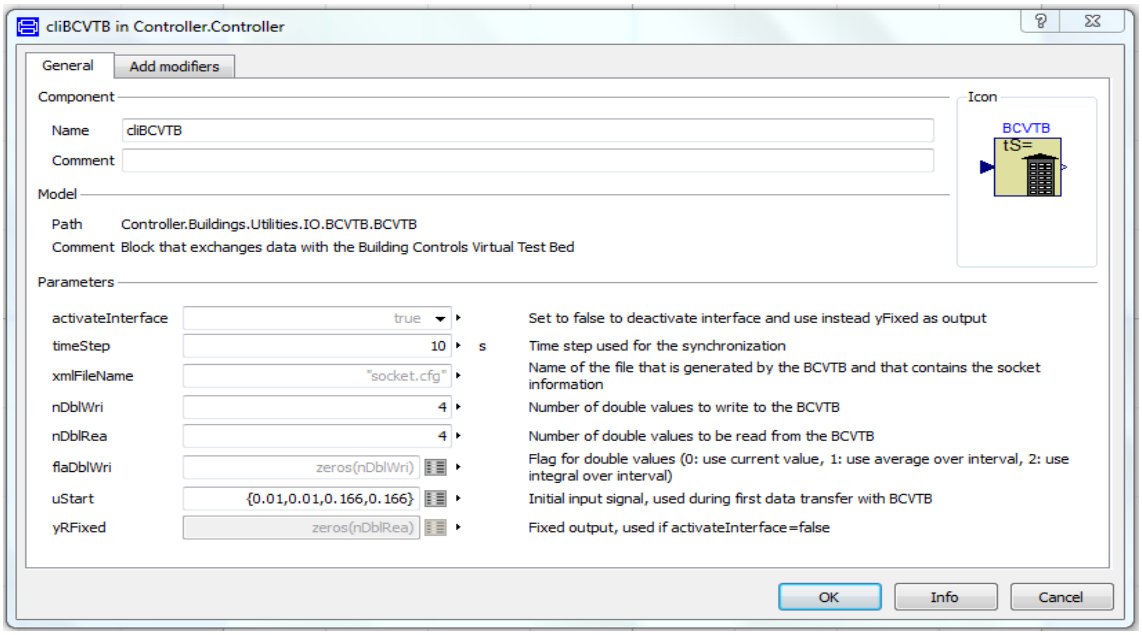

Figure 58: BCVTB Block

Now routing inputs and outputs to the BCVTB block is done using the multiplexer and demultiplexer blocks from modelica library. The inputs and outputs were connected to the BCVTB block through array slots (ports) which were given numbers as designation. The order of connected signals to the block should be concerned to ensure, that the right signal is transferred to the right submodel in Ptolemy II interface. (see Figure 59)

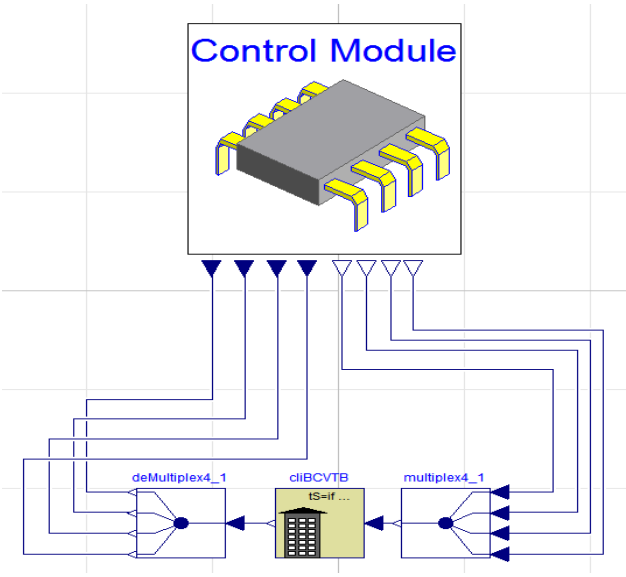

Figure 59: Control Module Configured Layout

In Dymola, all the inputs to the BCVTB block are actually outputs from the simulator actor in Ptolemy II at the same array slot, while all the inputs to the simulator actor in Ptolemy II are actually outputs from the BCVTB block in Dymola. (see Figure 60)

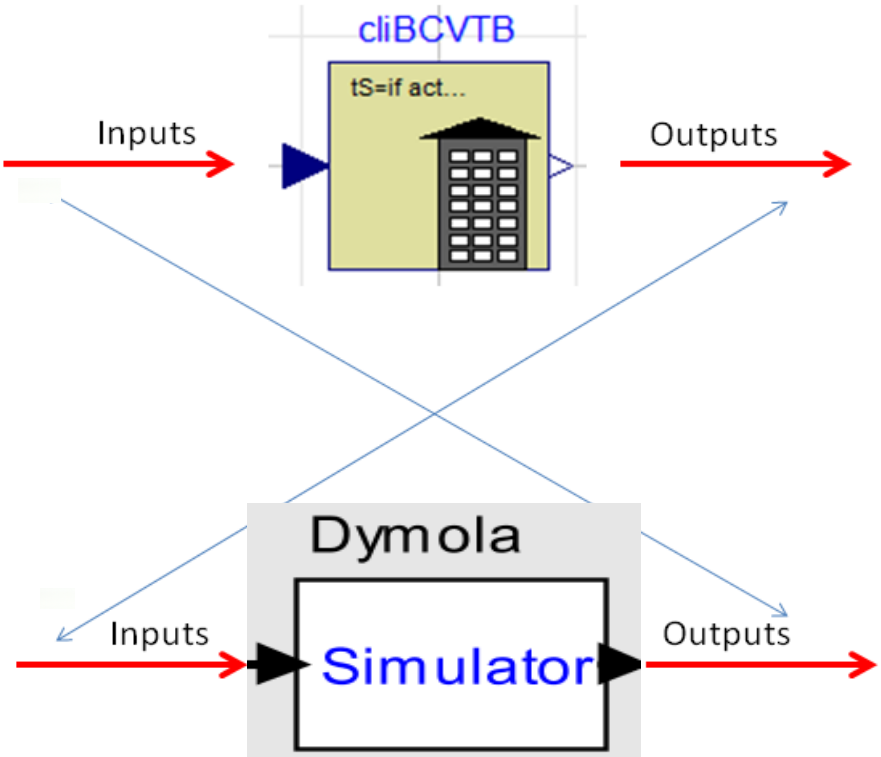

Figure 60: Data Exchange between Dymola and BCVTB

To reduce the number of transferred signals, constant values; which are not subjected to change during simulation, have been used directly inside the models where they belong (e.g. Cabin air mass flow rate).

Table 8: Inputs and Outputs to the BCVTB Block in the Control Module

Variables / Array no.	Inputs	Outputs	Initial values of inputs
1	Stg_pump_EM	TemperaturevorEM	0.01
2	Stg_pump_Battery	TemperaturevorBattery	0.01
3	NTK_mdot_air_kgps	TemperaturevorFC	0.166
4	mdot_kw_kgps	TemperaturenachFC	0.166

2.4.3.2 Configuring LT and Battery Models

Similar to the control module, the LT and Battery models have also been reconfigured to group out the inputs and outputs into and from the models and to be transferred to Ptolemy II through the BCVTB block in Dymola. (see Figure 61)

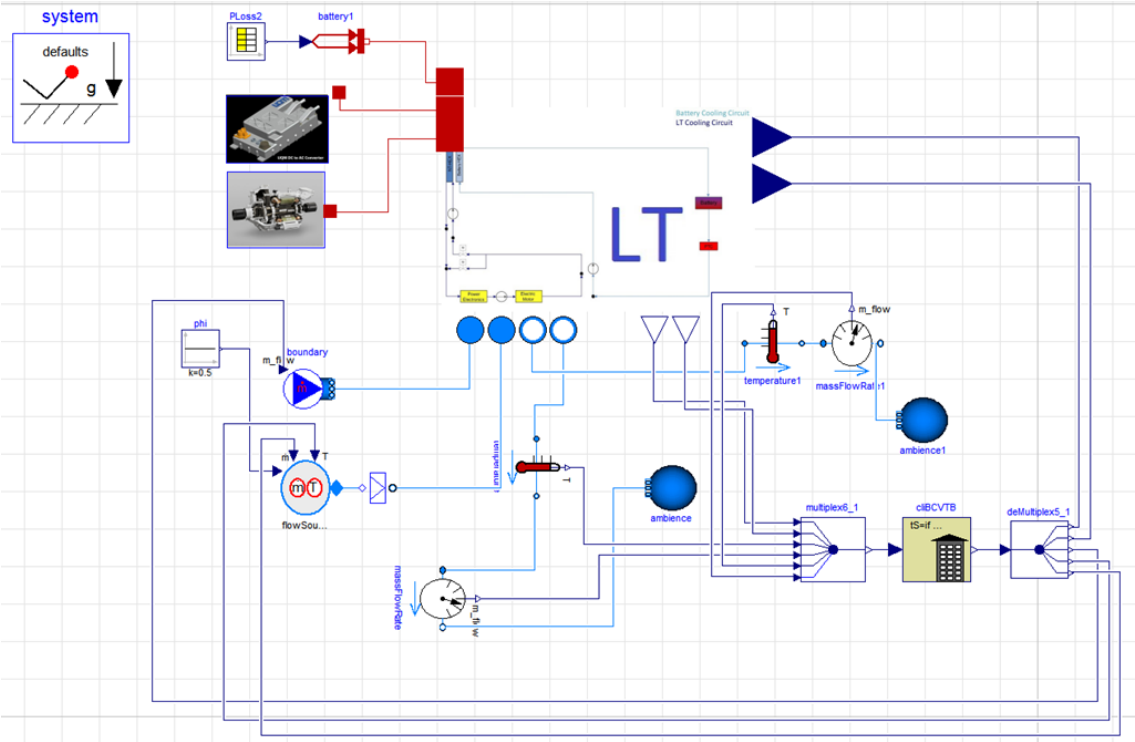

Figure 61: LT and Battery Configured Models' Layout in BCVTB

Table 9: Inputs and Outputs to the BCVTB Block in the LT and Battery Models

Variables / Array no.	Inputs	Outputs	Initial values of inputs
1	TemperaturevorEM	Stg_pump_EM	303.15
2	TemperaturevorBattery	Stg_pump_Battery	303.15
3	Temp_air_out_Battery_HEX	NTK_mdot_air_kgps	303.15
4	air_massflow_out_Battery_HEX	Temp_air_in_NT_HEX	0.166
5	Temp_air_out_NT_HEX	air_mass_flow_in_NT_HEX	303.15
6	air_massflow_out_NT_HEX	-	0.05

In order to couple the submodels from the air side, properties like mass flow rate and temperature were sensed and sent as signals to BCVTB block. These signals are then used as inputs to flow sources in the recipient submodel connected in Ptolemy II interface for coupling.

Because air flow properties in output ports should be measured, these ports are connected to flow sinks and both temperature and mass flow rate signals are measured and sent to the BCVTB block.

2.4.3.3 Configuring A/C Model

Similar to the Control Module, LT and Battery models, the A/C model has been also reconfigured to group out the inputs and outputs into and from the model and to be transferred to Ptolemy II through the BCVTB block in Dymola. (see Figure 62)

The air properties fed to the evaporator are constant and hence, there was no need to transfer them in a form of input and output signals to the BCVTB.

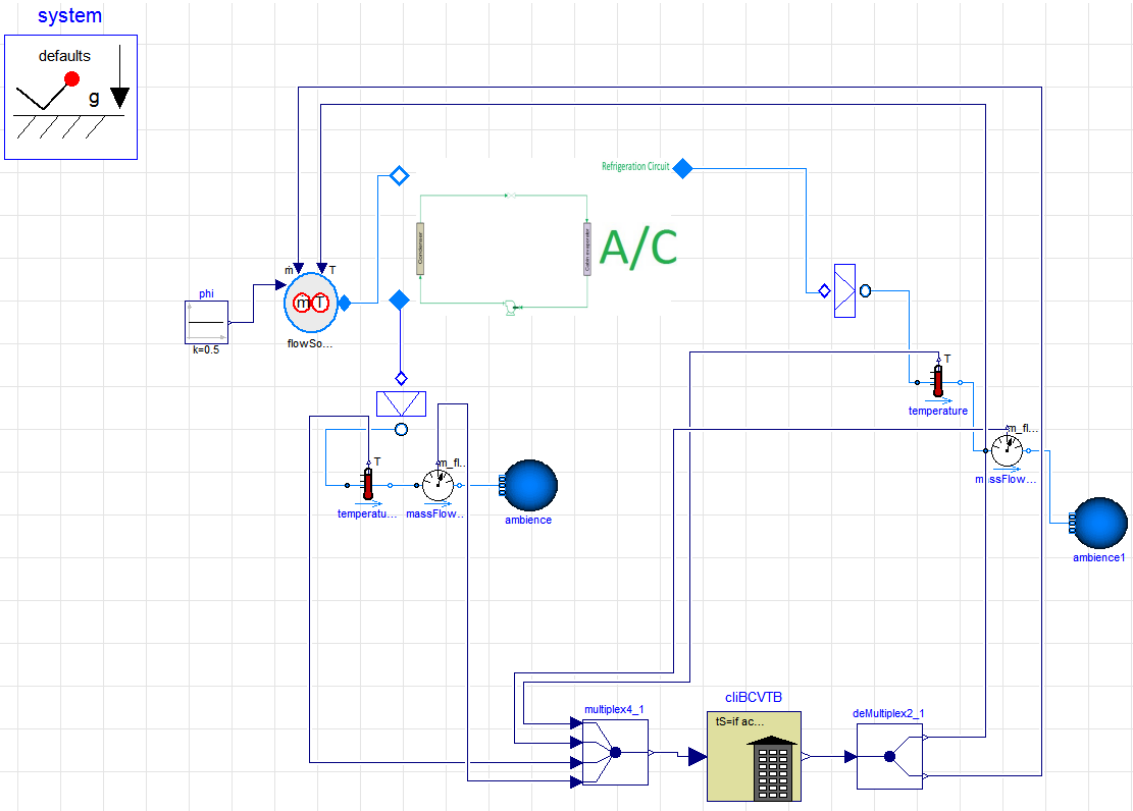

Figure 62: A/C Configured Model Layout in BCVTB

Table 10: Inputs and Outputs to the BCVTB Block in the A/C Model

Variables / Array no.	Inputs	Outputs	Initial values of inputs
1	Temp_air_in_NT_HEX	Temp_air_out_Battery_HEX	315
2	air_mass_flow_in_NT_HEX	air_mass_flow_out_Battery_HEX	0.166
3	Temp_air_in_Cabin_HEX	-	314.15
4	air_mass_flow_in_Cabin_HEX	-	0.06

2.4.3.4 Configuring HT Model

Similar to the former models, the HT model has been also reconfigured to group out the inputs and outputs into and from the model and to be transferred to Ptolemy II through the BCVTB block in Dymola. (see Figure 63)

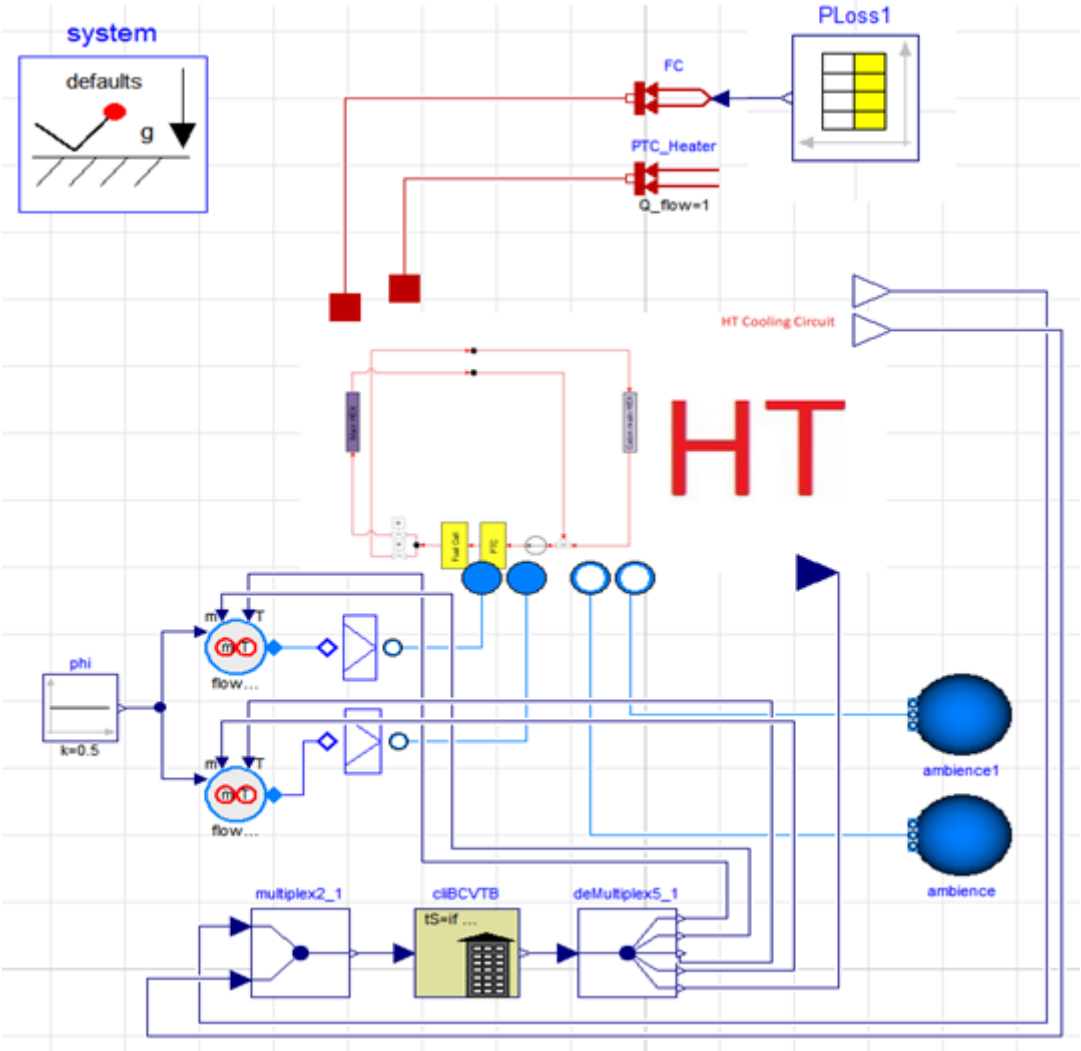

Figure 63: HT Configured Model Layout in BCVTB

Table 11: Inputs and Outputs to the BCVTB Block in the HT Model

Variables / Array no.	Inputs	Outputs	Initial values of inputs
1	TemperaturevorFC	Temp_air_in_Main_HEX	303.15
2	TemperaturenachFC	air_mass_flow_in_Main_HEX	303.15
3	-	Temp_air_in_Cabin_HEX	-
4	-	air_mass_flow_in_Cabin_HEX	-
5	-	mdot_kw_kgps	-

2.4.4 General Model Layout in BCVTB

Just like in Dymola, the general model will consist of connecting the submodels all together from the air side in the HEXs concerning the arrangement that was set from the beginning.

As simulating each model requires input data from others, the layout will have the structure of a closed loop with feedback signals. Since the air flow starts from the Battery model and passes through the A/C and HT models, the general layout in Figure 64 has all the connections denoting the outputs and inputs from and to each model depending on the required input signals for simulation and output signals for running the other models.

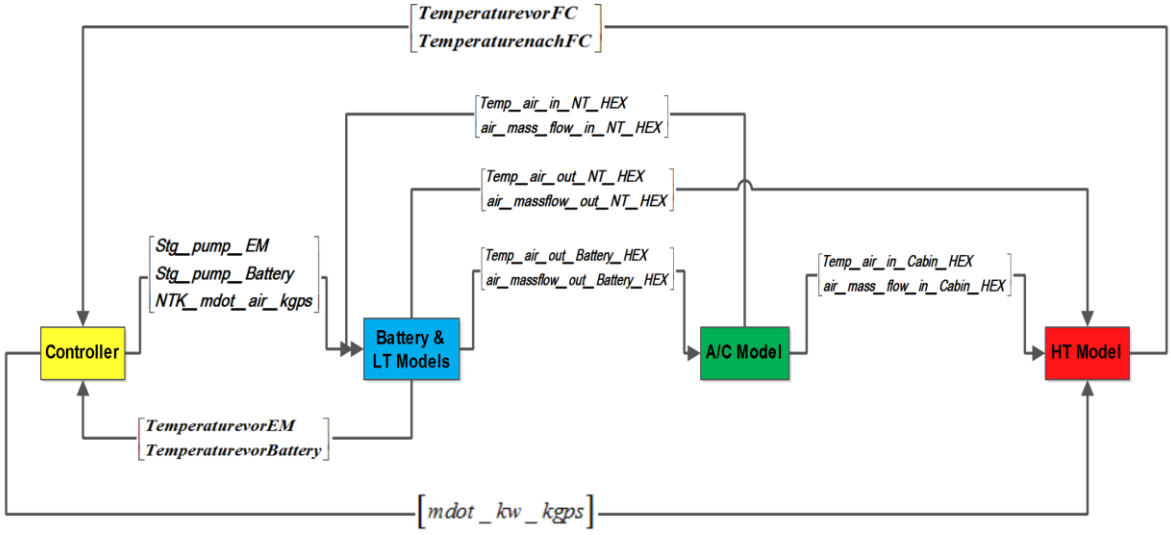

Figure 64: Conceptual Architecture of the General Model in Ptolemy II

The structure above was chosen to satisfy the direction of the air flow which starts from the Battery model in the engine compartment and the A/C model in the passenger compartment. The feedback lines will contain the output signals that should be transferred as a input data to run other models.

The order of the actors in the structure above could be changed but the order of the input and output signals in the arrays connected to the BCVTB block in each model should also be reconfigured to match with the proper array slots in each corresponding model.

For each model, a separate folder has been established and the contents of the "dymola-room" example from Ptolemy II library have been copied and pasted except the file "TwoRoomsTotal.mo" which will be substituted with the model developed.

Each folder should basically have:

1- bcvtb.h C/C++ file to allow the Dymola simulation environment to establish a socket connection with BCVTB.
2- build.xml file to pass the port number where the inputs and outputs are transferred from the server to the client program.
3- simulation.log file where all the info regarding the compilation and the simulation run should be stored.
4- simulateAndExit.mos which is a Modelica script file that contains the model name, path, start-time, stop-time and tolerance of the simulation.

In each folder, the model name, path, start and stop time of the simulation and tolerance should be changed in the modelica script file (simulateAndExit).

In the script file (line 11), the script (method: "radau") has been added to specify the solver with which the simulation in Dymola should be running.

Also to stop Dymola from closing after the co-simulation execution, the script (exit();) in line 12 has been deleted.

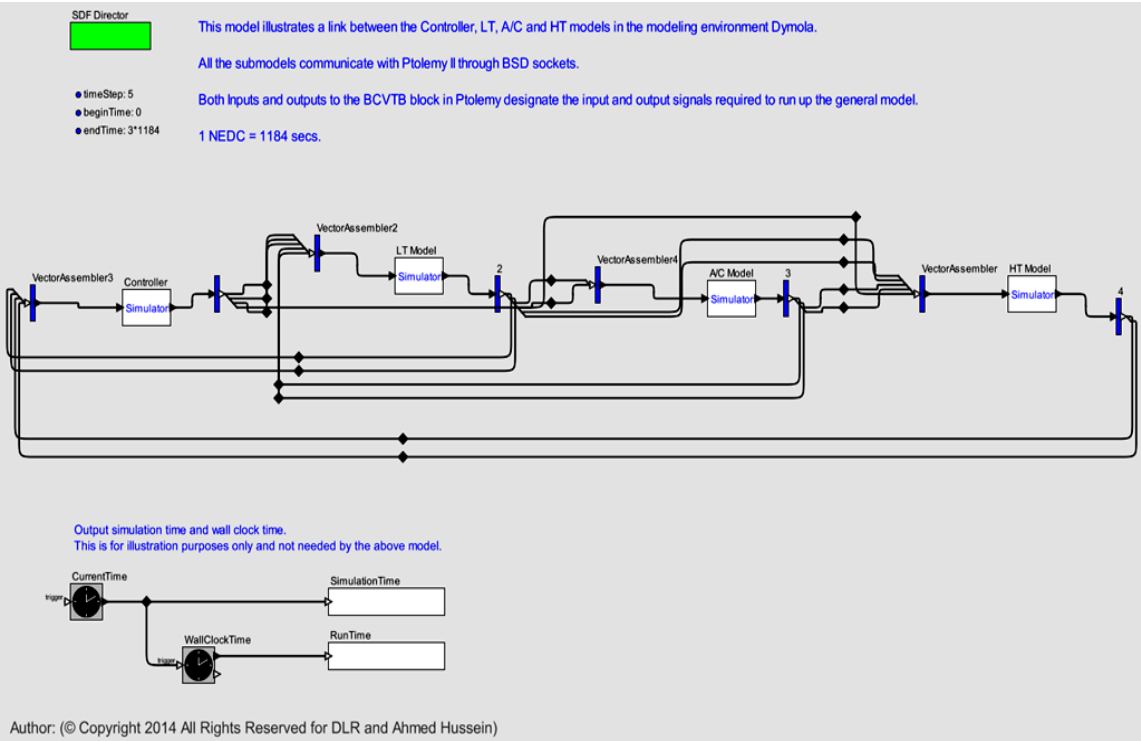

Figure 65: General Model Coupled in Ptolemy II

In translation to Figure 64, Figure 65 represents the layout of the general model after coupling all submodels in Ptolemy II interface.

The Synchronous Data Flow (SDF) director is a MoC that controls the communication of the actors which are connected to simulation programs. In SDF, each actor is fired only when a fixed, pre-specified number of tokens (inputs) is available on each of its input ports. In the SDF domain, each actor produces a fixed, pre-specified number of output tokens at each firing.

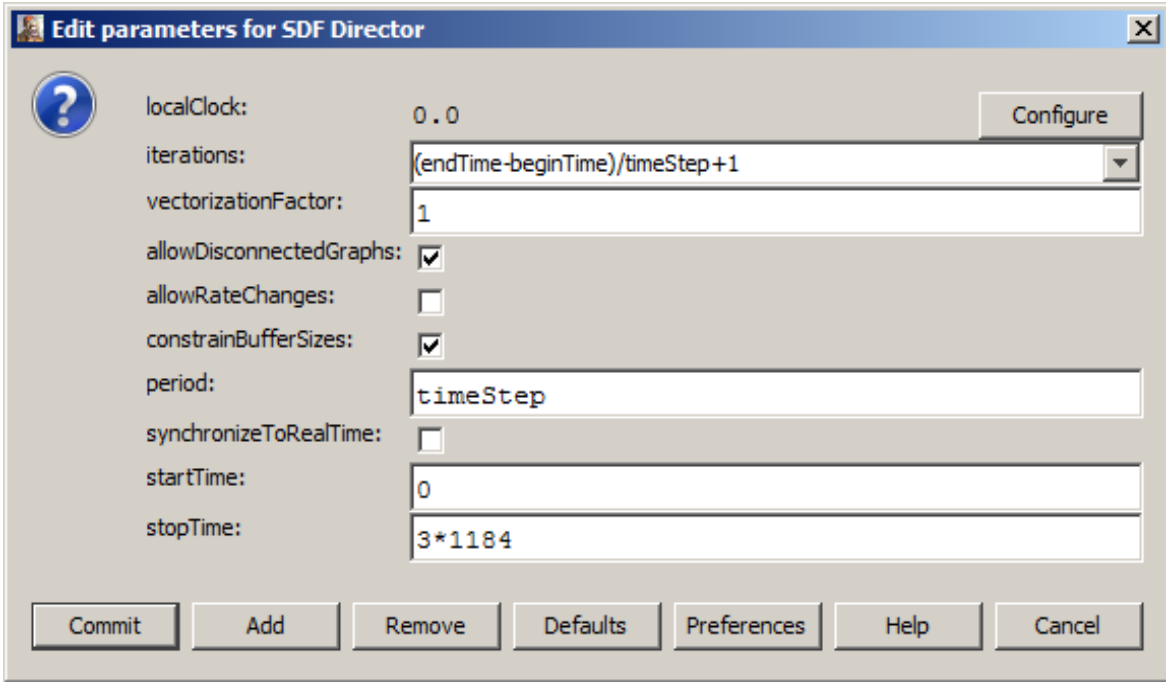

Figure 66: SDF Director

As shown in Figure 66, the simulation start and stop times as well as the iterations are specified in prior to the initialization of the co-simulation. Other options are to allow disconnected graphs in case that a model has skipped the data exchange in a certain simulation time step.

There's also a possibility to synchronize the simulation time with the real time.

In Figure 65, the interface of the general model in BCVTB consists of a Director, 4 Simulators (Actors), Relations (Black Diamonds), connectors, Vectors (signals) assemblers and disassemblers.

The 4 simulators (actors) denote all the submodels which form the cooling and air conditioning circuits in the FCEV (one actor for each submodel).

The actors (models) are connected with connectors through relations of width=1. The width of a connector or a relation is the sum of the signals transported per each path.

2.4.5 Data Transport between Actors in BCVTB

Data transport is depicted in Figure 67. The originating actor E1 has an output port P1, indicated in the figure with an arrow in the direction of token flow. The destination actor E2 has an input port P2, indicated in the figure with another arrow.

E1 calls the send() method of P1 to send a token t (signal) to a remote actor. The port obtains a reference to a remote receiver (via the IO Relation in the BCVTB block in Dymola model) and calls the put() method of the receiver, passing it the token. The destination actor retrieves the token by calling the get() method of its input port, which in turn calls the get() method of the designated receiver (Department of Electrical Engineering and Computer Sciences, University of California at Berkeley, April 1, 2008).

xvi

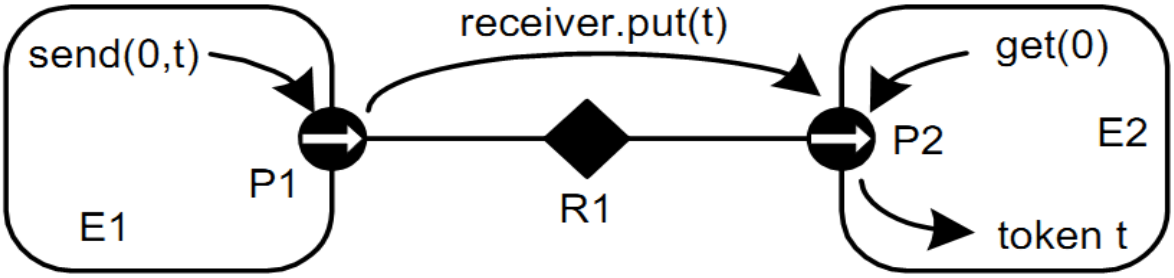

Figure 67: Data Transport between Actors in BCVTB

In Figure 67, message passing is mediated by the IO Port class. Its send() method obtains a reference to a remote receiver, and calls the put () method of the receiver, passing it the token t. The destination actor retrieves the token by calling the get () method of its input port.

Since the IO Ports of the actors are single ports, an advantage has been taken by using the vector assemblers and disassemblers in Ptolemy II interface to connect more than one relation at a single port.

2.4.6 Co-simulation Results and Validation

The model in Ptolemy II is supervised by SDF director as a MoC which demands the so-called firing of the individual simulators every 5 seconds (TimeStep=5).

The simulation time stopped at 3500 s which is equivalent to a 3 NEDCs. The simulation real runtime was 4223 s.

- **Electric Motor**

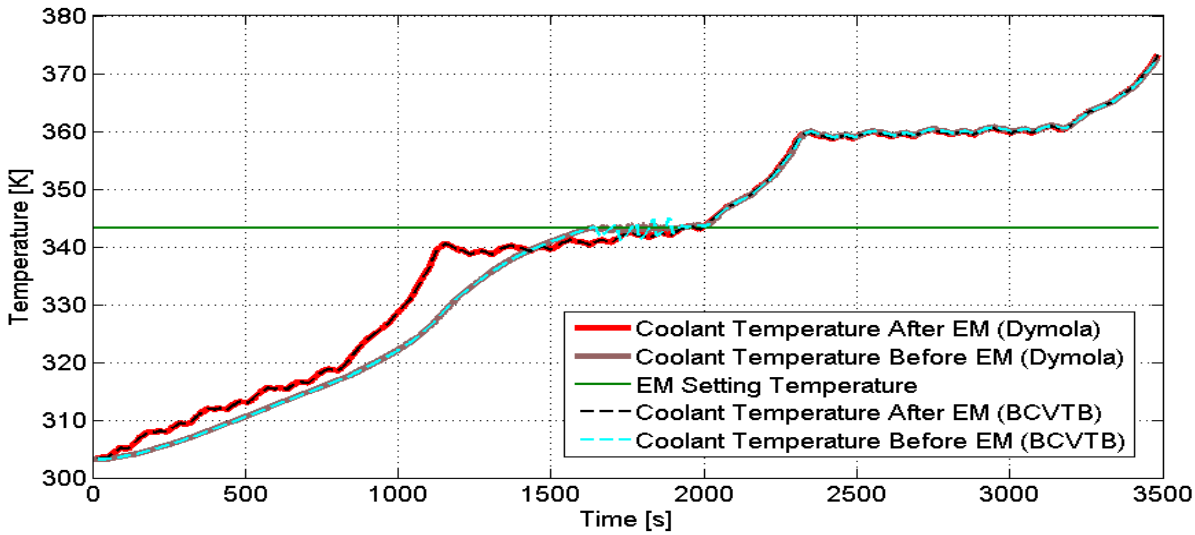

Figure 68: Comparison between EM Cooling Effect in BCVTB and Dymola

- **Power Electronics Module**

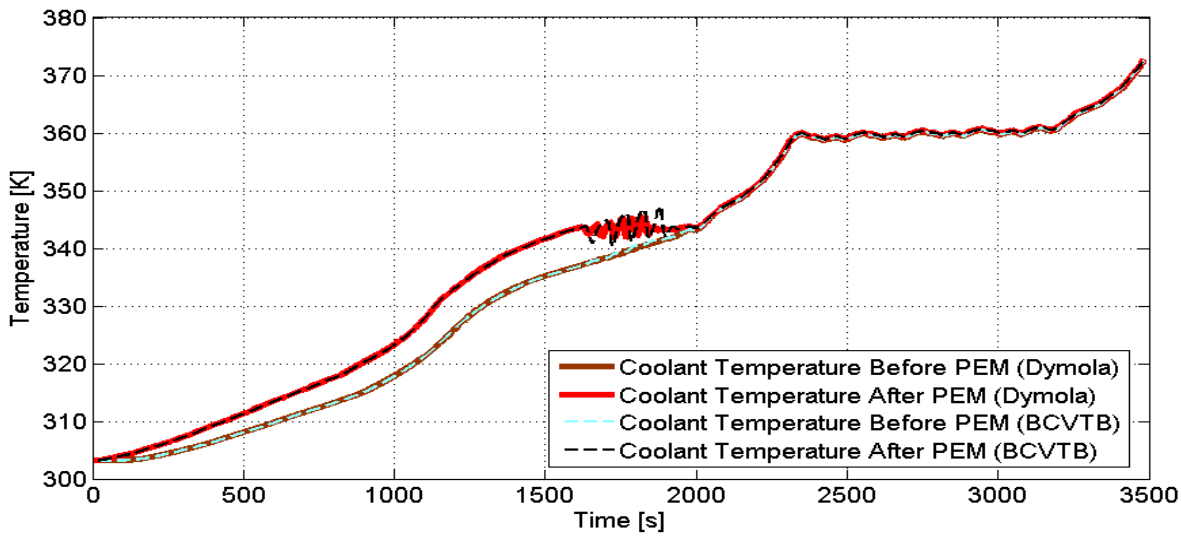

Figure 69: Comparison between PEM Cooling Effect in BCVTB and Dymola

- **Battery**

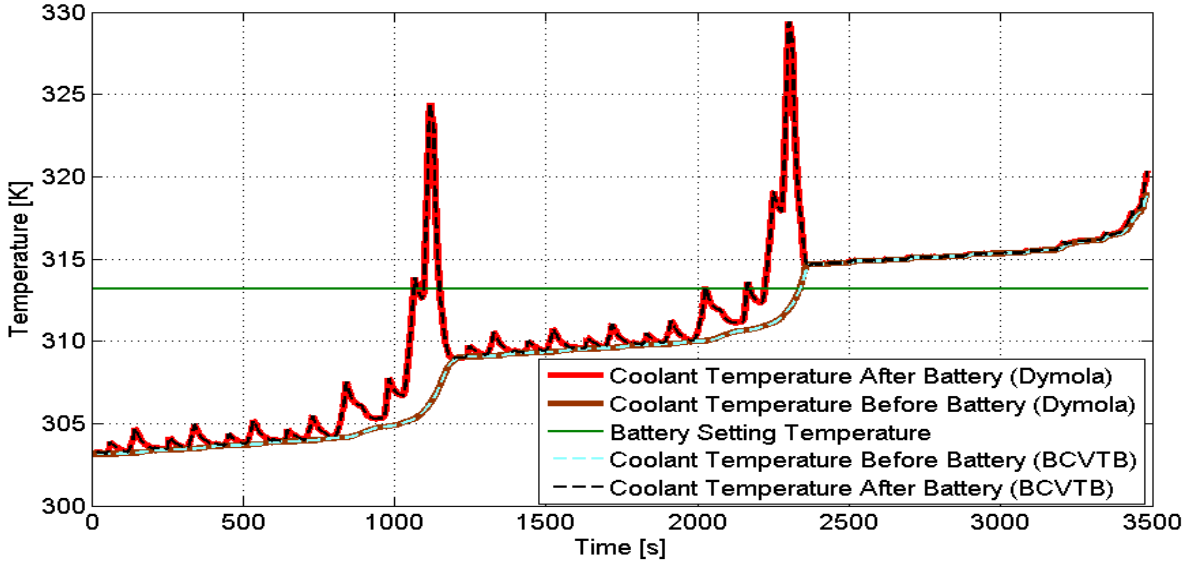

Figure 70: Comparison between Battery Cooling Effect in BCVTB and Dymola

- **Fuel Cell**

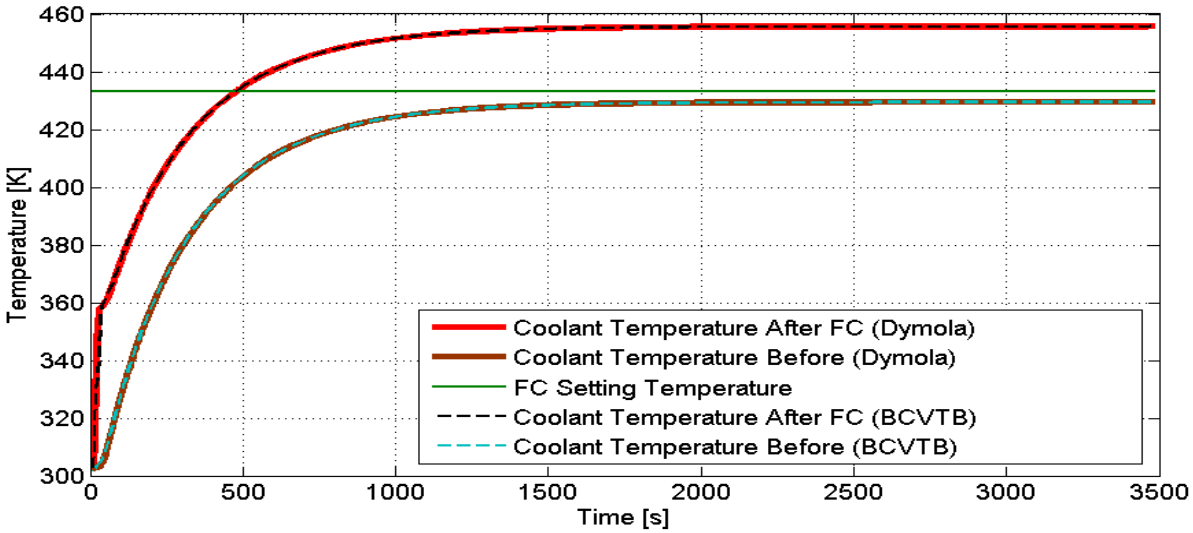

Figure 71: Comparison between FC Cooling Effect in BCVTB and Dymola

- **A/C Cycle's COP**

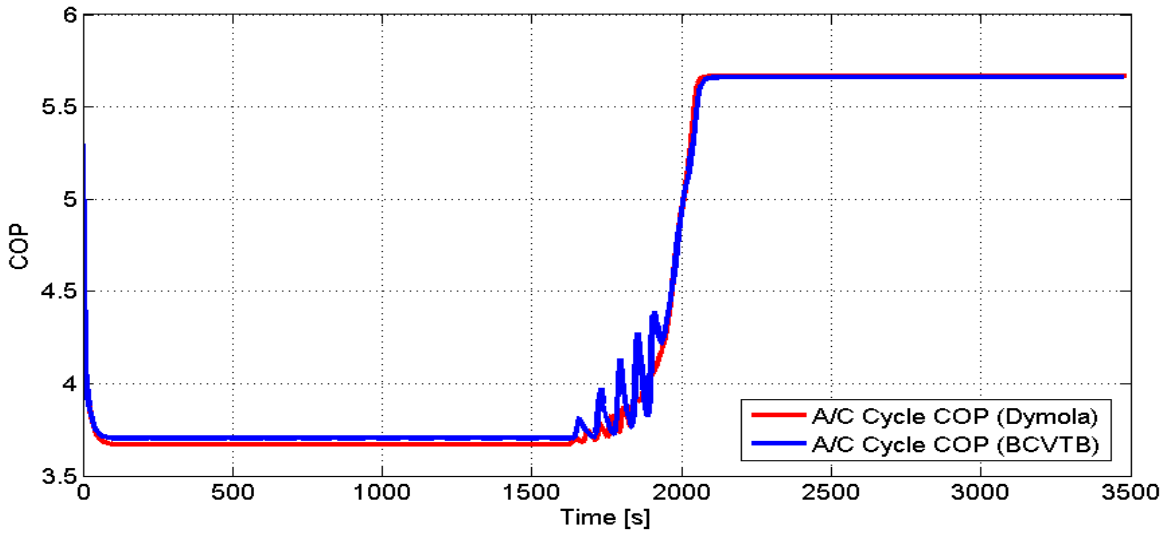

Figure 72: Comparison between COP in BCVTB and Dymola

- **A/C Cycle's Evaporator Outlet Air Temperature**

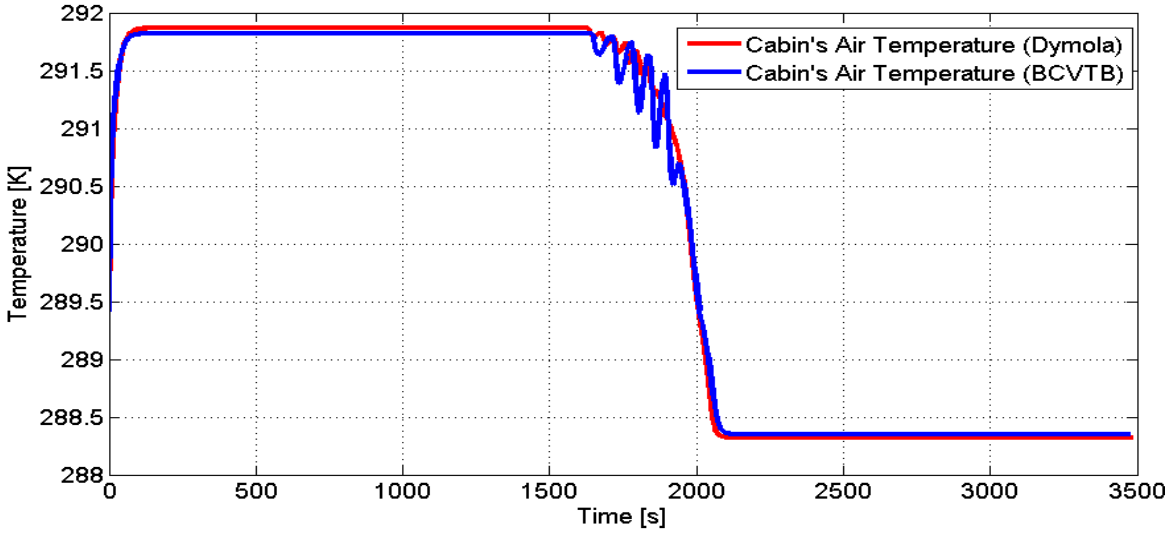

Figure 73: Comparison between Cabin's Air Temperature in BCVTB and Dymola

Referring to the co-simulation results, they have shown symmetry to the coupling results from Dymola in each submodel. The curves in most cases have collaterally progressed with the results from Dymola and sometimes congruently. This has indicated a satisfactory range of accuracy consistent with the intended validation of coupling.

Using equation (8) and for co-simulation in BCVTB with TimeStep=5 and 10 s, the accuracy of the synchronized data exchange; at similar temporal point, has been calculated at 99 % and 98 %; respectively, when compared with coupling in Dymola.

$$Accuracy_{TimeStep}(\%) = 1 - \frac{data\ point_{TimeStep} - data\ point_{Dymola}}{data\ point_{Dymola}} \cdot 100 \qquad (8)$$

2.5 Comparison and Conclusion

Stating the differences between coupling in Dymola and BCVTB was one of the main objectives in this thesis from the beginning. A comparison between coupling in both softwares should widen the recognition of advantages and disadvantages of both coupling approaches.

Table 12: Comparison between Dymola and BCVTB Coupling Tools

Coupling Tool / Factor	Dymola	BCVTB
Coupling accuracy	Higher (because error tolerance in Dymola could be reduced, a higher accuracy would be obtained on the account of the simulation time).	Lower (using SDF as MoC does not enable the user to control the error tolerance. Also between 2 different synchronization time steps, all values from BCVTB are extrapolated uniformly. So depending on the actual graph and the synchronization step size in Dymola, the single errors could sum up to an amount which causes the model to fail any validation. However, in thermal systems which react very slowly, co-simulation with BCVTB might be considered sufficiently accurate).
Speed of simulation	13380 s	4223 s at TimeStep=5 (3 x speed in Dymola).
Ease of interface	Easier (object-oriented).	Easy (actor-oriented).
Flexibility of model exchange	Low	High

Considering the comparison above, Dymola has shown more appropriateness as a modelling tool. However for complex systems, BCVTB has shown more suitability for coupling and co-simulation but often, on the account of resulted data accuracy.

Although the cooling strategy represented in this thesis might not have shown a high degree of sufficiency, it still has paved the way for assorted and diverse cooling techniques in either alternative simulation models or developed ones to be introduced.

Stochastically, this thesis could contribute among others in cultivating more integrated and sophisticated models representing the FCEV. Especially, when Dymola software has been introduced as a powerful modelling and simulation tool along with the BCVTB with high co-simulation and coupling capabilities.

3 Acknowledgment

Although this thesis was done by a one-man-band, the achievements would never have been the same without the support, encouragement and assistance from the following people. Prof. Dr.- Ing. Peter Treffinger for recommending me for this position at the beginning and his industrious endeavours for supporting his students, not only scientifically but also personally by consolidating their self confidence and decision making skills. Dr. Michael Schier and Dipl.- Ing. Mounir Nasri for supporting me with knowledge and assistance throughout the whole period of the master thesis and for being containing not only on professional levels but also on the personal. Dipl.- Ing. Holger Dittus, Dipl.- Ing. Dave Dickinson, Dipl.- Ing. Michael Schmitt for their aid and assistance with which I could fully concentrate to achieve the goals of this scientific work and without which I wouldn't have been somewhat oriented towards the aims of my work.

I would like also to thank the BCVTB software developers team (Michael Wetter and Thierry Nouidui) at Lawrence Berkeley National Laboratory, Berkeley, CA, USA for their technical support in using the software and for their breadth of mind being good listeners and real helpers.

I am also grateful for the warm welcome and behaviour shown to me by all the staff of the institute being one of them, one of a successful team. My family for all your love, support and encouragement.

A heartfelt thanks go out to the love of my life, whom without her love and support I wouldn't have gotten further to approach this far in my life… To my Sarah.

4 Bibliography

i. AAA (American Automobile Association) World Magazine, Jan-Feb 2011, p.53, January 28, 2014.

ii. BEE Bundesverband Erneuerbare Energie e.V., January 28, 2014.

iii. Mana Mirzaei, Integration of OpenModelica into the Multi-paradigm Modelling Environment of Ptolemy ll, March 04, 2014.

iv. http://www.kleenspeed.com/ev-components/, November 28, 2013.

v. Booß, C. Lefebvre, F.-J. Löpmeier, G. Müller-Westermeier, S. Pietzsch, W. Riecke, H.-H. Schmitt, Die Witterung in Deutschland 2010, February 17, 2014.

vi. R. Fischer, Elektrische Maschinen (Hanser Verlag, 2006), p.385, February 17, 2014.

vii. Martin März, Andreas Schletz, Bernd Eckardt, Sven Egelkraut, Hubert Rauh, Fraunhofer IIS, Power Electronics System Integration for Electric and Hybrid Vehicles, 18 February, 2014.

viii. http://www.examiner.com. November 30, 2013.

ix. The Dow Chemical Co., DOWFROST product information, February 20, 2014.

x. www.modelica.org, Standardization of Thermo-Fluid Modelling in Modelica.Fluid, February 24, 2014.

xi. ESSO AG, Properties of Organic Heat Carriers, March 07, 2014.

xii. AIR LIQUIDE Co., R134-a Manual, March 07, 2014.

xiii. http://simulationresearch.lbl.gov/bcvtb, January 31, 2014.

xiv. http://ptolemy.eecs.berkeley.edu/ptolemyII/index.htm, January 31, 2014.

xv. http://escholarship.org/uc/item/7cp597jf, January 31, 2014.

xvi. http://ptolemy.eecs.berkeley.edu/papers/05/ptIIdesign2-software/, February 03, 2014.

xvii. Dassault Systèmes AB, Dymola (Dynamic Modelling Laboratory) User Manual 1, May, 2012.

xviii. Mounir Nasri, Holger Dittus, Auslegung eines RangeExtender-Antriebsstrangs mit Hochtemperatur-PEM-Brennstoffzelle, 09, 2013.

xix. Dipl.-Ing. Markus Auer (Institut für Verbrennungsmotoren und Kraftfahrwesen Universität Stuttgart), Dipl.-Ing. Sina Krug (Zentrum für Sonnenenergie- und Wasserstoff-Forschung Baden-Württemberg), Gesamtfahrzeugsimulation eines Batterieelektrischen Fahrzeugs, August 30, 2013.

Appendices

Appendix A

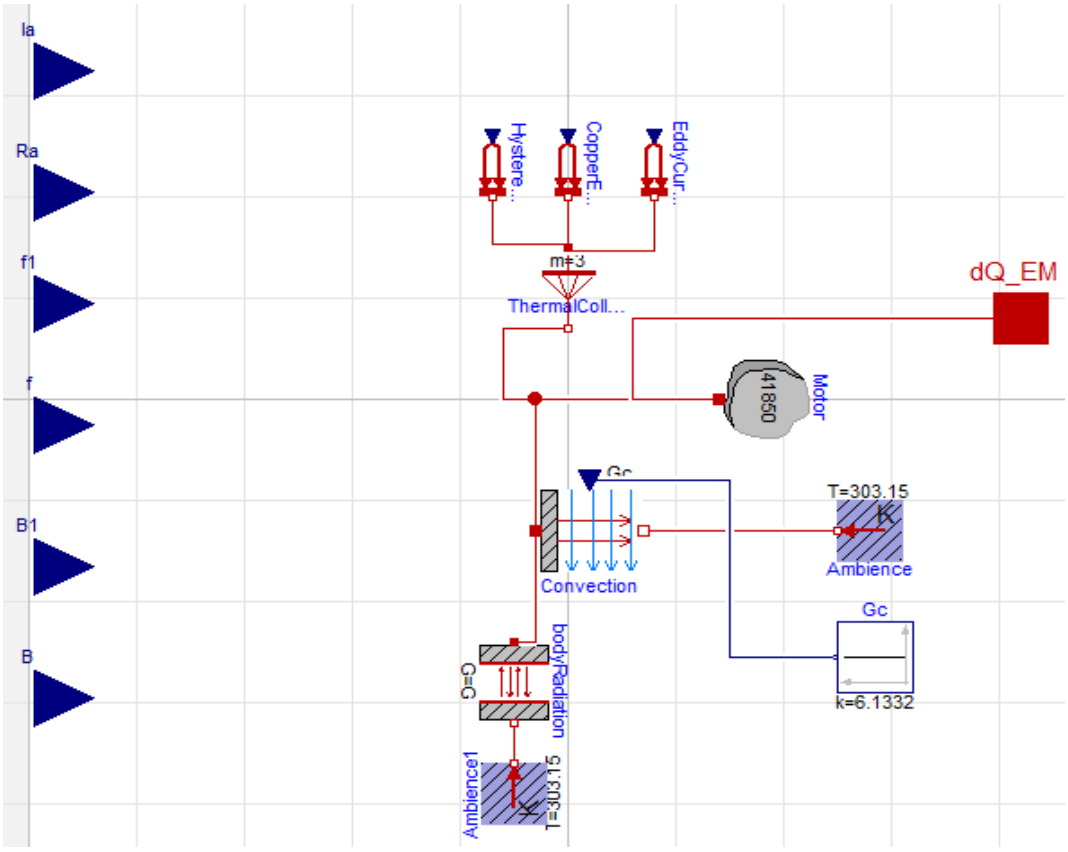

Figure 74: EM Thermal Submodel

In Figure 74, the other approach of EM thermal modelling is introduced. As mentioned before, that this model has been excluded to fast up the simulation speed. The heat load out of this model is a product of the calculated energy losses inside the EM.

The main equations used for calculating energy losses are:

$$\begin{aligned} Copper\ Energy\ Losses\ (W_c) &= 3 \cdot \left(\frac{I_a}{\sqrt{3}}\right)^2 \cdot R_a \\ Hysteresis\ Energy\ Losses\ (W_h) &= \sum \cdot \left(\frac{f}{100}\right) \cdot B^2 \\ Eddy\ Current\ Losses\ (W_r) &= \sum \cdot \left(\frac{f^2}{100}\right) \cdot B^2 \cdot t^2 \end{aligned} \tag{9}$$

Where,

I_a: $current\ per\ phase\ [A]$, B: $magnetic\ flux\ density\ [Wb]$

R_a: $coil\ resistance\ per\ phase\ [\Omega]$, f: $operating\ frequency\ [Hz]$

t: $magnetic\ steel\ plate\ thickness\ [m]$

$permeability\ of\ vacuum\ (\mu)$: $4\pi e^{-7} [H/m]$

Each of the former logged parameters from DLR test vehicle were fed to the above equations to calculate energy losses each second. Each prescribed heat flow in Figure 74 represents energy loss equation.

The sum of all equations is fed to the model above which is similar to the thermal model used in the system.

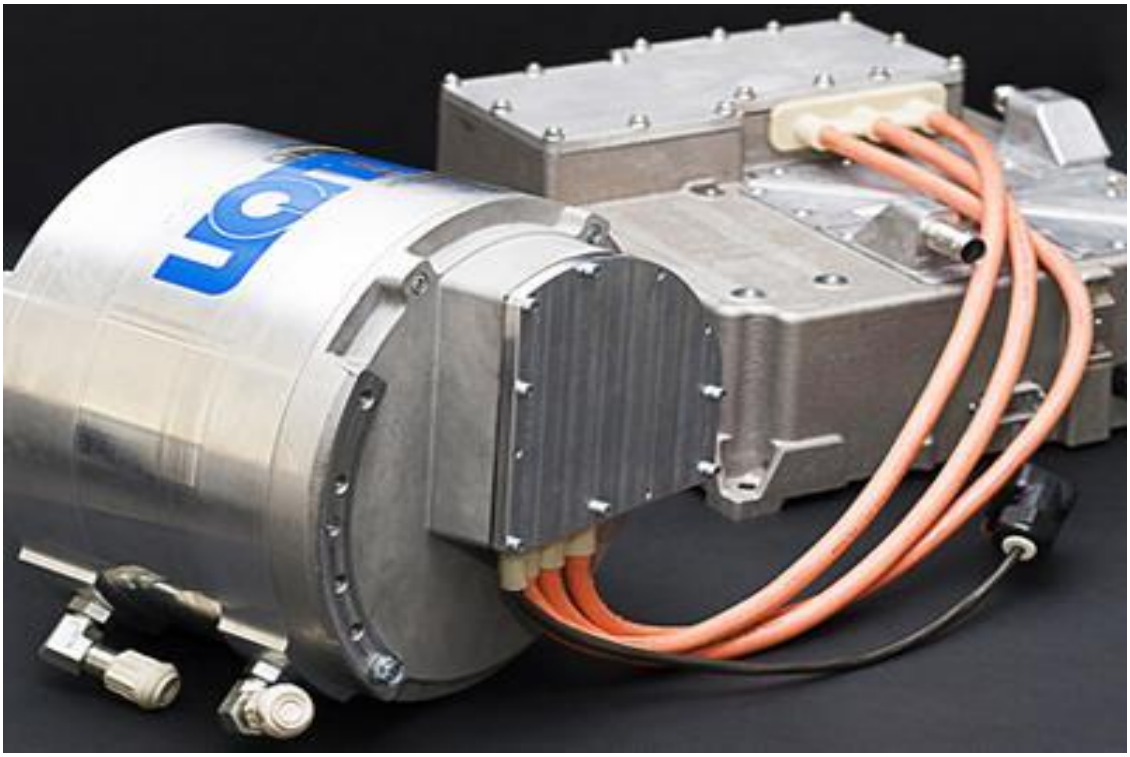

Figure 75: UQM both EM and PEM

Figure 75 shows how the EM and PEM would look like in reality. It is also apparent how the coolant inlet and outlet ports are attached to the cooling jacket around the EM.

Appendix B

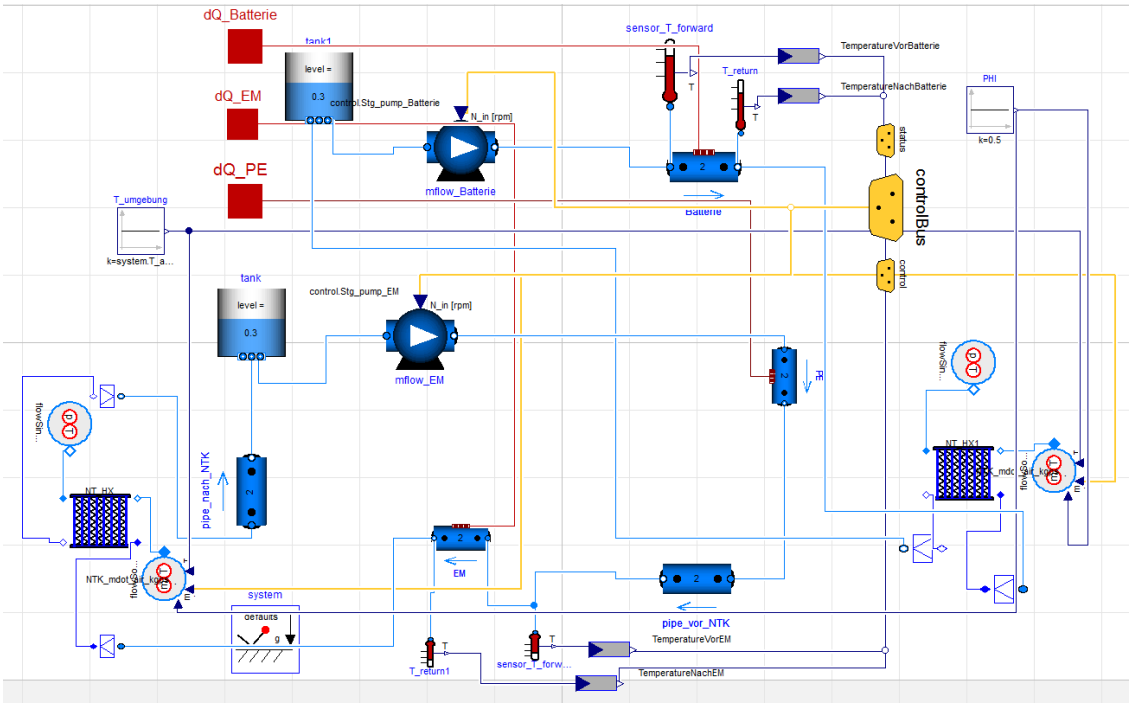

Figure 76: LT and Battery Models with A/C HEXs

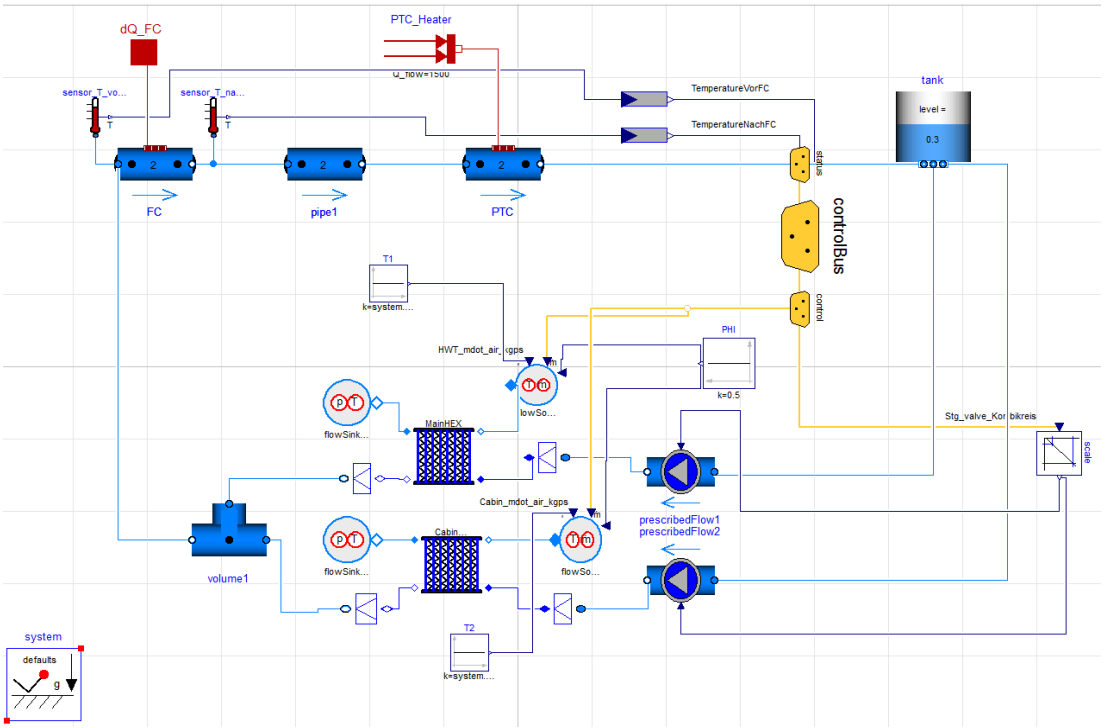

Figure 77: HT Model with A/C HEXs

As mentioned before, that the first approach when choosing the HEXs was to choose them from the A/C library. In Figure 76 and Figure 77, the layouts of LT, Battery and HT models using HEXs from A/C library are illustrated.